République Algérienne démocratique et populaire

Ministère de l'Enseignement Supérieur et de la Recherche Scientifique

Université de Hamma Lakhdar –El Oued

Faculté de Technologie

Département de génie électrique

Mémoire présenté par:

ZEGHIB Okba

En vue de l'obtention du diplôme de doctorat en LMD

Filière: **Electrotechnique**

Option: **Optimisation et gestion d'énergie**

Diagnostic et commande tolérante aux fautes par l'approche du modèle flou de Takagi-Sugeno dédiés à la machine asynchrone

Soutenu le : 18/09/2019

Devant le jury composé de:

Nom et Prénom	*Grade*	*Affiliation*	*Position*
BEN ATTOUS Djilani	***Professeur***	***Université d'El Oued***	***Président***
ALLAG Abdelkrim	***Professeur***	***Université d'El Oued***	***Encadreur***
BETKA Achour	***Professeur***	***Université de Biskra***	***Examinateur***
ALLOUI Lotfi	***Professeur***	***Université de Biskra***	***Examinateur***
KHENE Mohamed Lotfi	***Professeur***	***Université de Biskra***	***Examinateur***
CHEMSA Ali	***MCA***	***Université d'El Oued***	***Examinateur***

2018/2019

People's Democratic Republic of Algeria

Ministry of Higher Education and Scientific Research

University of Hamma Lakhdar –El Oued

Faculty of Sciences and Technology

Department of Electrical Engineering

Thesis presented by:

ZEGHIB Okba

For the purpose of obtaining a doctorate degree in LMD

Sector: **Electrical Engineering**

Option: **Optimization and energy management**

Diagnosis and faults tolerant control based on the Takagi-Sugeno fuzzy approach dedicated to the asynchronous machine

Defensed the : 18/09/2019

In front of the Jury composed of:

Full name	*Grade*	*Affiliation*	*Position*
BEN ATTOUS Djilani	***Professor***	***El Oued University***	***President***
ALLAG Abdelkrim	***Professor***	***El Oued University***	***Supervisor***
BETKA Achour	***Professor***	***Biskra University***	***Examiner***
ALLOUI Lotfi	***Professor***	***Biskra University***	***Examiner***
KHENE Mohamed Lotfi	***Professor***	***Biskra University***	***Examiner***
CHEMSA Ali	***MCA***	***El Oued University***	***Examiner***

2018/2019

Abstract

The purpose of the research presented in this thesis is to propose a methodology for the control and observation of the induction motor (IM) based on the algorithms based on the mean value theorem (MVT) and the transformations by sector non-linearity approach. In the first step, the different control techniques of electric drives were identified and analyzed. A parallel distributed control (PDC) approach is then developed.

In the field of low power, the removal of the mechanical speed sensor can be of economic interest and improve operational safety. We have presented two categories of methods that allow to reconstitute and control this rotor speed quantity; the MVT observer and the robust MVT controller respectively. All the solutions have been validated by numerical simulation and affirmed by experimental tests to compare the accuracy and dynamics characteristics of the different methods with the MVT control. Finally, new approaches to localization and fault detection and Fault-tolerant control (FTC) based on the Takagi-Sugeno (T-S) representation have been addressed once the defective model of the IM is established. The results of the various simulation tests and the different experimental trials put into evidence the robustness and the success properties of the proposed algorithms. The thesis ends with a review of our contribution in terms of research.

Keywords:

induction motor, mean value theorem, sector non-linearity approach, parallel distributed control, MVT observer, robust MVT controller, Takagi-Sugeno representation, Fault-tolerant control.

ملخص

الغرض من البحث المقدم في هذه الرسالة هو اقتراح منهجية للتحكم ومراقبة المحرك الحثي استناداً إلى الخوارزميات المستندة إلى نظرية القيمة المتوسطة (MVT) والتحولات حسب نهج القطاع غير الخطي. في الخطوة الأولى ، تم تحديد تقنيات التحكم المختلفة لمحركات الأقراص الكهربائية وتحليلها. ثم يتم تطوير نهج التحكم المتوازي الموزع(PDC) .

في مجال الطاقة المنخفضة ، يمكن أن يكون إزالة جهاز استشعار السرعة الميكانيكية ذا فائدة اقتصادية ويحسن من السلامة التشغيلية. لقد قدمنا فئتين من الأساليب التي تسمح بإعادة تشكيل ومراقبة كمية سرعة دوارالمحرك الحثي؛ مراقب MVT ووحدة تحكم قوية اعتمادا على MVT على التوالي. تم التحقق من صحة جميع الحلول من خلال محاكاة عددية وأكدتها الاختبارات التجريبية لمقارنة دقة وديناميكية خصائص الأساليب المختلفة مع التحكم MVT. وأخيرًا ، تم التعامل مع أساليب جديدة للتوطين وكشف الأعطاب والتحكم في التسامح عند حدوث الاعطال (FTC) على أساس تمثيل Takagi -Sugeno (T-S) بمجرد إنشاء النموذج المعيب من المحرك الحثي. نتائج اختبارات المحاكاة المختلفة والتجارب التجريبية المختلفة وضعت دليلاً على متانة و نجاح للخوارزميات المقترحة. تنتهي الرسالة بمراجعة مساهمتنا من حيث البحث.

الكلمات المفتاحية

المحرك الحثي, نظرية القيمة المتوسطة, القطاع غير الخطي, مراقبMVT , وحدة تحكم قوية اعتمادا على MVT, والتحكم في التسامح عند حدوث الاعطال.

Résumé

L'objectif de la recherche présentée dans cette thèse est de proposer une méthodologie de contrôle et d'observation du moteur asynchrone (MAS) basée sur des algorithmes basés sur le théorème de la valeur moyenne (MVT) et sur les transformations par secteurs non linéaires. Premièrement, les différentes techniques de contrôle des entraînements électriques ont été identifiées et analysées. Une approche de contrôle distribué parallèle (PDC) est ensuite développée.

Dans le domaine des faibles puissances, le retrait du capteur de vitesse mécanique peut présenter un intérêt économique et améliorer la sécurité de fonctionnement. Nous avons présenté deux catégories de méthodes permettant de reconstituer et de contrôler cette quantité de vitesse de rotor; l'observateur MVT et le contrôleur MVT robuste, respectivement. Toutes les solutions ont été validées par simulation numérique et confirmées par des tests expérimentaux afin de comparer les caractéristiques de précision et de dynamique des différentes méthodes avec le contrôle MVT. Enfin, de nouvelles approches de localisation et de détection de pannes et de commande tolérante au défaut (FTC) basées sur la représentation du Takagi-Sugeno (T-S) ont été abordées une fois que le modèle défectueux du MAS est établi. Les résultats des différents tests de simulation et des différents essais expérimentaux mettent en évidence la robustesse et les propriétés de réussite des algorithmes proposés. La thèse se termine par une revue de notre contribution en termes de recherche.

Mots-clés :

Moteur asynchrone, théorème de la valeur moyenne, secteurs non linéaire approche, observateur MVT, contrôleur MVT robuste, représentation du Takagi-Sugeno , commande tolérante au défauts

Acknowledgment

I first want to prostrate thanking **ALLAH** Almighty for giving me the courage and the patience to complete this work in good conditions.

This thesis is the result of several years of hard and team work . Therefore there is a large number of people to whom I owe my utmost thanks and gratitude.

I would like to express my sincere gratitude to my supervisor Prof. **Dr. Allag Abdelkrim** for his encouragement and guidance throughout the study. I also thank him not only for his technical assists but for his friendship in due course of development of the thesis.

Also, I thank the PhD student **Mr. Hamidani** Bilal for their help and continuous sensory and moral support during my studies.

Finally, my special thanks go to **Dr. Nik Rumzi bin Nik Idris**, **Prof. Dr. Zainal bin Salem**, **Mr. Kermadi Mostafa** for their help during the experimental stage of this work.

A big thank goes to the Department of Electrical Engineering and the College of Engineering at the University of **Hamma Lakhdar** in El Oued and **Mohammed Kheider** in Biskra for offering me the opportunity to pursue this Doctoral study.

Dedication

To my dear parents,

To my fiancée

To my brothers and sisters,

In memory of my grandparents,

To my uncles, aunts, and cousins,

And to all who count for me.

List of publications

Journals

1- O. Zeghib, A. Allag, M. Allag, and B. Hamidani, "An Extended MVT Observer Designed for Induction Motor Drive," *Mediterranean Journal of Measurement and Control*, vol. 13, pp. 805-811, 2017.

2- O. Zeghib, A. Allag, M. Allag, and B. Hamidani, "A robust extended H∞ observer based on the mean value theorem designed for induction motor drives," *International Journal of System Assurance Engineering and Management*, February 08 2019.

3- B. Hamidani, A. Allag, A. Allag, and O. Zeghib, "Sensorless Non-linear Control Applied to a PMSM Machine Based on New Extended MVT Observer," *Journal of Electrical Engineering & Technology*, pp. 1-9, 2019.

4- M. Allag, A. Allag, O. Zeghib and B. Hamidani, " ROBUST H_∞ CONTROL BASED ON THE MEAN VALUE THEOREM FOR INDUCTION MOTOR DRIVE," *Journal of Control, Automation and Electrical Systems*, 2019.

Conferences

1- O. ZEGHIB, A. ALLAG, B. HAMIDANI and M. ALLAG, "Input-output linearizing control of Induction Motor based on a newly extended MVT Observer Design," *2018 International Conference on Communications and Electrical Engineering (ICCEE)*, El Oued, Algeria, 2018, pp. 1-6.

2- B. Hamidani, A. Allag, O. Zeghib and A. Allag, "An extended H∞ observer based on the mean value theorem approach applied to open loop FOC of PMSM drive," *2018 International Conference on Communications and Electrical Engineering (ICCEE)*, El Oued, Algeria, 2018, pp. 1-8.

Table of contents

Chapter 1: Introduction

Chapter 2: State of art about controllers and observers of non-linear systems and faults detection

Chapter 3: Mean value theorem and T-S fuzzy approach for non-linear systems; design and stability analysis

Chapter 4: Control and states estimation of the induction motor based on the MVT theory

Chapter 5: Diagnosis and fault tolerant control of the induction motor based on the T-S fuzzy approach

Chapter 6: Conclusions and future works

Appendixes

List of figures

Chapter 2: State of art about controllers and observers of non-linear systems and faults detection

Chapter 4: Control and states estimation of the induction motor based on the MVT theory

Chapter 5: Diagnosis and fault tolerant control of the induction motor based on the T-S fuzzy approach

Nomenclatures and Abbreviations

$x(t)$	State vector
$\hat{x}(t)$	Estimated state vector
$x_r(t)$	Reference state vector
$e(t)$	State estimation error
$u(t)$	Input vector
$y(t)$	Output vector
$n(t)$	disturbance vector
w_r, w_s	Rotor and stator speed
w_{rr}	Rotor speed reference
w_{sr}	Electrical stator speed reference
θ_r	Rotor position
Ψ_{rd}, Ψ_{rq}	The (*d*,*q*) Rotor flux
Ψ_r	Rotor flux reference
i_{sd}, i_{sq}	The (*d*,*q*) stator currents
U_{ds}, U_{qs}	The (*d*,*q*) stator voltages
U_{dsr}, U_{qsr}	The (*d*,*q*) open loop controls
L_r, L_s	Rotor and stator inductances
R_r, R_s	Rotor and stator resistances
J	Moment of inertia
b	Friction coefficient
P_n	Nominal power of the induction motor
n_p	Pole pair number
T_L	Load torque
M	Mutual inductance

L_0	Observer gain
MVT	Mean value theorem
IM	Induction motor
T-S	Takagi-Sugeno
P	Proportional
PI	Proportional Integral
LPV	Linear parameter varying
LTI	Linear time invariant
LMI's	Linear matrix inequalities
PWM	Pulse width modulation
FOC	Field-oriented control
HP	Horsepower
DTC	Direct torque control
PDC	Parallel distributed compensator
PMSM	Permanent magnet synchrounous machine
FTC	Fault tolerant control

Chapter 1:
Introduction

1.1 General presentation:

Induction machine (IM) receives its name from the fact that electrical current is induced in the rotor by magnetic fields generated by the stator windings. It is therefore required that the rotor of an IM contains an electrically conducting material. In fact, if the rotor is a solid cylinder of metal the machine could operate as an IM, though not a very good one. This conducting material may consist of two or three phase windings similar to those on the stator, this is known as a wound rotor IM, but many induction machine rotors have a squirrel cage design.

The IM's had the most uses among the electrical machines in industrial applications due to their simple, high efficiency, high power density and higher torque to weight ratio. Owing to the intrinsic nonlinear coupling between the dynamics of the electrical part and of the mechanical part, strongly coupled time-varying systems, the rotor variables are not measurable, inaccessibility for the rotor flux, system-parameter variations, and IM's are multivariable nonlinear, the IM drives feedback control and state's estimation are so difficult[1] .

It is known that the occurrence of such fault can degrade the control performances and in some cases lead to the instability of the system. Consequently, many strategies for fault detection and isolation (FDI) and fault-tolerant control (FTC) are introduced to tolerate the fault effect and maintain system stability[1-3]. Generally speaking, fault tolerant control is a control that possesses the ability to accommodate system failures automatically, maintain overall system stability, and acceptable performance even in the faulty situation.

1.2 Background

Due to the disadvantages of nonlinear systems, many authors are tried to transfer the nonlinear and coupling systems as specific forms of systems, such as Lipschitz systems. Different approaches have been after studied according to the IM, among them, the high gain observer in [4] and the using of the flux linkage observer as in [5], many other strategies were proposed in literature among them: sliding mode observers, an extended Kalman filter, a Model Reference Adaptive System (MRAS) observers, nonlinear Luenberger observers and others. In detail, an extended sliding mode observer to estimate the rotor flux for IM control was proposed in [6] and the authors in [7] propose a second-order sliding mode observer for the sensor-less control of IM drives, whereas in [8] Regaya et al. present an adaptive sliding mode speed observer for IM drive control. An extended Kalman filter method for the speed and the flux observation of the IM was illustrated in [9, 10]. The MRAS observers are used for the IM control as in [11] where the authors proposed an MRAS observer for the IM control that estimates the speed and the rotor flux, wherein [12] Kandoussi et al. propose an improved MRAS observer for sensorless control of the IM drives. Nonlinear Luenberger observers were proposed for the IM speed servo drive in [13]. A nonlinear observer was used to estimate the IM flux which proved to be satisfactory as in [14]. A technique relied on the changing of the original system into a linear system was proposed by Alonge et al. in [15].

Many modern control techniques have been designed to overcome the tracking problem. Adaptive control methods are proposed in [16, 17], fuzzy control has been treated in [18, 19] and a sliding mode and backstepping controls have been adopted by [20] and [21] respectively. In [16] a backstepping adaptive control for IM was designed with uncertainties, while the authors in [17] propose an adaptive controller based on sliding mode neuro-fuzzy control of an IM without mechanical sensors. A fuzzy self-tuning speed control of indirect field oriented control of IMs is studied in [18], the paper [19] shows a novel fuzzy sliding mode structure for the speed control of IMs. DTC of IM with feedback linearization has been presented in [22].

In all mentioned estimation and control methods above it was so difficult to reach them owing to the strong conditions, the dependency between the observers or controllers and the states of the

IM and they haven't any systematic methodology for proving the stability conditions and, moreover, the existence of the transformation in the IM system through the decoupling block.

1.3 Research motivation

To remedy the disadvantages of the previous observation methods and the control concepts which have been quoted above, a controller or observer based on the MVT approach [23, 24]makes sure to do so.

The MVT approach was recently used in [25-27] for the observation of the states of IM's drives, where the authors transfer the nonlinear model of the IM into the Lipschitz form and use the MVT and sector non-linearity approaches to find the observer gain by solving the LMI's which are obtained from the Lyapunov theory. The contribution of this thesis is to use the MVT theory combined with sector non-linearity approach in order to estimate the extended states of the IM (the ordinary states and, moreover, the rotor position and the load torque) with a minimum disturbance effect to the estimation error. The used approach is based on the transfer of the nonlinear system of the IM into the Lipschitz form, then the nonlinear error dynamics of the proposed observer designed for the IM is expressed as a convex combination of known matrices with time-varying coefficients as LPV systems. Using the Lyapunov theory [28], the stability conditions are obtained and expressed in terms of LMI's that are solved through the YALMIP software in order to obtain the observer gain. The important idea of the MVT observers is to find the observer gain so as that the nonlinear and coupling model of the IM drive makes as in linear model feedback control theory taking into consideration a minimum effect of the disturbance to the estimation error. The main advantage of the MVT approach in this work is to find observer gain which is calculated offline with a proven methodology that stabilizes the estimation error of the IM even in presence of a disturbances and doesn't depend on the states of the IM contrarily as in other technics for the estimation of the states of the nonlinear systems.

In this work, the design of various controllers for FOC of IM based on MVT applied to a class of Lipchitz nonlinear system are presented. In [29], the MVT theory has been applied to design the controller for a FOC of PMSM, but only simulation work is presented. In this thesis, the controller is designed based on the state space feedback and MVT is applied to the nonlinear error dynamic of the controller. It is then can be considered as a convex combination of a linear parameter varying

(LPV) system. The structure of the proposed controls is similar to that of the P and PI controllers. By using Lyapunov stability conditions, the linear matrix inequalities (LMIs) is obtained. Subsequently, the gains of the controllers are obtained by solving the LMI's. This thesis demonstrates the feasibility and effectiveness of the proposed controllers, despite its simple implementation. The controller managed to follow the references with variation with a minimum tracking error even in presence of various disturbances.

In our work, we exploit the performances of the FTC for state feedback tracking control for IM drive using the T–S fuzzy approach. The aim is to guarantee the stability and the operating in safe despite the occurrence of the speed and current sensors faults. First, we construct an augmented system containing the tracking error and the estimation error. Then, a fuzzy descriptor observer-based fault-tolerant tracking controller is developed.

1.4 Research aim and objectives

1.4.1 Research aim

The study aims to the control and the observation of the IM based on the MVT and PDC approaches. It further seeks to develop a control or state observation for the IM where the model is taken as it (without any transformations) and in the same time the controller or the observer gains are gotten offline (no dependency with the IM states) with the stability is of them should has a proven and systematic methodology contrarily to other methods. The work includes the development FTC of a mechanical sensor fault based on the T-S fuzzy model of the IM through the PDC approach.

1.4.2 Research objectives

The main research goal of this work is to simplify and to reduce the price of the control or the observer for IM with efficiency and performance similar to previous methods. In order to fulfill the research goal a number of objectives are identified and prioritized as follows:

Objective 1: develop an MVT observer that does not depend on the states of the IM and can estimate faults, parameters and of course the IM states.

Objective 2: develop a robust MVT controller that makes the IM subject to control conditions even in presences of perturbations (load, faults and parameters variations…).

Objective 3: avoid any type of transformation in the non-linear model of the IM because for example when the decoupling exists, we are in reality examine a linear model.

Objective 4: check the effectiveness of the approaches through various simulation and experimental tests.

Objective 5: develop an FTC approach based T-S model to protect the electrical machines against the partial or full loss of them.

1.5 Structure of the thesis

This thesis is organized as follows:

The previous works for the observation and the control of the nonlinear systems and some reviews about the faults are given in Chapter 2. Firstly, The review mainly focused on FOC and DTC, and state observers such as Kalman filter and others, the previous works are discussed briefly and compared with each other. Secondly, the most popular faults in the IM and their effects is clearly proposed.

Chapter 3 presents the MVT approach for the class of non-linear systems and moreover the T-S model of non-linear systems. The stability of each kind is discussed and through the Lyapunov theory either for controllers or either for observers.

Chapter 4 presents a generalized dynamic mathematical model of the IM which can be used to construct various equivalent circuit models in the d-q rotating reference frame, firstly. Then, the design of controllers and observers for the IM based on the MVT theory is presented. These observers and controllers based on the MVT approach are checked through illustrative simulation tests and also with different experiments in order to prove the effectiveness of the MVT approach.

Chapter 5 is devoted to the FTC approach for the IM based on the PDC approach. The sensor fault is chosen for the FTC concept. the design of the robust control that makes the IM submit to

control conditions even in the presence of the sensor faults, and an extended observer that estimate the sensor fault with the states of the IM, where the stability of all the system is proven.

Chapter 6 presents conclusions based on the findings and outlines perspectives for future work.

References

[1] H. B. Zina, M. Allouche, M. Souissi, M. Chaabane, and L. Chrifi-Alaoui, "Robust sensor fault-tolerant control of induction motor drive," *International Journal of Fuzzy Systems*, vol. 19, pp. 155-166, 2017.

[2] H. b. Zina, M. Allouche, M. Souissi, M. Chaabane, L. Chrifi-Alaoui, and M. Bouattour, "Descriptor observer based fault tolerant tracking control for induction motor drive," *automatika*, vol. 57, pp. 703-713, 2016.

[3] H. B. Zina, M. Allouche, M. Souissi, M. Chaabane, L. Chrifi-Aloui, and C. France, "Fault Tolerant Control for Induction Motor Drive Using Descriptor Approach," 2015.

[4] J. H. Ahrens and H. K. Khalil, "High-gain observers in the presence of measurement noise: A switched-gain approach," *Automatica*, vol. 45, pp. 936-943, 2009.

[5] M. Manohar and S. Das, "Current sensor fault-tolerant control for direct torque control of induction motor drive using flux-linkage observer," *IEEE Transactions on Industrial Informatics*, vol. 13, pp. 2824-2833, 2017.

[6] O. Asseu, M. A. Kouacou, T. R. Ori, Z. Yéo, M. Koffi, and X. Lin-Shi, "Nonlinear Control of an Induction Motor Using a Reduced-Order Extended Sliding Mode Observer for Rotor Flux and Speed Sensorless Estimation," *Engineering*, vol. 2, p. 813, 2010.

[7] L. Zhao, J. Huang, H. Liu, B. Li, and W. Kong, "Second-order sliding-mode observer with online parameter identification for sensorless induction motor drives," *IEEE Transactions on Industrial Electronics*, vol. 61, pp. 5280-5289, 2014.

[8] C. B. Regaya, F. Farhani, A. Zaafouri, and A. Chaari, "An adaptive sliding-mode speed observer for induction motor under backstepping control," *Int J Innov Comput I*, vol. 11, pp. 763-771, 2017.

[9] Z. Yin, G. Li, Y. Zhang, J. Liu, X. Sun, and Y. Zhong, "A Speed and Flux Observer of Induction Motor Based on Extended Kalman Filter and Markov Chain," *IEEE Transactions on Power Electronics*, vol. 32, pp. 7096-7117, 2017.

[10] S. Meziane, R. Toufouti, and H. Benalla, "Nonlinear control of induction machines using an extended kalman filter," *Acta Polytechnica Hungarica,* vol. 5, pp. 41-58, 2008.

[11] S. Zaidi, F. Naceri, and R. Abdssamed, "Input-Output Linearization of an Induction Motor Using MRAS Observer," *International Journal of Advanced Science and Technology,* vol. 68, pp. 49-56, 2014.

[12] Z. Kandoussi, Z. Boulghasoul, A. Elbacha, and A. Tajer, "Sensorless Control of Induction Motor Drives Using an Improved MRAS Observer," *Journal of Electrical Engineering & Technology,* vol. 12, pp. 1456-1470, 2017.

[13] J. Gacho and M. Zalman, "IM based speed servodrive with luenberger observer," *Journal of Electrical Engineering,* vol. 61, p. 149, 2010.

[14] C.-W. Park and S. Lee, "Nonlinear observer based control of induction motors," *Electrical Engineering (Archiv fur Elektrotechnik),* vol. 90, pp. 107-113, 2007.

[15] F. Alonge, M. Cirrincione, M. Pucci, and A. Sferlazza, "A Nonlinear Observer for Rotor Flux Estimation of Induction Motor Considering the Estimated Magnetization Characteristic," *IEEE Transactions on Industry Applications,* vol. 53, pp. 5952-5965, 2017.

[16] A. Zaafouri, C. B. Regaya, H. B. Azza, and A. Châari, "DSP-based adaptive backstepping using the tracking errors for high-performance sensorless speed control of induction motor drive," *ISA transactions,* vol. 60, pp. 333-347, 2016.

[17] T. Orlowska-Kowalska, M. Dybkowski, and K. Szabat, "Adaptive sliding-mode neuro-fuzzy control of the two-mass induction motor drive without mechanical sensors," *IEEE Transactions on Industrial Electronics,* vol. 57, pp. 553-564, 2010.

[18] M. Masiala, B. Vafakhah, J. Salmon, and A. M. Knight, "Fuzzy self-tuning speed control of an indirect field-oriented control induction motor drive," *IEEE Transactions on Industry Applications,* vol. 44, pp. 1732-1740, 2008.

[19] F. Barrero, A. Gonzalez, A. Torralba, E. Galvan, and L. G. Franquelo, "Speed control of induction motors using a novel fuzzy sliding-mode structure," *IEEE Transactions on Fuzzy Systems,* vol. 10, pp. 375-383, 2002.

[20] C. Lascu, I. Boldea, and F. Blaabjerg, "Direct torque control of sensorless induction motor drives: a sliding-mode approach," *IEEE Transactions on Industry Applications,* vol. 40, pp. 582-590, 2004.

[21] C. Kwan and F. L. Lewis, "Robust backstepping control of induction motors using neural networks," *IEEE Transactions on Neural Networks*, vol. 11, pp. 1178-1187, 2000.

[22] C. Lascu, S. Jafarzadeh, M. S. Fadali, and F. Blaabjerg, "Direct torque control with feedback linearization for induction motor drives," *IEEE Transactions on Power Electronics*, vol. 32, pp. 2072-2080, 2017.

[23] G. Phanomchoeng, "State, parameter, and unknown input estimation problems in active automotive safety applications," 2011.

[24] A. Zemouche, M. Boutayeb, and G. I. Bara, "Observer Design for Nonlinear Systems: An Approach Based on the Differential Mean Value Theorem," in *Decision and Control, 2005 and 2005 European Control Conference. CDC-ECC'05. 44th IEEE Conference on*, 2005, pp. 6353-6358.

[25] M. Y. Hammoudi, A. Allag, M. Becherif, M. Benbouzid, and H. Alloui, "Observer design for induction motor: an approach based on the mean value theorem," *Frontiers in Energy*, vol. 8, pp. 426-433, 2014.

[26] O. Zeghib, A. Allag, M. Allag, and B. Hamidani, "An Extended MVT Observer Designed for Induction Motor Drive," *Mediterranean Journal of Measurement and Control*, vol. 13, pp. 805-811, 2017.

[27] O. Zeghib, A. Allag, M. Allag, and B. Hamidani, "A robust extended H∞ observer based on the mean value theorem designed for induction motor drives," *International Journal of System Assurance Engineering and Management*, February 08 2019.

[28] D. Ichalal, B. Marx, S. Mammar, D. Maquin, and J. Ragot, "How to cope with unmeasurable premise variables in Takagi–Sugeno observer design: Dynamic extension approach," *Engineering Applications of Artificial Intelligence*, vol. 67, pp. 430-435, 2018.

[29] A. Allag, A. Benakcha, M. Allag, I. Zein, and M. Y. Ayad, "Classical state feedback controller for nonlinear systems using mean value theorem: closed loop-FOC of PMSM motor application," *Frontiers in Energy*, vol. 9, pp. 413-425, 2015.

Chapter 2:

State of art about controllers and observers of non-linear systems and faults detection

2.1 Introduction:

In the chapter, we have presented some works and methods for the IM control those are used now in the industry with their benefits and drawbacks, and we illustrate also the last observers in the literature review, each observer is mentioned with their advantages and disadvantages. Finally, we talk about the famous faults in the induction motor (causes, consequences, the percentage of happening,…).

The current chapter is organized as follows: in the first section, the previous control technics for the IM are distinctly presented. Whereas, the last observers in the literature review for the state's estimation of the IM are proposed after. In the following section, the Fault types in the IM motor are presented. At last this chapter are closed by a conclusion.

2.2 State of Art about control of non-linear systems

In the literature review, there are many control types was of control for nonlinear systems were added to the electrical machines. in control theory there is no perfect method, any control approach has advantages and drawbacks at the same time. In followings, we mention many kinds of control for nonlinear systems with their benefits and drawbacks.

2.2.1 Scalar control

The scalar control method is based on varying two parameters simultaneously. This speed can be varied by increasing or decreasing the supply frequency, though this results in a change of impedances. This change of impedances then also increases or decreases the current. If the current

is small, the motor torque decreases. If the frequency decreases or the voltage increases, the coils can be burned or saturation can occur in the iron of the coils. To avoid these problems, it is necessary to vary the frequency and the voltage at the same time[1]. Scalar control is cheap and easy to implement, though it is not as sufficient in controlling drives with dynamic behavior. Overall, the scalar control is low-performance, but stable.

2.2.2 Vector control (FOC)

Field-oriented vector control makes it possible to uncouple the field components into two independent, single-controlled currents instead: The flux-producing current and the torque producing current. With vector-based control, you can achieve tighter speed control, higher starting torque, and higher low-speed torque[2]. With a field-oriented vector, you can control the currents independently, allowing it to operate with fast responses, making it much more appropriate for dynamic drives. the main disadvantages of the vector control are the huge computational capability required and the compulsory good identification of the motor parameters.

2.2.3 DTC control

DTC has a very fast response and simple structure which makes it be more popular used in the industrial world. This method of control implies a comparative control of the torque and the stator fluxes which must fall into two separate certain bands (limits) to be applicable[3]. In DTC it's possible to control directly the stator flux and the torque by selecting the appropriate inverter state.

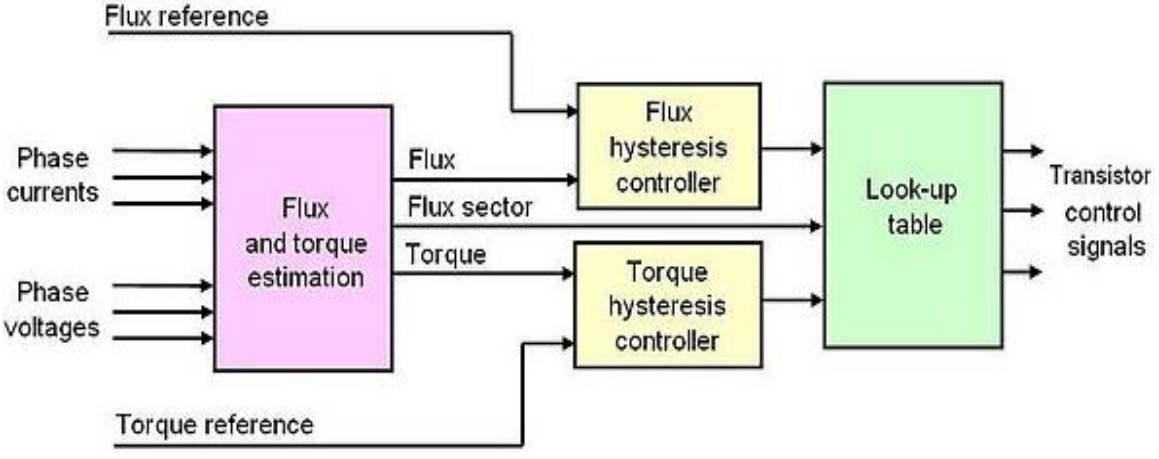

Figure 2.1 Illustrative scheme of the DTC

2.2.4 Adaptive control

The origin of adaptive control goes back to 1950: automation engineers quickly realized that a controller with fixed parameters was not always able to ensure the desired performance, for example in the case where the parameters of the system varied with time. Adaptive control strategies include direct methods, such as MRAC, whose objective is to design a reference model whose performance coincides with that of the closed-loop system. The command is to eliminate any divergence between the response of the model and that of the system regardless of the input signal and the disturbance conditions (internal or external). Indirect methods are based on the real-time identification of the process and the placement of poles. Each method uses different techniques but for the same purpose the cancellation of the error between the reference and the model output [4, 5].

2.2.5 Sliding mode control

SMC is a particularly interesting technique. it dates back to the 1970s with Utkin's work[6]. The principle consists in bringing, whatever the initial conditions, the point representative of the evolution of the system on a hypersurface of the phase space by the integration of switching elements in the control law. The SMC scheme is a well-known robust control scheme for dynamic uncertain systems. However, SMC suffers from the dangerous chattering effect which prevents them from being extensively used in practice. Also, the performance of sliding mode control depends heavily on the sliding surface. If the sliding surface is not designed properly, it may lead to adverse effects[7].

2.2.6 Backstepping control

The technique of backstepping appeared in the 1990s by P. Kokotovic. The history of the backstepping is summarized in [8]and the approach is extensively studied. Nonlinear control with input-state linearization or input-output leads to the cancellation of nonlinearities that might be useful. Backstepping is less restrictive and does not force the system to become linear. The basic idea of backstepping is to synthesize the control law in a recursive way. Some components of the state vector are considered "virtual commands" and intermediate control laws are developed. Backstepping is strictly applied to triangular non-linear systems[8]. The process terminates when the final external control is reached.

2.2.7 Fuzzy control

The fuzzy logic, introduced by Lotfi Zadeh [9], Fuzzy models have the property of approximating any nonlinear function. The main advantage of fuzzy logic control is that it is possible to "do without" an explicit model of the process [10]. This approach is based on two concepts: that of the decomposition of a discourse universe of one or more variables measured in the form of linguistic symbols: "small", "medium", "large" ... and rules coming from of the expertise of the human operator, which express, again, in the form of a language, how the system controls must evolve according to the variables. Fuzzy systems can be classified into three groups: linguistic Fuzzy systems or Mamdani systems, relational fuzzy systems, and functional consequence systems, or known as T-S Kang fuzzy systems.

2.3 State of Art on the state's estimation of non-linear systems

There are various types of observers in literature for the state's estimation, for the nonlinear systems, this topic becomes a challenge in the actually researches, except the observers for nonlinear systems those are considered so difficult. In this part we will describe some kinds of observers for nonlinear systems:

2.3.1 Kalman filter

The purpose of Kalman filter is to predict the trajectory of a moving system in real time, updating the estimate at the previous epoch by exploiting the new observations and the dynamics of the system (assumed to be predictable). This estimate is sub-optimal with respect to the joint use of all the data in post-processing, which can be obtained by Least Squares (batch solution).

Despite the stability and convergence of evidence established in the case of linear systems and can’t be extended generally to the case of nonlinear systems, this method remains the most popular and widely studied in the field of nonlinear observation systems[11, 12]. In the next figure, the different steps to the state's estimation by Kalman filter was illustrated.

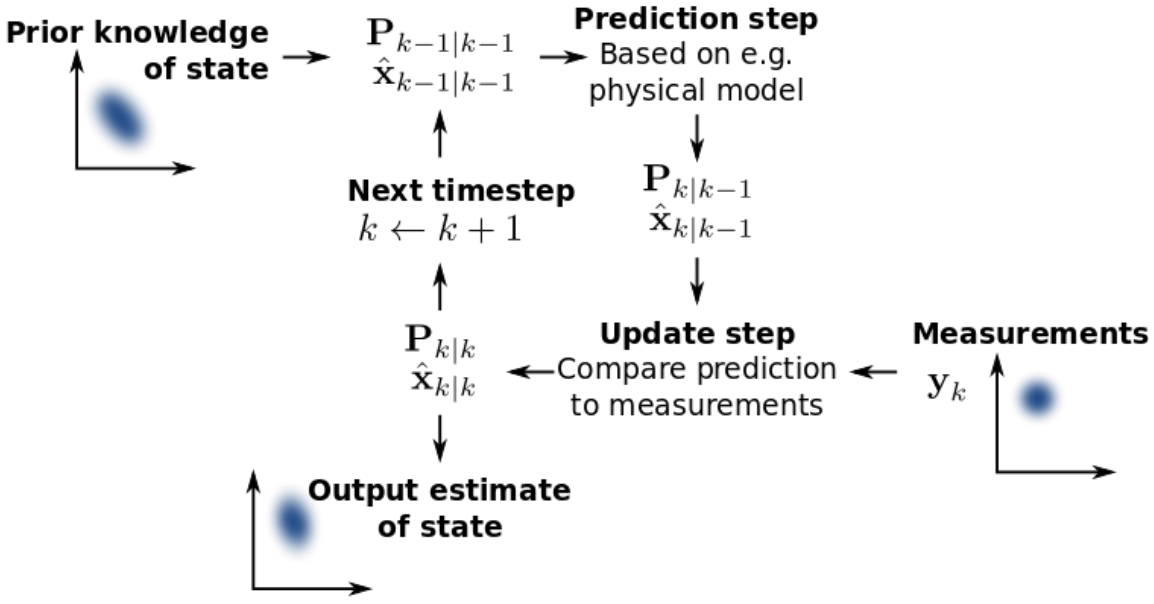

Figure 2.2 Different steps of Kalman filtering

2.3.2 Sliding mode observer

Based on the same theory of the SMC, The sliding mode observer uses non-linear high-gain feedback to drive estimated states to a hypersurface where there is no difference between the estimated output and the measured output. The non-linear gain used in the observer is typically implemented with a scaled switching function. Hence, due to this high-gain feedback, the vector field of the observer has a crease in it so that observer trajectories slide along a curve where the estimated output matches the measured output exactly. So, if the system is observable from its output, the observer states will all be driven to the actual system states. Additionally, by using the sign of the error to drive the sliding mode observer, the observer trajectories become insensitive to many forms of noise. Hence, some sliding mode observers have attractive properties similar to the Kalman filter but with a simpler implementation.[13, 14].

2.3.3 Non-linear Leuenberger observer

The Luenberger observer has been proposed by[15], the idea of this technique is to add a second gain inside the non-linear part depend on the estimated states of the system to the constant gain of

the Luenberger observer. This type of observer can cause instabilities that manifest themselves away from the point of operation, that is why it is rarely used in practice[16].

2.3.4 High gain observers

High gain observers are observers based on Lyapunov stability conditions, they appear for the first time in 1973 by[17]. The principle of this kind of observers is to get a high gain of the observer that make up for the non-linearity terms of the system. The high gain observers have some advantages such as they are relatively simple to design as you do not need to solve complex differential equations nor use complicated formulae. For a large class of nonlinear systems, they can provide global or semi-global stability results for a large class of systems. They can be relatively fast. In spite of high gain observers have the previous benefits, they have some drawbacks as they are sensitive to measurement noise, they suffer from the 'peaking' phenomenon, where, due to the high-gain, there is an initial sharp spike in the response of the state estimates. This phenomenon can cause instability for some types of systems[18].

2.4 Faults in IM drive

2.4.1 Fault types

IM's may encounter several fault conditions, which can lead to additional maintenance costs and unscheduled downtime, resulting in an overall loss of production and financial income. More than 80% of electromechanical conversion in industrial drives belongs to the IM. Furthermore, the total number of operating electrical machines in the world was around 16.1 billion in 2011, with a growth rate of about 50% in the last five years [19]. In general, various surveys on studying IM machine faults have categorized the most common fault mechanisms. The more statistical results, based on the statistical report of the Motor Reliability Working Group of the IEEE-Industry Applications Society, which surveyed 1141 motors, and the Electrical Power Research Institute (EPRI), which surveyed 6312 motors, can be summarized in the results depicted in figure 2.3 [19, 20].

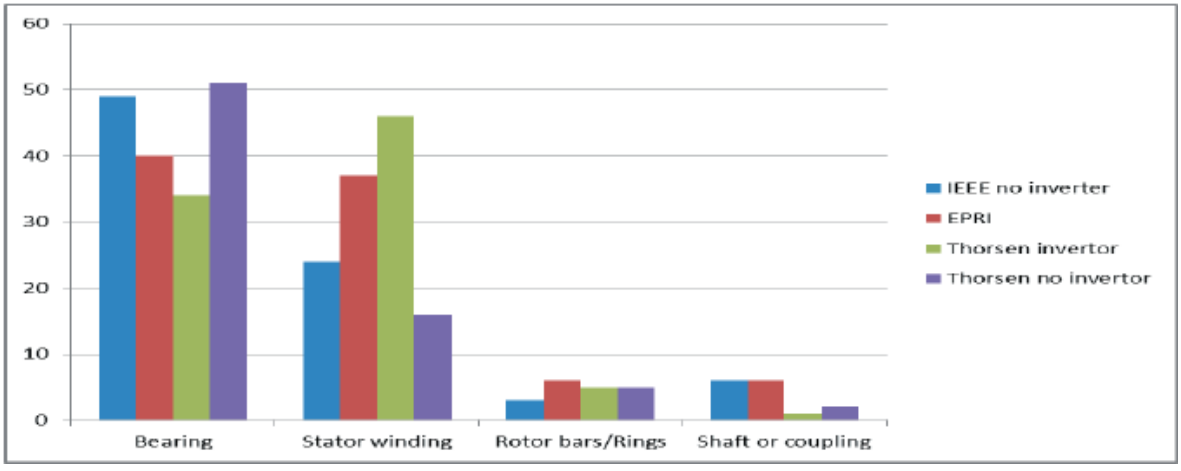

Figure 2.3 The percentage of common faults in IM's

2.4.2 Stator Faults

Stator faults are usually related to insulation failures. Several studies have shown that 30%− 40% of IM failures are due to stator winding breakdowns[21]. Stator winding consists of coils of insulated copper wire placed in the stator slots, while the stator winding faults start due to the insulation breakdown between two adjacent turns in a coil for the same phase; this fault is usually called a turn to turn fault or inter-turn short circuit. Therefore, this type of fault will produce extra heat and imbalance in the magnetic field of the machine. The extra local heat between two or more shorted turns will cause further damage to the neighboring turn's insulation until the occurrence of a catastrophic failure, such as phase failures, phase to phase failures, phase to ground failures, or phase to phase to ground failures.

In fact, the majority of these defects are due to a combination of various stresses acting on the stator, which can be classified into thermal, electrical, mechanical, and environmental factors.

Inter-turn short circuits in stator windings constitute a category of faults that are most common in IM's drives. Typically, short circuits in stator windings occur between turns of one phase, between turns of two phases, or between turns of all phases. Moreover, short circuits between winding conductors and the stator core also occur[22].

2.4.3 Rotor Faults

Rotor faults now account for around 5-10% of the total IM failures. The reasons for rotor bar and end ring breakage are several and are mainly caused by [19, 23]:

- ✓ Magnetic stresses caused by electromagnetic forces, unbalanced magnetic pull, electromagnetic noise, and vibration.
- ✓ Residual stresses due to manufacturing problems
- ✓ Thermal stresses due to thermal overload and unbalance; hot spots or excessive losses or sparking.
- ✓ Dynamic stresses arising from shaft torques, centrifugal forces, and cyclic stresses.
- ✓ Environmental stresses caused, for example, contamination and abrasion of rotor material due to chemicals or moisture.
- ✓ Mechanical stresses due to loose laminations, fatigued parts, or bearing failure.

On the other hand, rotor type faults, lead to speed fluctuation, torque pulsation, changes of the frequency component in the supplying current of the motor, temperature increase, arcing in the rotor, and vibration of the machine. These side effects can be utilized in detecting and classifying this type of fault. Therefore, early detection of the rotor asymmetry is essential not only for the rotor protection but also for reducing some other types of motor failures.

2.4.4 Bearing Faults

As figure 2.3 indicate, around 40% of faults in IM's come from bearing faults[24]. In general, the rolling element bearing consists of one inner and outer ring, while a set of rolling elements are located in between. Standard shapes of rolling elements include the ball, cylindrical roller, tapered roller, needle roller, etc. Usually, the rolling elements in a bearing are arranged or guided in a cage, in order to ensure uniform spacing between elements to prevent mutual contact. The different faults occurring in a rolling-element bearing can be classified according to the damaged element as ball defect, inner raceway defect, and outer raceway defect. The rolling element bearing is one of the most critical components when rotating IM's because the large majority of problems arise from bearing faults. Therefore, both the detection and diagnosis of mechanical faults in rolling element bearings are very important for the reliable operation of an IM[25].

2.4.5 Sensor Faults

A sensor fault represents the difference between the actual value of a physical quantity and its measurement, it may be partial or total. the first produces a signal with more or less matching with the true value, this type of fault, appears in the form of bias, drift, drop in efficiency or a calibration defect. The second fault produces a value that is not related to the quantity to be measured, it is due for example to a total disconnection between the information source and the sensor[26].
In this thesis, the recent fault was taken into consideration for the diagnosis and the FTC approach based on the T-S fuzzy approach as will presented later in chapter 5.

2.5 Conclusion

In this chapter, we have presented some literature review of the control, the state's estimation and some types of faults according to the three-phase IM. Firstly, we have mentioned the known control methods those are used in the industry with their benefits and drawbacks. Then, different kinds of observers were also proposed. At last, we have present the famous faults in the IM's drives and their causes and consequences. We illustrate these works with their disadvantages in order to show the effectiveness of the MVT approach that is based on the T-S representation of the non-linear system and how it remedy the disadvantages of the previously technics. The topic of the next chapter is the T-S representation of non-linear systems and the MVT approach and the stability analysis for the two concepts.

References

[1] B. K. Bose, "Scalar decoupled control of induction motor," *IEEE transactions on industry applications*, pp. 216-225, 1984.

[2] S. Bozhko, S. Kovbasa, Y. Nikonenko, and S. Peresada, "Direct vector control of induction motors based on rotor resistance-invariant rotor flux observer," in *2018 IEEE International Conference on Electrical Systems for Aircraft, Railway, Ship Propulsion and Road Vehicles & International Transportation Electrification Conference (ESARS-ITEC)*, 2018, pp. 1-6.

[3] C. Lascu, S. Jafarzadeh, M. S. Fadali, and F. Blaabjerg, "Direct torque control with feedback linearization for induction motor drives," *IEEE Transactions on Power Electronics,* vol. 32, pp. 2072-2080, 2017.

[4] S. Maiti, C. Chakraborty, Y. Hori, and M. C. Ta, "Model reference adaptive controller-based rotor resistance and speed estimation techniques for vector controlled induction motor drive utilizing reactive power," *IEEE Transactions on Industrial Electronics,* vol. 55, pp. 594-601, 2008.

[5] C. Chan, W. Leung, and C. Ng, "Adaptive decoupling control of induction motor drives," *IEEE Transactions on industrial electronics,* vol. 37, pp. 41-47, 1990.

[6] V. Utkin, "Variable structure systems with sliding modes," *IEEE Transactions on Automatic control,* vol. 22, pp. 212-222, 1977.

[7] Z. Yan, C. Jin, and V. Utkin, "Sensorless sliding-mode control of induction motors," *IEEE Transactions on Industrial Electronics,* vol. 47, pp. 1286-1297, 2000.

[8] G. Bastin and J.-M. Coron, "Backstepping Control," in *Stability and Boundary Stabilization of 1-D Hyperbolic Systems*, ed: Springer, 2016, pp. 219-228.

[9] L. A. Zadeh, "On fuzzy algorithms," in *Fuzzy Sets, Fuzzy Logic, And Fuzzy Systems: Selected Papers by Lotfi A Zadeh*, ed: World Scientific, 1996, pp. 127-147.

[10] C. W. De Silva, *Intelligent control: fuzzy logic applications*: CRC press, 2018.

[11] M. Hoshiya and E. Saito, "Structural identification by extended Kalman filter," *Journal of engineering mechanics,* vol. 110, pp. 1757-1770, 1984.

[12] F. Alonge, T. Cangemi, F. D'Ippolito, A. Fagiolini, and A. Sferlazza, "Convergence analysis of extended Kalman filter for sensorless control of induction motor," *IEEE Transactions on Industrial Electronics,* vol. 62, pp. 2341-2352, 2015.

[13] V. Utkin, J. Guldner, and J. Shi, *Sliding mode control in electro-mechanical systems*: CRC press, 2009.

[14] Y. Shtessel, C. Edwards, L. Fridman, and A. Levant, "Conventional sliding mode observers," in *Sliding Mode Control and Observation*, ed: Springer, 2014, pp. 105-141.

[15] M. Arcak and P. Kokotovic, "Nonlinear observers: A circle criterion design," in *Decision and Control, 1999. Proceedings of the 38th IEEE Conference on*, 1999, pp. 4872-4876.

[16] G. Ciccarella, M. Dalla Mora, and A. Germani, "A Luenberger-like observer for nonlinear systems," *International Journal of Control,* vol. 57, pp. 537-556, 1993.

[17] F. Thau, "Observing the state of non-linear dynamic systems," *International journal of control,* vol. 17, pp. 471-479, 1973.

[18] H. K. Khalil and L. Praly, "High-gain observers in nonlinear feedback control," *International Journal of Robust and Nonlinear Control,* vol. 24, pp. 993-1015, 2014.

[19] M. O. Mustafa, "On Fault Detection, Diagnosis and Monitoring for Induction Motors," Luleå tekniska universitet, 2015.

[20] W. T. Thomson and M. Fenger, "Current signature analysis to detect induction motor faults," *IEEE Industry Applications Magazine*, vol. 7, pp. 26-34, 2001.

[21] A. Siddique, G. Yadava, and B. Singh, "A review of stator fault monitoring techniques of induction motors," *IEEE transactions on energy conversion,* vol. 20, pp. 106-114, 2005.

[22] A. M. Da Silva, "Induction motor fault diagnostic and monitoring methods," Marquette University, 2006.

[23] M. Hajiaghajani and S. Madani, "A new method for analysis of rotor broken bar fault in induction machines," in *Electric Machines and Drives, 2005 IEEE International Conference on*, 2005, pp. 1669-1674.

[24] Y. Han and Y. Song, "Condition monitoring techniques for electrical equipment: A literature survey," *IEEE power engineering review*, vol. 22, pp. 59-59, 2002.

[25] M. B. Gülmezoğlu and S. Ergin, "An approach for bearing fault detection in electrical motors," *European Transactions on Electrical Power*, vol. 17, pp. 628-641, 2007.

[26] M. Y. HAMMOUDI, "Contribution à la commande et à l'observation dans l'association convertisseurs machine," Université Mohamed Khider-Biskra, 2015.

Chapter 3:

Mean value theorem and T-S fuzzy approach for non-linear systems; design and stability analysis

3.1 Introduction

In order to avoid the drawbacks of the previous methods for control and observation of non-linear systems (mentioned in the last chapter), the MVT approach and PDC approach based T-S models are very interesting to do so. Both of the MVT and the T-S mathematical representation of nonlinear systems are introduced at the level of the model of the nonlinear system. They allow representing any nonlinear system, whatever its complexity, by a simple structure based on linear models interpolated by nonlinear functions positive or null and bounded for the T-S approach and a Mean model for the MVT approach. These models make it possible to accurately represent nonlinear systems. They have a simple structure with interesting properties making them easily exploitable from a mathematical point of view and allowing the extension of some results from the linear domain to nonlinear systems. The fuzzy model (T-S) proposed by [1, 2] where the MVT theory was proposed by [3]. In the following, the MVT approach for the case of non-linear systems and the continuous representation T-S will be discussed.

3.2 Mean value theorem

3.2.1 problem statement

This section presents an efficient methodology for designing observers for the class of nonlinear systems described by:

$$\begin{cases} \dot{x} = Ax + \varphi(x) + g(u,y) \\ y = Cx \end{cases} \tag{3.1}$$

where x is the state vector, u is the input vector and y is the output measurement vector. A *and* C are appropriate matrices. The functions $\varphi(x)$ and $g(u,y)$ are nonlinear. The function $\varphi(x)$ is assumed to be differentiable.

The observer will be assumed to be of the form

$$\dot{\hat{x}} = A\hat{x} + \varphi(\hat{x}) + g(u,y) + L(y - C\hat{x}) \tag{3.2}$$

The estimation error introductions are then seen to be given by

$$\dot{e} = (A - LC)e + (\varphi(x) - \varphi(\hat{x})) \tag{3.3}$$

Where $e = x - \hat{x}$ and L is the observer gain.

3.2.2 Mean value theorem for bounded Jacobian systems

In this sub-section, we present mathematical tools which are used subsequently to develop the observer gain in the next section. First, we present the scalar mean value theorem and the mean value theorem for vector functions. Then, we define the canonical basis for writing a vector function with a composition form. Lastly, we present a new modified form of the mean value theorem for vector functions.

Lemma 3.1: Scalar MVT

Let consider $f(x)$ be a function continuous on $[a,b]$ and differentiable on (a,b). There exist numbers $c \in (a,b)$ such as[4]:

$$f(a) - f(b) = \left.\frac{df}{dx}\right|_{x=c} \times (a - b) \tag{3.4}$$

The equation (3.4) can also be rewritten as

$$f(a) - f(b) = \left(\delta_1 \left.\frac{df}{dx}\right|_{x=c_1} + \delta_2 \left.\frac{df}{dx}\right|_{x=c_2}\right) \times (a - b) \qquad \delta_1, \delta_2 > 0, \quad \delta_1 + \delta_2 = 1 \tag{3.5}$$

Where $c_1, c_2 \in (a,b)$ and δ_1, δ_2 are parameters depend on the value of a and b.

The proof of Lemma 3.1 is presented in [5].

Lemma 3.2: MVT for a vector function[6]

Let consider $f(x)$ be a function continuous on $[a,b]$ and differentiable on the convex hull of a set (a,b) with a Lipchitz continuous gradient ∇f . There exist numbers $c \in (a,b)$ such as

$$f(a) - f(b) = \nabla f(c) \times (a-b) \tag{3.6}$$

However, we cannot directly use the mean value theorem of equation (3.6), since is a varying parameter that continuously changes with the values of a and b. Thus $\nabla f(c)$ is an unknown and changing matrix. We need to modify the mean value theorem before it can be utilized.

Lemma 3.3: canonical basis [3]

Let's define the vector function as

$$f(x) = \left[f_1(x), f_2(x), \dots, f_q(x)\right]^T \tag{3.7}$$

Where $f_i(x)$ is the i^{th} component of $f(x)$

The function $f(x)$ can be written as

$$f(x) = \sum_{i=1}^{q} e_q(i) f_i(x) \tag{3.8}$$

Where

$$e_q(i) = (0,\dots,0,1,0,\dots,0), \qquad i = 1,2,\dots,q \tag{3.9}$$

Now, we are ready to state and prove a modified form of the mean value theorem for a vector function.

Theorem 3.1: modified MVT for a vector function [6]

Let consider $f(x)$ be a function continuous on $[a,b]$ and differentiable on the convex hull of a set (a,b) with a Lipchitz continuous gradient ∇f . There exist ${\delta_{ij}}^{max}$ and ${\delta_{ij}}^{min}$ for $i,j = 1,2,\dots n$ such that:

$$f(a)-f(b)=\left[\left(\sum_{i,j=1}^{n,n} {Z_{ij}}^{max}{\delta_{ij}}^{max}\right)+\left(\sum_{i,j=1}^{n,n} {Z_{ij}}^{min}{\delta_{ij}}^{min}\right)\right](a-b) \tag{3.10}$$

Where

$${h_{ij}}^{max} \geq max\left(\frac{\partial f_i}{\partial x}\right) \; and \; {h_{ij}}^{min} \leq min\left(\frac{\partial f_i}{\partial x}\right) \; \forall x \in (a,b)$$

And

$${Z_{ij}}^{max} = e_n(i){e_n}^T(j){h_{ij}}^{max} \; and \; \; {Z_{ij}}^{min} = e_n(i){e_n}^T(j){h_{ij}}^{min}$$

Based on Lemma 3.2, we have

$$f(a)-f(b)=\nabla f(c)\times(a-b)=\begin{bmatrix} \frac{\partial f_1}{\partial x_1} & \frac{\partial f_1}{\partial x_2} & \cdots & \frac{\partial f_1}{\partial x_n} \\ \frac{\partial f_2}{\partial x_1} & \frac{\partial f_2}{\partial x_2} & \cdots & \frac{\partial f_2}{\partial x_n} \\ \vdots & \vdots & \ddots & \vdots \\ \frac{\partial f_n}{\partial x_1} & \frac{\partial f_n}{\partial x_2} & \cdots & \frac{\partial f_n}{\partial x_n} \end{bmatrix}[(a-b)] \tag{3.11}$$

Lemma 3.1 shows that each derivative function can be replaced with a convex combination of 2 values of the derivative of the function. Hence, the derivative function $\frac{\partial f_i(c)}{\partial x_j}$ can be replaced by

$$\begin{gathered} \frac{\partial f_i}{\partial x_j}(c)={\delta_{ij}}^{max}\frac{\partial f_i}{\partial x_j}(\gamma)+{\delta_{ij}}^{min}\frac{\partial f_i}{\partial x_j}(\varepsilon) \\ {\delta_{ij}}^{max},{\delta_{ij}}^{min}>0, \qquad {\delta_{ij}}^{max}+{\delta_{ij}}^{min}=1 \end{gathered} \tag{3.12}$$

Where

$$\gamma=(\gamma_1,\gamma_2,\dots,\gamma_n) \;\; and \;\; \varepsilon=(\varepsilon_1,\varepsilon_2,\dots,\varepsilon_n) \; with \; \gamma,\varepsilon \in (a,b)$$

The values of $\frac{\partial f_i}{\partial x_j}(\gamma)$ and $\frac{\partial f_i}{\partial x_j}(\varepsilon)$ need to be chosen as follows in order to satisfy lemma 1

$$\frac{\partial f_i}{\partial x_j}(\gamma) = {h_{ij}}^{max} \geq max\left(\frac{\partial f_i}{\partial x_j}\right), \qquad and \qquad \frac{\partial f_i}{\partial x_j}(\varepsilon) = {h_{ij}}^{min} \leq min\left(\frac{\partial f_i}{\partial x_j}\right) \tag{3.13}$$

Then the equation (3.12) can be rewritten as

$$\begin{gathered} \frac{\partial f_i}{\partial x_j}(c) = {\delta_{ij}}^{max} {h_{ij}}^{max} + {\delta_{ij}}^{min} {h_{ij}}^{min} \\ {\delta_{ij}}^{max}, {\delta_{ij}}^{min} > 0, \qquad {\delta_{ij}}^{max} + {\delta_{ij}}^{min} = 1 \end{gathered} \tag{3.14}$$

With ${\delta_{ij}}^{max}\ and\ {\delta_{ij}}^{min}$ are parameters that vary with the value of a and b. Subsequently, the equation (3.11) become as

$$\begin{aligned} f(a) - f(b) = & \begin{bmatrix} {\delta_{11}}^{max}{h_{11}}^{max} & {\delta_{12}}^{max}{h_{12}}^{max} & \dots & {\delta_{1n}}^{max}{h_{1n}}^{max} \\ {\delta_{21}}^{max}{h_{21}}^{max} & {\delta_{22}}^{max}{h_{22}}^{max} & \cdots & {\delta_{2n}}^{max}{h_{2n}}^{max} \\ \vdots & \vdots & \ddots & \vdots \\ {\delta_{n1}}^{max}{h_{n1}}^{max} & {\delta_{n2}}^{max}{h_{n2}}^{max} & \dots & {\delta_{nn}}^{max}{h_{nn}}^{max} \end{bmatrix} [(a-b)] \\ & + \begin{bmatrix} {\delta_{11}}^{min}{h_{11}}^{min} & {\delta_{12}}^{min}{h_{12}}^{min} & \dots & {\delta_{1n}}^{min}{h_{1n}}^{min} \\ {\delta_{21}}^{min}{h_{21}}^{min} & {\delta_{22}}^{min}{h_{22}}^{min} & \cdots & {\delta_{2n}}^{min}{h_{2n}}^{min} \\ \vdots & \vdots & \ddots & \vdots \\ {\delta_{n1}}^{min}{h_{n1}}^{min} & {\delta_{n2}}^{min}{h_{n2}}^{min} & \dots & {\delta_{nn}}^{min}{h_{nn}}^{min} \end{bmatrix} [(a-b)] \end{aligned} \tag{3.15}$$

Use the canonical basis from Lemma 3.3, then $f(a) - f(b)$ can be written as

$$f(a) - f(b) = \left[\left(\sum_{i,j=1}^{n,n} {Z_{ij}}^{max}{\delta_{ij}}^{max}\right) + \left(\sum_{i,j=1}^{n,n} {Z_{ij}}^{min}{\delta_{ij}}^{min}\right)\right](a-b) \tag{3.16}$$

Where ${Z_{ij}}^{max} = e_n(i){e_n}^T(j){h_{ij}}^{max}\ and\ {Z_{ij}}^{min} = e_n(i){e_n}^T(j){h_{ij}}^{min}$

${h_{ij}}^{max} \geq max\left(\frac{\partial f_i}{\partial x_j}\right)$ and ${h_{ij}}^{min} \leq min\left(\frac{\partial f_i}{\partial x_j}\right)$

The equation (3.16) can be modified as

$$f(a) - f(b) = \left(\sum_{r=1}^{r} {\delta_{ij}}^{r}\, \tilde{A}_i\right)(a-b) \tag{3.17}$$

With

$r = 1,2 \;\; {\delta_{ij}}^{1} = {\delta_{ij}}^{max} \;\; and \;\; {\delta_{ij}}^{2} = {\delta_{ij}}^{min}$

And

$$\tilde{A}_i = \sum_{i,j,r=1}^{n,n,r} {Z_{ij}}^{r}$$

$r = 1,2 \;\; {Z_{ij}}^{1} = {Z_{ij}}^{max} \;\; and \;\; {Z_{ij}}^{2} = {Z_{ij}}^{min}$

3.2.3 Non-linear observer

Based on the equation (3.17) the dynamics of the estimation error (3.3) can be expressed as

$$\dot{e} = (A - LC)e + \left(\sum_{r=1}^{2} {\delta_{ij}}^{r} \tilde{A}_i\right)(x - \hat{x}) \tag{3.18}$$

Then the dynamics of the estimation error can be expressed as follows

$$\dot{e} = (A - LC + \sum_{r=1}^{2} {\delta_{ij}}^{r} \tilde{A}_i)e \tag{3.19}$$

Due

$$\sum_{r=1}^{2} {\delta_{ij}}^{r} = {\delta_{ij}}^{max} + {\delta_{ij}}^{min} = 1$$

It's possible to rewrite the dynamics of the estimation error as the next final form

$$\dot{e} = \sum_{r=1}^{2} {\delta_{ij}}^{r} (A - LC + \tilde{A}_i)e \tag{3.20}$$

3.2.3.1 stability analysis

In this subsection, and in order to get the observer gain, the stability is studied by the Lyapunov quadratic function that's given as follows[7]

$$V(e(t)) = e^T(t)Pe(t) \tag{3.21}$$

The stability is checked when the derivative of the Lyapunov function (3.21) is lower than zero

$$\dot{V}(e(t)) \leq 0 \tag{3.22}$$

The state estimation error asymptotically converges to zero if there exists a matrix $P = P^T > 0$ such as the following LMI's be verified:

$$A^T P + PA + \tilde{A}_i^T P + P\tilde{A}_i - MC - M^T C^T + \tilde{\alpha}P < 0 \tag{3.23}$$

Where

$\tilde{\alpha}$ is a coefficient depend reversely on the response time of the estimation error

And $i = (1,2,\dots,2n)$

Then the observer gain can be easily gotten by solving the LMI's (3.23). the observer gain is calculated as

$$L = P^{-1}M \tag{3.24}$$

3.2.4 Non-linear controller

Approximately the same for the observer case, the tracking error introductions are then seen to be given by

$$\dot{e_c} = (A - BK)e_c + (\varphi(x) - \varphi(x_c)) \tag{3.25}$$

Where $e = x - x_c$ with x_c is the reference state and K is the controller gain.

By introducing the MVT approach mentioned above to $\varphi(x) - \varphi(x_c)$, the final form of the tracking error becomes as

$$\dot{e_c} = \sum_{r=1}^{2} {\delta_{ij}}^{r} (A - BK + \bar{\bar{A}}_i) e_c \tag{3.26}$$

3.2.4.1 stability analysis

In this subsection, and in order to get the controller gain, the stability is studied by the Lyapunov quadratic function that's given as follows[8, 9]

$$V(e(t)) = {e_c}^T(t) P e_c(t) \tag{3.27}$$

The stability is checked when the derivative of the Lyapunov function (3.27) is lower than zero

$$\dot{V}(e_c(t)) \leq 0 \tag{3.28}$$

The state estimation error asymptotically converges to zero if there exists a matrix $P = P^T > 0$ such as the following LMI's be verified:

$$AP + PA^T + \bar{\bar{A}}_i P + P{\bar{\bar{A}}_i}^T - BY - B^T Y^T + \alpha P < 0 \tag{3.29}$$

Where

α is coefficient depend reversely on the response time of the tracking error

And $i = (1,2, \dots, 2n)$

Then the controller gain can be easily gotten by solving the LMI's (3.29). the controller gain is calculated as

$$K = YP^{-1} \tag{3.30}$$

3.3 T-S fuzzy model

3.3.1 T-S representation

The T–S fuzzy model is described by fuzzy IF-THEN rules which represent local linear input-output relations of a nonlinear system. The main feature of this model is to express the local dynamics of each fuzzy implication (rule) by a linear system model. The overall fuzzy model of the system is achieved by the fuzzy blending of the linear system models[10].

consider the following non-linear system

$$\dot{x}(t) = f\big(x(t), u(t)\big) \tag{3.31}$$

Where f is a function. $x(t) = [x_1(t)\, x_2(t) \ldots\, x_n(t)\,]$ is the state vector and $u(t) = [u_1(t)\, u_2(t) \ldots\, u_n(t)\,]$is the input vector. Based on the sector nonlinearity concept [11], we can exactly represent the system (3.31) with the T-S fuzzy model (3.32)

Model rule *i*:

If $z_1(t)$ is F_{i1} and … and $z_p(t)$ is F_{ip} then

$$\dot{x}_i(t) = A_i x(t) + B_i u(t) \qquad i = 1,2, \ldots, n \tag{3.32}$$

Where $z_j(t)$ ($j = 1,2, \ldots, p$) is the premise variable. The membership function associated with the i^{th} Model rule and j^{th} premise variable component is denoted by F_{ij} . the n denotes the number of model rules. Each $z_j(t)$ is a measurable time-varying quantity that may be states, measurable external variables and/or time. The defuzzification process of the model (3.32) can be represented as [11]:

$$\dot{x}(t) = \sum_{i=1}^{n} \mu_i(z(t)) \big(A_i x(t) + B_i u(t)\big) \qquad i = 1,2, \ldots, n \tag{3.33}$$

Where

$z(t) = \big[z_1(t)\, z_2(t) \ldots z_p(t)\big]$

And

$$\sum_{i=1}^{n} \mu_i(z(t)) = \frac{h_i\big(z(t)\big)}{\sum_{i=1}^{n} h_i\big(z(t)\big)}$$

$$h_i(z(t)) = \prod_{j=1}^{p} F_{ij}\left(z_j(t)\right)$$

It should be noted from the properties of membership functions that the following relations hold.

$$\sum_{i=1}^{n} h_i(z(t)) > 0, \quad h_i(z(t)) \geq 0, \quad i = 1,2, \dots n$$

Hence

$$\sum_{i=1}^{n} \mu_i(z(t)) = \frac{h_i(z(t))}{\sum_{i=1}^{n} h_i(z(t))} \geq 0 \qquad \sum_{i=1}^{n} \mu_i(z(t)) = 1$$

In T-S modeling, we often find the terms: premises variables, membership functions, areas of operation and defuzzification. These are specified by the following definitions:

- **Premises variables:** noted $z(t)$. Known and accessible quantities allow evaluation of membership functions. They may depend on the measurable state variables and / or the command

- **Membership functions:** noted $h_i(z(t))$. they are nonlinear functions depending on the premises variables associated with the different zones of operation. They make it possible to translate the contribution of a local model LTI corresponding to an operating point with respect to the operating zone of the system. Thus, they ensure the gradual transition from a local LTI model to neighboring local models.

- **Areas of operation:** represented by domains l_i obtained via the decomposition of the operating space of the system l. With $l = \cup_i l_i$.

- **Defuzzification:** defuzzification transforms the fuzzy output set into a numeric value. Defuzzification is an art more than science in such a way that one never finds a systematic

method to choose a defuzzification strategy, except simplicity. The best-known methods are Method of maximum, average maxima method, the center of gravity method,…

3.3.2 Getting T-S model

Various approaches can be used to get the fuzzy T-S model as the direct method of obtaining through the knowledge model[12], get the fuzzy model by identification method[1, 2] and by the linearization around various operation points[13].

In this work, we will talk about another approach for the getting of the fuzzy T-S model of non-linear systems that is named " Sector non-linearity approach".

- **Sector non-linearity approach**

This method guarantees the construction of a T-S model representing exactly the nonlinear model on a compact space of the state variables. Note that the sector non-linearity approach allows associating an infinite number of T-S models for a nonlinear system according to the division of the nonlinearities realized. A systematic approach is based on the following lemma:

Lemma 3.4 [14]:

Either $f(x(t))$ is a bounded function, so there are always two function $\gamma_1(x(t))$ and $\gamma_2(x(t))$ and also two scalars α and β such as:

$$f\big(x(t)\big) = \alpha \times \gamma_1\big(x(t)\big) + \beta \times \gamma_2(x(t)) \tag{3.34}$$

Where

$\gamma_1\big(x(t)\big) + \gamma_2\big(x(t)\big) = 1$ and $\gamma_1\big(x(t)\big), \gamma_2(x(t)) > 0$

- **Proof**

Under the consideration of the function $f\big(x(t)\big)$ is bounded such as $\alpha \leq f\big(x(t)\big) \geq \beta$, then it's possible to write the nonlinear function as indicated previously in (3.34) with

$\alpha \leq \min\left(f(x(t))\right)$ and $\beta \geq \max\left(f(x(t))\right)$,

$$\gamma_1(x(t)) = \frac{f(x(t)) - \alpha}{\beta - \alpha} \; and \; \gamma_2(x(t)) = \frac{\beta - f(x(t))}{\beta - \alpha}$$

In this case, the T-S model (3.34) represent exactly the nonlinear system and there are 2^n Fuzzy rules, with n representing the number of non-linearities of the real system.

3.3.3 Study of the stability of the T-S model

The simple structure of T-S models as interpolation of linear models local, allowed the researchers to exploit it in the analysis of the stability and the stabilization of nonlinear systems in all their complexities. Often the study of stability and stabilization uses Lyapunov's theory, including the second method. Stability properties can then be deduced by solving a set of LMI's[15]. If they prove to admit a solution, can be solved using tools from the field of convex optimization. In this section, we present a brief review of some approaches for studying the stability of T-S models and the synthesis of control laws. These approaches include the quadratic approach of Lyapunov, and LMI approaches.

3.3.3.1 Stability based Lyapunov approach

This class of function plays a very important role in the study of the stability and stabilization of the controllers and/or observers [13, 16, 17], and which will be used in this thesis, and it is of the form:

$$V(x) = x^T P x \tag{3.35}$$

With $P = P^T$

The principle of stability according to Lyapunov based on the behavior of the dynamic system from the perspective of its total energy. This energy is generally represented by a function $V(x(t))$ of the state x of the system. The sign of this function and its time derivative in a certain neighborhood of the equilibrium point gives information on the stability of the system. The stability theory of Lyapunov uses many concepts (for more details, see [11]). The main result shows that for a continuous time autonomous system $\dot{x} = f(x(t))$; the origin is a globally

asymptotically stable equilibrium point, if there is a positive function satisfying the following conditions:

$$\begin{cases} V(x(t)) > 0 \\ \dot{V}(x(t)) < 0 \\ V(0) = 0, \ V(\infty) \to \infty \end{cases} \tag{3.36}$$

- **Quadratic stability**

The approach proposed in this section is based on the quadratic Lyapunov functions defined by (3.35). This is to look for a Lyapunov function such that stability conditions (continuous system) are checked.

The T-S model in open loop is presented as follows:

$$\dot{x}(t) = \sum_{i=1}^{n} \mu_i(z(t)) \left(A_i x(t)\right) \tag{3.37}$$

The stability of the T-S model was firstly given by [16]

Theorem 3.2: (for continues case) [16]

The equilibrium of the T-S model (3.36) is asymptotically stable if there is a matrix $P = P^T > 0$ such as:

$$A_i{}^T P + P A_i < 0 \tag{3.38}$$

- **proof**

$$\dot{V}(x(t)) = \dot{x}^T(t)Px(t) + x^T(t)P\dot{x}(t) = x^T(t)\left[\sum_{i=1}^{n} \mu_i\big(z(t)\big)\left(A_i{}^T P + P A_i\right)\right]x(t)$$

$So \quad \dot{V}(x(t)) < 0 \qquad if \qquad A_i{}^T P + P A_i < 0$

3.3.4 Stabilization of T-S models

One of the first ideas for stabilizing these models is to use linear state returns. These have quickly been supplanted by a control law that allows taking into account the nonlinearities of fuzzy models known as PDC (Parallel Distributed Compensation)[18].

3.3.4.1 PDC concept

This concept uses a linear control law for each sub-model. The result is nonlinear in general. The idea is to create a compensator for each rule of the fuzzy model. The procedure is as follows:

- ✓ Fuzzy T-S representation of the controlled system
- ✓ Each control rule is designed from the previously defined fuzzy model rule.
- ✓ A control gain by state feedback constitutes the conclusion part of each fuzzy sub-model such that the control is as:

$$u(t) = \sum_{j=1}^{n} \mu_j\big(z(t)\big) K_j x(t)$$

Now, based on the PDC concept, it's possible to rewrite the system (3.31) as follows:

$$\dot{x}(t) = \sum_{i=1}^{n}\sum_{j=1}^{n} \mu_i(z(t))\mu_j(z(t))\big(A_i - B_i K_j\big)x(t) \tag{3.39}$$

We define

$G_{ij} = A_i - B_i K_j$

Then

$$\begin{aligned}\dot{x}(t) = \sum_{i=1}^{n}\sum_{j=1}^{n} \mu_i\big(z(t)\big)\mu_j\big(z(t)\big)\big(G_{ij}\big)x(t) \\ + 2\sum_{i=1}^{n}\sum_{j=1}^{n} \mu_i\big(z(t)\big)\mu_j\big(z(t)\big)\left(\frac{G_{ij}+G_{ji}}{2}\right)x(t) +\end{aligned} \tag{3.40}$$

Theorem 3.3: (Continues case)[12]

The equilibrium of the T-S model is asymptotically stable if there is a matrix $P = P^T$ and K_j such as:

$$G_{ii}{}^T P + P G_{ii} < 0 \tag{3.41}$$
$$\left(\frac{G_{ij} + G_{ji}}{2}\right)^T P + P\left(\frac{G_{ij} + G_{ji}}{2}\right) < 0$$

With

$\mu_i(z(t))\mu_j(z(t)) = 0$ and $G_{ij} = A_i - B_i K_j$

3.4 Conclusion

In this chapter, we have presented the MVT concept and the approach based on the T-S representation (PDC) in order to design the controllers and the observers for the class of the non-linear systems.

Based on the MVT concept, the design of controllers or the observers are so simple due to the unique gain of each of them and also have and also the MVT approach has a proven and a systematic methodology in order to prove the stability of non-linear systems. The PDC approach allows to get the controller and the observer gains with a methodical way and the stability is proven through the Lyapunov function.

The topic of the next chapter will the design, the simulation tests and the experimental trials of controllers and observers based on the MVT approach applied to the IM, whereas the PDC approach based on the T-S model will be designed for the FTC of the IM in the fifth chapter.

References

[1] T. Takagi and M. Sugeno, "Fuzzy identification of systems and its applications to modeling and control," *IEEE transactions on systems, man, and cybernetics*, pp. 116-132, 1985.

[2] M. Sugeno and G. Kang, "Structure identification of fuzzy model," *Fuzzy sets and systems*, vol. 28, pp. 15-33, 1988.

[3] A. Zemouche, M. Boutayeb, and G. I. Bara, "Observer Design for Nonlinear Systems: An Approach Based on the Differential Mean Value Theorem," in *Decision and Control, 2005 and 2005 European Control Conference. CDC-ECC'05. 44th IEEE Conference on*, 2005, pp. 6353-6358.

[4] O. Zeghib, A. Allag, M. Allag, and B. Hamidani, "A robust extended H∞ observer based on the mean value theorem designed for induction motor drives," *International Journal of System Assurance Engineering and Management*, February 08 2019.

[5] P. Sahoo and T. Riedel, *Mean value theorems and functional equations*: World Scientific, 1998.

[6] G. Phanomchoeng, "State, parameter, and unknown input estimation problems in active automotive safety applications," 2011.

[7] O. Zeghib, A. Allag, M. Allag, and B. Hamidani, "An Extended MVT Observer Designed for Induction Motor Drive," *Mediterranean Journal of Measurement and Control*, vol. 13, pp. 805-811, 2017.

[8] A. Allag, A. Benakcha, M. Allag, I. Zein, and M. Y. Ayad, "Classical state feedback controller for nonlinear systems using mean value theorem: closed loop-FOC of PMSM motor application," *Frontiers in Energy*, vol. 9, pp. 413-425, 2015.

[9] M. Allag, A. Allag, A. Abrar, I. Zein, and M. Ayad, "Controller Design for Nonlinear Systems using Takagi Sugeno Model: Closed Loop-FOC of IM Motor Application," *Journal of Electrical Engineering and Electronic Technology*, vol. 2016, 2017.

[10] K. Tanaka and H. O. Wang, *Fuzzy control systems design and analysis: a linear matrix inequality approach*: John Wiley & Sons, 2004.

[11] K. Tanaka, H. Ohtake, and H. O. Wang, "A descriptor system approach to fuzzy control system design via fuzzy Lyapunov functions," *IEEE Transactions on Fuzzy Systems*, vol. 15, pp. 333-341, 2007.

[12] K. Tanaka, T. Ikeda, and H. O. Wang, "Fuzzy regulators and fuzzy observers: relaxed stability conditions and LMI-based designs," *IEEE Transactions on fuzzy systems,* vol. 6, pp. 250-265, 1998.

[13] H. O. Wang, K. Tanaka, and M. Griffin, "Parallel distributed compensation of nonlinear systems by Takagi-Sugeno fuzzy model," in *Fuzzy Systems, 1995. International Joint Conference of the Fourth IEEE International Conference on Fuzzy Systems and The Second International Fuzzy Engineering Symposium., Proceedings of 1995 IEEE Int*, 1995, pp. 531-538.

[14] Y. Morère, "Mise en oeuvre de lois de commande pour les modèles flous de type Takagi-Sugeno," Valenciennes, 2001.

[15] S. Boyd, L. El Ghaoui, E. Feron, and V. Balakrishnan, *Linear matrix inequalities in system and control theory* vol. 15: Siam, 1994.

[16] K. Tanaka and M. Sugeno, "Stability analysis and design of fuzzy control systems," *Fuzzy sets and systems,* vol. 45, pp. 135-156, 1992.

[17] J. Yoneyama, M. Nishikawa, H. Katayama, and A. Ichikawa, "Output stabilization of Takagi–Sugeno fuzzy systems," *Fuzzy sets and Systems,* vol. 111, pp. 253-266, 2000.

[18] K. Tanaka, T. Hori, and H. O. Wang, "A fuzzy Lyapunov approach to fuzzy control system design," in *American Control Conference, 2001. Proceedings of the 2001*, 2001, pp. 4790-4795.

Chapter 4:

Control and states estimation of the induction motor based on the MVT theory

4.1 Introduction:

IM's are widely utilized in industrial motion systems, for their reliability, simple construction and jagged design, low operating costs, direct connection to the power supply, long lifespan and premium energy efficiency[1, 2].

In the current chapter, we will present the T-S form, of the IM, the design of the FTC approach based on the T-S fuzzy model of the IM and the simulation results and discussion and it's ended by a conclusion

4.2. IM machine modeling:

4.2.1. Three phase IM presentation:

The IM's are constructed from the stator which is connected to the power source and the rotor that spins inside the stator within a precisely engineered air gap. Currents are induced into the rotor via the air gap from the stator side. The stator and the rotor are made of highly magnetizable core sheet providing low eddy current and hysteresis losses[3]. Figure 4.1 shows an exploded view of a typical IM.

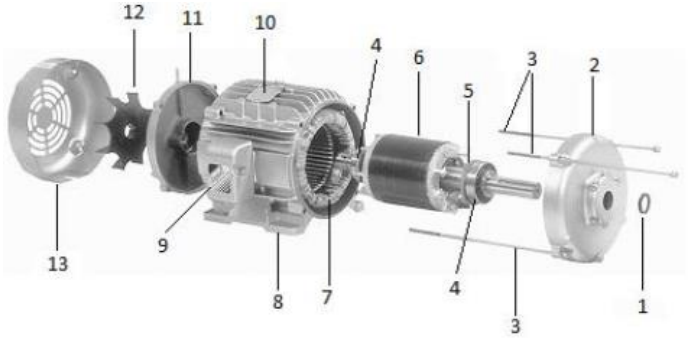

Item	Description	item	description	item	description
1	Shaft sealing ring	5	Spring washer	10	Rating plate
2	End shield	6	Rotor, complete	11	End Child
3	Assembly screws	7	Stator, complete	12	Cooling fan
4	Rolling-contact bearing	8	Housing foot	13	Cooling fan cover
		9	Terminal box, complete		

Figure 4.1 An enlarged view of typical IM[2]

- **The stator:**

The stator core is usually made of a doughnut-shaped stack of thin steel laminations with insulated slots. Slots are opening to the inside diameter holding the stator coils (windings) and held together by suitable means. Each core lamination is separated from the other. The teeth are separating the slots and carry the magnetic flux from the stator windings to the rotor through the air gap[2], figure 4.2(a) shows the stator core slots.

Stator windings are made from insulated copper wires embedded in the slots. A number of the identical array of uniform coils are twisted around each stator tooth. Coils are connected together to form the three-phase windings, circulated around the stator, and symmetrically located with respect to one another[2].

Currents in the stator windings are supposed of equal amplitude but differ in phase by one-third of a cycle ($^{2\pi}/_{3}$) forming a balanced three-phase set. As current flows through the coil on the first tooth, it creates a magnetic field of polarity that opposes the polarity of the opposite tooth, as shown in figure 4.2(b) [4].

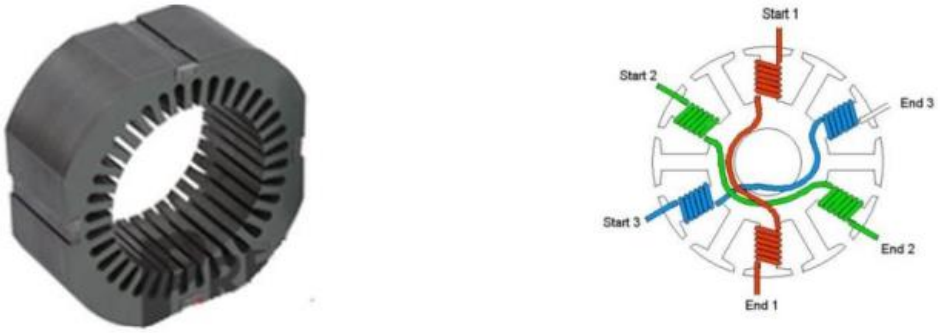

a) Stator core slots b) Windings distributions in stator slots

Figure 4.2 Stator slots and windings[5]

- **The rotor:**

The rotor is constructed of the shaft and cage conductors, as shown in Figure 4.3. The rotor shaft is made up of a cylindrical cast iron core. The squirrel cage rotor windings consist of a number of heavy, straight and embedded copper or cast aluminum bars, regularly circulated about the periphery, and connected at both ends by end rings. The slots accommodate the rotor conductors and are skewed to minimize torque pulsations. Blades are attached to the end rings to function as a cooling fan[4].

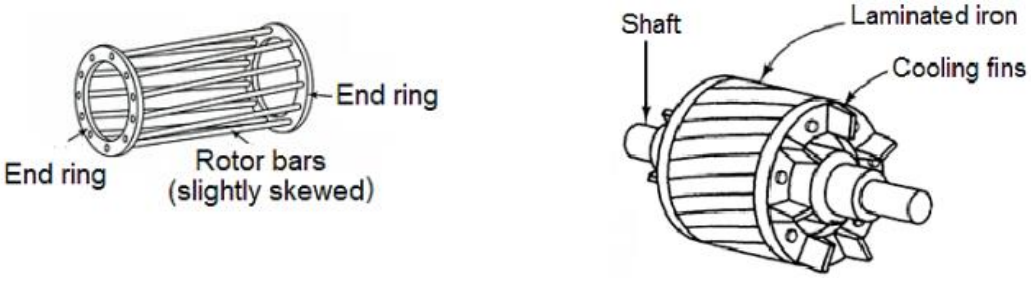

a) Cage construction b) assembled

Figure 4.3 Squirrel cage rotor[6]

4.2.2. The equivalent circuit of the IM drive:

Due to the similarity, in the steady-state case, the three-phase IM is generally represented in the same way as a three-phase transformer. The stator windings represent the primary windings and the rotor windings represent the secondary windings. The stator and rotor iron transfer the flux

between them acting as a core in the transformer [5]. Figure 4.4 presents the one phase equivalent circuit of the three-phase IM.

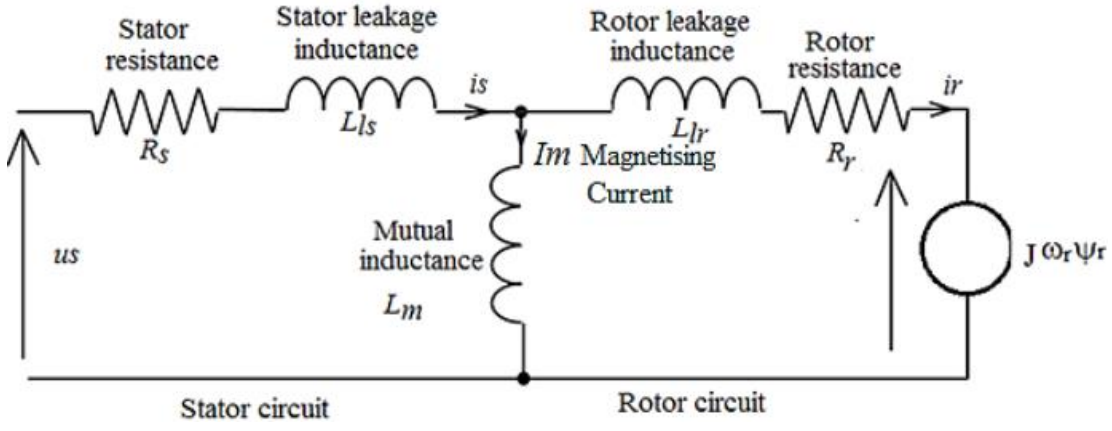

Figure 4.4 Per-phase IM equivalent circuit [2]

4.2.3. Study of the electromechanical equations:

4.2.3.1 Electrical equations:

The electrical equations of the IM can be divided into two terms linked with stator and rotor circuits, the equations (4.1) present the stator and the rotor electrical equations:

$$\begin{cases} [V_s] = [R_s] \times [I_s] + \dfrac{d[\emptyset_s]}{dt} \Big\}_{stator} \\ [V_r] = 0 = [R_r] \times [I_r] + \dfrac{d[\emptyset_r]}{dt} \Big\}_{rotor} \end{cases} \tag{4.1}$$

Where

$$[V_{s,r}] = \begin{bmatrix} V_{s,r\,A} \\ V_{s,r\,B} \\ V_{s,r\,C} \end{bmatrix}, [I_{s,r}] = \begin{bmatrix} I_{s,r\,A} \\ I_{s,r\,B} \\ I_{s,r\,C} \end{bmatrix}, [\emptyset_{s,r}] = \begin{bmatrix} \emptyset_{s,r\,A} \\ \emptyset_{s,r\,B} \\ \emptyset_{s,r\,C} \end{bmatrix}, [R_{s,r}] = \begin{bmatrix} R_{s,r} & 0 & 0 \\ 0 & R_{s,r} & 0 \\ 0 & 0 & R_{s,r} \end{bmatrix}$$

4.2.3.2 Magnetic equations:

The magnetic equations of the IM drive are related to the stator and the rotor parts, and can be presented as the following matrix form[7]:

$$\begin{cases}[\emptyset_s] = [L_{ss}] \times [I_s] + M_{sr}[R(\theta_r)] \times [I_r]\}_{stator} \\ [\emptyset_r] = [L_{rr}] \times [I_r] + M_{sr}[R(\theta_r)] \times [I_s]\}_{rotor}\end{cases} \quad (4.2)$$

With:

$$[L_{ss}] = \begin{bmatrix} L_s & M_s & M_s \\ M_s & L_s & M_s \\ M_s & M_s & L_s \end{bmatrix}, [L_{rr}] = \begin{bmatrix} L_r & M_r & M_r \\ M_r & L_r & M_r \\ M_r & M_r & L_r \end{bmatrix},$$

And

$$[R(\theta_r)] = \begin{bmatrix} \cos(\theta_r) & \cos(\theta_r + {}^{2\pi}/_{3}) & \cos(\theta_r + {}^{4\pi}/_{3}) \\ \cos(\theta_r + {}^{4\pi}/_{3}) & \cos(\theta_r) & \cos(\theta_r + {}^{2\pi}/_{3}) \\ \cos(\theta_r + {}^{2\pi}/_{3}) & \cos(\theta_r + {}^{4\pi}/_{3}) & \cos(\theta_r) \end{bmatrix}$$

Where:

L_s, L_r: are the stator and rotor proper inductance of one phase respectively.

M_s, M_r: are the stator and the rotor mutual inductance between two phases respectively.

M_{sr}: represent the maximum mutual inductance between a one stator phase and the rotor phase.

4.2.3.3 Mechanical equation of the IM drive:

The next equation illustrates the mechanical operation of the IM which is depended on the rotor speed an torque as indicated as follows:

$$J\frac{d\omega_r}{dt} = T_{em} - b\omega_r - T_L \quad (4.3)$$

Where:

ω_r: is the rotor speed, where its unity is $\left[{}^{rad}/_{sec}\right]$.

b: is the friction coefficient.

T_{em}, T_L: is the electromagnetic torque (depend on the stator and rotor currents) and load torque respectively.

The model of the IM obtained has the disadvantage of being relatively complex insofar as the matrices contain variable elements as a function of the rotation angle θ_r.

To remedy the previously disadvantage, the IM model in two axes rotating frame make sure to do so based on the application of a mathematical tool known as the Park Transformation.

4.2.4. Vector model in two axes rotating frame:

4.2.4.1. The Park transformation:

The park transformation allows to transfer a three-phase system (a,b,c) to another three-phase system (d,q,o), where its third component is null if we consider the (a,b,c) system is balanced, the figure 4.5 shows the passage using the park transformation from (a,b,c) to (d,q,o) axes:

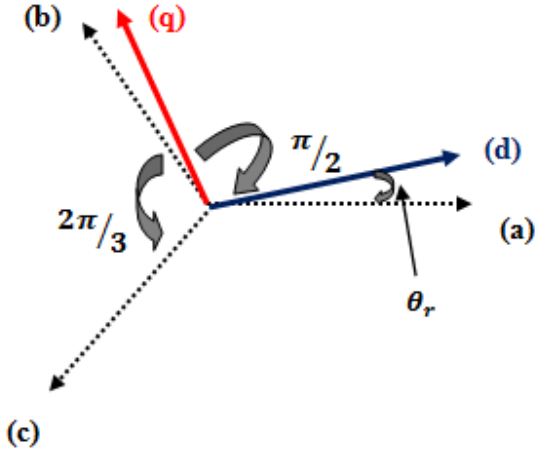

Figure 4.5 Park transformation axes

4.2.4.2. The Park transformation matrices:

The passage and the inverse passage from a three axes system (a,b,c) to two axes system in the rotating frame (d,q,o) need necessary to use the next matrices $P(\theta_r)$ and $P^{-1}(\theta_r)$ respectively.

$$[P(\theta_r)] = \frac{\sqrt{2}}{\sqrt{3}}\begin{bmatrix} \cos(\theta_r) & \cos(\theta_r - {}^{2\pi}/_{3}) & \cos(\theta_r - {}^{4\pi}/_{3}) \\ -\sin(\theta_r) & -\sin(\theta_r - {}^{2\pi}/_{3}) & -\sin(\theta_r - {}^{4\pi}/_{3}) \\ {}^{1}/_{\sqrt{2}} & {}^{1}/_{\sqrt{2}} & {}^{1}/_{\sqrt{2}} \end{bmatrix} \quad (4.4)$$

$$[P^{-1}(\theta_r)] = \frac{\sqrt{2}}{\sqrt{3}}\begin{bmatrix} \cos(\theta_r) & -\sin(\theta_r) & {}^{1}/_{\sqrt{2}} \\ \cos(\theta_r - {}^{2\pi}/_{3}) & -\sin(\theta_r - {}^{2\pi}/_{3}) & {}^{1}/_{\sqrt{2}} \\ \cos(\theta_r - {}^{4\pi}/_{3}) & -\sin(\theta_r - {}^{4\pi}/_{3}) & {}^{1}/_{\sqrt{2}} \end{bmatrix} \quad (4.5)$$

The application of the park transformation to (4.1), (4.2) and (4.3) allows to get the followings equations [7]:

$$\begin{cases} \left.\begin{aligned} U_{sd} &= R_s i_{sd} + \frac{d\emptyset_{sd}}{dt} \\ U_{sq} &= R_s i_{sq} + \frac{d\emptyset_{sq}}{dt} \end{aligned}\right\}_{\boldsymbol{stator}} \\ \left.\begin{aligned} 0 &= R_r i_{rd} + \frac{d\emptyset_{rd}}{dt} + \omega_r \emptyset_{rq} \\ 0 &= R_r i_{rq} + \frac{d\emptyset_{rq}}{dt} + \omega_r \emptyset_{rd} \end{aligned}\right\}_{\boldsymbol{rotor}} \end{cases} \quad (4.6)$$

And

$$\begin{cases} \left.\begin{aligned} \emptyset_{sd} &= L_s i_{sd} + M i_{rd} \\ \emptyset_{sq} &= L_s i_{sq} + M i_{rq} \end{aligned}\right\}_{\boldsymbol{stator}} \\ \left.\begin{aligned} \emptyset_{rd} &= L_r i_{rd} + M i_{sd} \\ \emptyset_{rq} &= L_r i_{rq} + M i_{sq} \end{aligned}\right\}_{\boldsymbol{rotor}} \end{cases} \quad (4.7)$$

And the mechanic equation of the IM becomes as:

$$J\frac{d\omega_r}{dt} = T_{em} - b\omega_r - T_L \quad (4.8)$$

Whereas:

$$T_{em} = n_p \frac{M}{L_r}\left(\emptyset_{rd} i_{sq} - \emptyset_{rq} i_{sd}\right)$$

4.2.4.3. State space form of the IM

From equations (4.6) and (4.7) it's possible to rewrite the IM model in the state space form where the stator currents (i_{sd} and i_{sq}), the rotor fluxes ($\emptyset_{rd}$ and $\emptyset_{rq}$) and the rotor speed (ω_r) are considered as the state variables . with $x(t)$ is the state vector, $u(t)$ is the input vector and $y(t)$ is the output vector, the state model of the IM can be represented as:

$$\begin{cases} \dot{x}(t) = f(x(t)) + Bu(t) + v(t) \\ y(t) = Cx(t) \end{cases} \tag{4.9}$$

Where:

$$f(x(t)) = \begin{bmatrix} -\gamma i_{sd} + \omega_s i_{sq} + \dfrac{k_s}{\tau_r}\emptyset_{rd} + k_s n_p \omega_r \emptyset_{rq} \\ -\omega_s i_{sd} - \gamma i_{sq} - k_s n_p \omega_r \emptyset_{rd} + \dfrac{k_s}{\tau_r}\emptyset_{rq} \\ \dfrac{M}{\tau_r} i_{sd} - \dfrac{1}{\tau_r}\emptyset_{rd} + \left(\omega_s - n_p \omega_r\right)\emptyset_{rq} \\ \dfrac{M}{\tau_r} i_{sq} - \left(\omega_s - n_p \omega_r\right)\emptyset_{rd} - \dfrac{1}{\tau_r}\emptyset_{rq} \\ \dfrac{n_p M}{J L_r}\left(\emptyset_{rd} i_{sq} - \emptyset_{rq} i_{sd}\right) - \dfrac{b}{J}\omega_r \end{bmatrix} \tag{4.10}$$

With

$$\gamma = \left(\frac{1}{\sigma\tau_s} + \frac{1-\sigma}{\sigma\tau_r}\right), \quad k_s = \frac{M}{\sigma L_s L_r}, \qquad \tau_r = \frac{L_r}{R_r}, \quad \tau_s = \frac{L_s}{R_s}, \quad \sigma = 1 - \frac{M^2}{L_s L_r},$$

And

$$x(t) = [i_{sd} \quad i_{sq} \quad \emptyset_{rd} \quad \emptyset_{rq} \quad \omega_r]^T$$

$$B = \begin{bmatrix} \dfrac{1}{\sigma Ls} & 0 & 0 & 0 & 0 \\ 0 & \dfrac{1}{\sigma Ls} & 0 & 0 & 0 \end{bmatrix}^T$$

$$u(t) = \begin{bmatrix} U_{sd} \\ U_{sq} \end{bmatrix}$$

$$v(t) = \begin{bmatrix} 0 & 0 & 0 & 0 & -\frac{1}{J} T_L \end{bmatrix}^T$$

$$C = \begin{bmatrix} 1 & 0 & 0 & 0 & 0 \\ 0 & 1 & 0 & 0 & 0 \end{bmatrix}$$

4.3. References generator and Open Loop FOC:

The desired states of the IM are obtained taking in consideration the FOC conditions, where the importance of the FOC theory is to make the coupled and the nonlinear system of IM behave as a direct current (DC) machine with a constant flux; this is through the proportionality between the torque and the q-axis stator current (i_{sq}).

4.3.1 References generator:

In this part, the reference states are obtained by the exploitation of the FOC strategy by considering the rotor flux is aligned to the d-axis as the next equation indicates:

$$\begin{cases} \emptyset_{rd} = \emptyset_r \\ \emptyset_{rq} = 0 \end{cases} \tag{4.11}$$

The substitution of the states of the system (4.9) by the desired states: $[i_{sdr} \quad i_{sqr} \quad \emptyset_r \quad 0 \quad \omega_{rr}]^T$ in it make sure to have references under the FOC conditions[8], we obtain:

$$\begin{bmatrix} \dot{i}_{sdr} \\ \dot{i}_{sqr} \\ \dot{\emptyset}_r \\ 0 \\ \dot{\omega}_{rr} \end{bmatrix} = \begin{bmatrix} -\gamma i_{sdr} + \omega_{sr} i_{sqr} + \frac{k_s}{\tau_r} \emptyset_r + \frac{1}{\sigma Ls} U_{sdr} \\ -\omega_{sr} i_{sdr} - \gamma i_{sqr} - k_s n_p \omega_{rr} \emptyset_r + \frac{1}{\sigma Ls} U_{sqr} \\ \frac{M}{\tau_r} i_{sdr} - \frac{1}{\tau_r} \emptyset_r \\ \frac{M}{\tau_r} i_{sqr} - (\omega_{sr} - n_p \omega_{rr}) \emptyset_r \\ \frac{n_p M}{J L_r} (\emptyset_r \, i_{sqr}) - \frac{b}{J} \omega_{rr} - \frac{1}{J} T_L \end{bmatrix} \tag{4.12}$$

Where:

$$\omega_{sr} = \frac{M}{\tau_r \emptyset_r} i_{sqr} + n_p \omega_{rr}$$

The reference of the q-axis rotor flux is chosen 0, while the desired of d-axis rotor flux is taken the same as the rated rotor flux, whereas the reference of the rotor speed is chosen as we like. Through the third and the last equations of the system (4.12), the reference states of the d and q-axis stator currents (i_{sdr}, i_{sqr}) are :

$$\begin{cases} i_{sdr} = \frac{\tau_r}{M}\left(\dot{\emptyset}_r + \frac{1}{\tau_r}\emptyset_r\right) \\ i_{sqr} = \frac{L_r}{\emptyset_r n_p M}\left(J\dot{\omega}_{rr} + b\omega_{rr} + T_L\right) \end{cases} \quad (4.13)$$

4.3.2 Open Loop FOC:

From the first two equations of (4.12) and using (4.13), the formula of the open loop FOC of the IM drive is obtained as follows[9]:

$$\begin{cases} U_{sdr} = \sigma Ls\left(\dot{i_{sdr}} + \gamma i_{sdr} - \omega_{sr} i_{sqr} - \frac{k_s}{\tau_r}\emptyset_r\right) \\ U_{sqr} = \sigma Ls\left(\dot{i_{sqr}} + \gamma i_{sqr} + \omega_{sr} i_{sdr} + k_s n_p \omega_{rr}\emptyset_r\right) \end{cases} \quad (4.14)$$

Although the simplicity of the open loop FOC that clear from the (4.14), it is possible to base on it in industrial applications. To prove the effectiveness of this approach, simulation results are mentioned in the next subsection.

- ✓ **Simulation results for open loop FOC:**

The simulation results for open loop FOC (OL-FOC) is obtained through the MATLAB/Simulink environment to the IM drive. The parameters of the used IM are mentioned in Appendix A.

The reference of the rotor speed is chosen as 50, 100 and 200 rad/sec, respectively. Where the rotor flux, the d-axis was 0.4 Wb and the q-axis was 0 Wb in all simulation time. The references of the stator currents are taken as the equation (4.13).

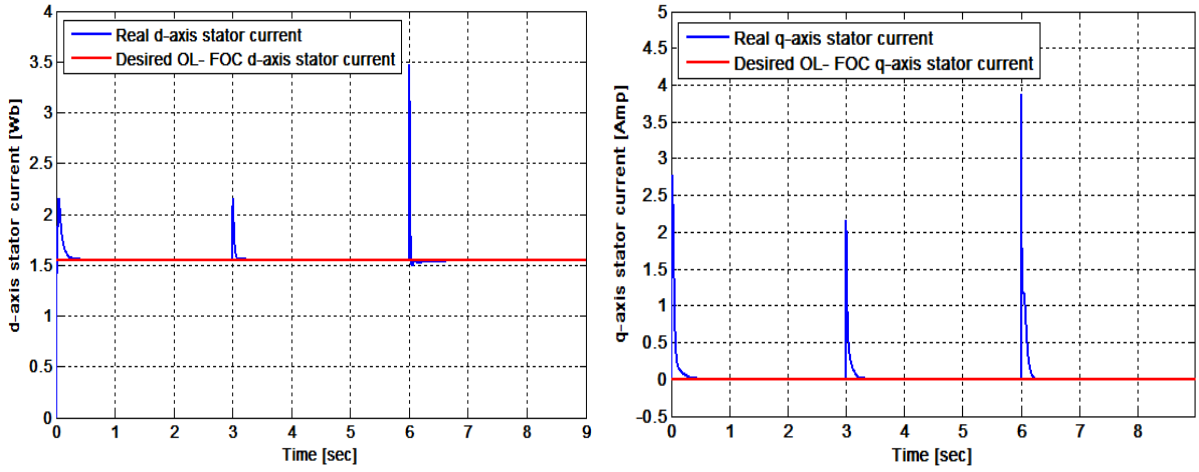

a) **b)**

Figure 4.6 The real d and q-axis stator currents and the their open loop references

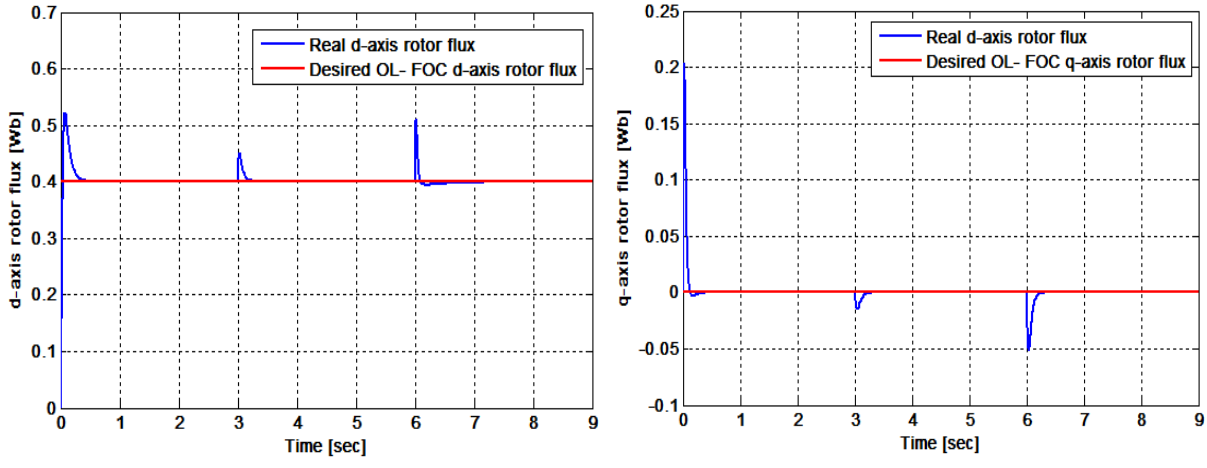

a) **b)**

Figure 4.7 The real d and q-axis rotor fluxes and the their open loop references

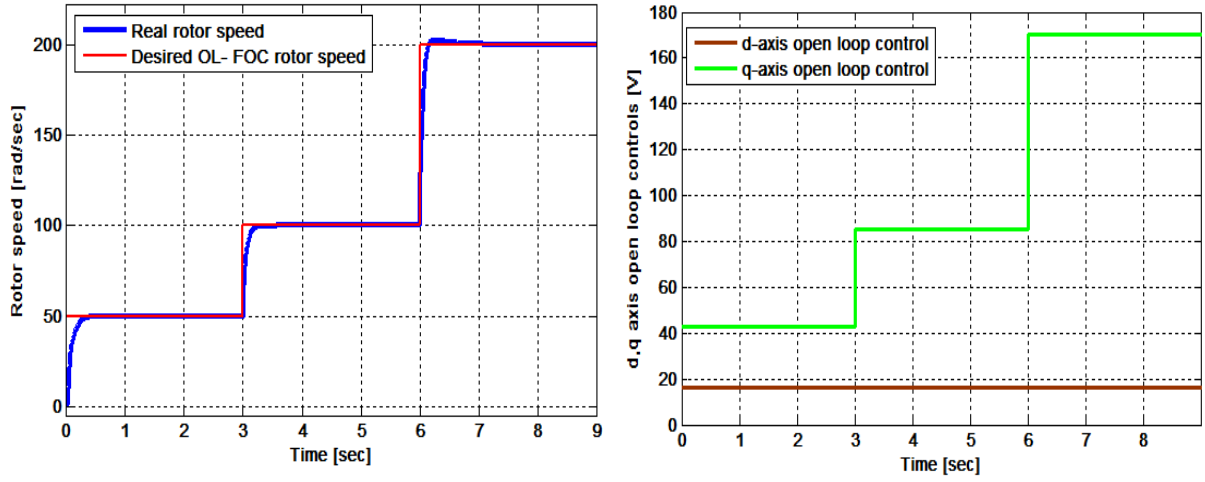

a) **b)**

Figure 4.8 The real rotor speed (a) and the open loop controls (b)

4.4 Control and states estimation of the IM based on the MVT theory

4.4.1 MVT controllers and observers design

4.4.1.1 Extended MVT observer for the load torque and the rotor position estimation:

The extended model chosen contains the usual dynamic model of the IM in the two axes rotating frame (4.9) and moreover the load torque and the rotor position in order to estimate them as chosen in[10]:

$$\begin{cases} \dot{x}(t) = f_e(x_e(t)) + B_e u(t) \\ y(t) = C_e x_e(t) \end{cases} \tag{4.15}$$

Where:

$$f_e(x_e(t)) = \begin{bmatrix} -\gamma i_{sd} + \omega_s i_{sq} + \frac{k_s}{\tau_r}\emptyset_{rd} + k_s n_p\,\omega_r \emptyset_{rq} \\ -\omega_s i_{sd} - \gamma i_{sq} - k_s n_p\,\omega_r \emptyset_{rd} + \frac{k_s}{\tau_r}\emptyset_{rq} \\ \frac{M}{\tau_r} i_{sd} - \frac{1}{\tau_r}\emptyset_{rd} + (\omega_s - n_p\,\omega_r)\emptyset_{rq} \\ \frac{M}{\tau_r} i_{sq} - (\omega_s - n_p\,\omega_r)\emptyset_{rd} - \frac{1}{\tau_r}\emptyset_{rq} \\ \frac{n_p M}{J L_r}(\emptyset_{rd}\, i_{sq} - \emptyset_{rq} i_{sd}) - \frac{b}{J}\omega_r - \frac{1}{J}T_L \\ 0 \\ \omega_r \end{bmatrix} \quad (4.16)$$

Where

$x_e = [i_{sd} \quad i_{sq} \quad \emptyset_{rd} \quad \emptyset_{rq} \quad \omega_r \quad T_L \quad \theta_r]^T$

$$B_e = \begin{bmatrix} \frac{1}{\sigma L s} & 0 & 0 & 0 & 0 & 0 & 0 \\ 0 & \frac{1}{\sigma L s} & 0 & 0 & 0 & 0 & 0 \end{bmatrix}^T$$

$$C_e = \begin{bmatrix} 1 & 0 & 0 & 0 & 0 & 0 & 0 \\ 0 & 1 & 0 & 0 & 0 & 0 & 0 \\ 0 & 0 & 0 & 0 & 1 & 0 & 0 \end{bmatrix}$$

The extended IM model can be represented in the following form:

$$\begin{cases} \dot{x_e}(t) = A_e x_e(t) + B_e u(t) + \varphi_e(x_e) \\ y(t) = C_e x_e(t) \end{cases} \quad (4.17)$$

With

$$A_e = \begin{bmatrix} -\gamma & 0 & \frac{k_s}{\tau_r} & 0 & 0 & 0 & 0 \\ 0 & -\gamma & 0 & \frac{k_s}{\tau_r} & 0 & 0 & 0 \\ \frac{M}{\tau_r} & 0 & -\frac{1}{\tau_r} & 0 & 0 & 0 & 0 \\ 0 & \frac{M}{\tau_r} & 0 & -\frac{1}{\tau_r} & 0 & 0 & 0 \\ 0 & 0 & 0 & 0 & -\frac{b}{J} & -\frac{1}{J} & 0 \\ 0 & 0 & 0 & 0 & 0 & 0 & 0 \\ 0 & 0 & 0 & 0 & 1 & 0 & 0 \end{bmatrix}$$

And

$$\varphi_e(x_e) = f_e(x_e(t)) - A_e x_e(t)$$

The estimated state can also be represented as the same form as the state of the IM:

$$\dot{\hat{x}}_e(t) = A_e \hat{x}_e(t) + B_e u(t) + L_e C_e\big(x_e(t) - \hat{x}_e(t)\big) + \hat{\varphi}_e(\hat{x}_e) \tag{4.18}$$

In the next equation, the estimation error is defined as:

$$e_e(t) = x_e(t) - \hat{x}_e(t) \tag{4.19}$$

Through (4.17) and (4.18), the dynamics of the estimation error is written as:

$$\dot{e_e}(t) = (A_e - L_e C_e) e_e(t) + (\varphi_e(x_e) - \hat{\varphi}_e(\hat{x}_e)) \tag{4.20}$$

Where:

In this part, the MVT approach is presented so as to develop the extended observer gain L_e. By the application of the MVT approach [10] (illustrated in last chapter (section 3.2)) to (4.20), the MVT approach to the dynamics of the estimation error can be exhibited as follows:

$$\dot{e_e}(t) = \left((A_e - L_e C_e) + \sum_{i=1}^{n} \sum_{j=1}^{n} e_n(i)\, e_n^T(j) \frac{\partial \varphi_i}{\partial x_j}\left(\xi^i\right) \right) e_e(t) \tag{4.21}$$

With n is the number of the states of the IM model.

The introducing of the sector nonlinearity approach after the using of the MVT allows to get the following dynamics of the following estimation error (section 3.2):

$$\dot{e_e}(t) = \sum_{r=1}^{2} \delta_{ij}^{r} \left(A_e - L_e C_e + A_i^*\right) e_e(t) \tag{4.22}$$

Where $\sum_{r=1}^{2} \delta_{ij}^{r} = 1$, $\xi \in [x, \hat{x}]$ and A_i^* depend on the maximum and the minimum of the IM states.

The stability of the state estimation error is studied so as to find the observer gain L_e by applying the quadratic Lyapunov function that is given as follows:

$$V\big(e(t)\big) = e^T(t) P e(t) \tag{4.23}$$

The state estimation error asymptotically converges to zero if there exists a matrix $P = P^T > 0$ such as the following LMI's are verified:

$$A_e^T P + P A_e + {A_i^*}^T P + P A_i^* - M C_e - M^T {C_e}^T + \alpha P < 0 \tag{4.24}$$

For $(i = 1, \cdots, 2n)$.

Where α is reversely depend on the response time of the estimation error

The solving of (4.24) by the exploiting of the YALMIP software computer allows obtaining the extended observer gain as:

$$L_e = P^{-1} M \tag{4.25}$$

Whereas

$$L_e = \begin{bmatrix} 10828 & -0.5693 & 2.8485^{-5} \\ 0.5376 & 11685 & 84.3298 \\ -2.4888 & 3.1130 & 2.4096^{-6} \\ -9.8266^{-5} & 1.3428 & 12.7270 \\ 0.0029 & 71.1755 & 3400.5 \\ -5.2944^{-5} & -1.3145 & -31.1879 \\ 0 & -6.5673^{-6} & 0.9999 \end{bmatrix}$$

4.4.1.2 Robust H_∞ controller based on the MVT approach

The important idea of this kind of control based on the MVT is to get the controller parameters that make the states of the IM track their references with a minimum effect of the disturbance on the control error.

The model of the IM that is used in this part is similar to the system mentioned previously in (4.9), with $v(t)$ is substituted by $Dn(t)$,

Where $D = \begin{bmatrix} 0 & 0 & 0 & 0 & -\frac{1}{J} \end{bmatrix}^T$ and $n(t) = T_L$

Passing by the T-S representation, we can represent the IM nonlinear system (4.9) as the Lipchitz form as [11]:

$$\begin{cases} \dot{x}(t) = A_0 x(t) + Bu(t) + \emptyset(x) + Dn(t) \\ y = Cx(t) \end{cases} \quad (4.26)$$

Where

$$\emptyset(x) = \sum_{i=1}^{r} \mu_i\big(x(t)\big)\left(\bar{A}_i x(t)\right)$$

And

$$A_0 = \frac{1}{r}\sum_{r=1}^{r} A_i \qquad \bar{A}_i = A_i - A_0$$

Where A_i, B_i and μ_i are obtained from the T-S model [9, 12].

The state vector of the control error is written as:

$$e(t) = x(t) - x_c(t) \tag{4.27}$$

Where x_c is the reference state and it's supposed as a stepwise signal, so the dynamics of the state error as the following form:

$$\dot{e}(t) = \dot{x}(t) - \dot{x}_c(t) = \dot{x}(t) = A_0 x(t) + Bu(t) + \emptyset(x) + Dn(t) \tag{4.28}$$

- ✓ **State feedback control**

The control law of the classical proportional controller has the following form:

$$u(t) = -K_0 e(t) \tag{4.29}$$

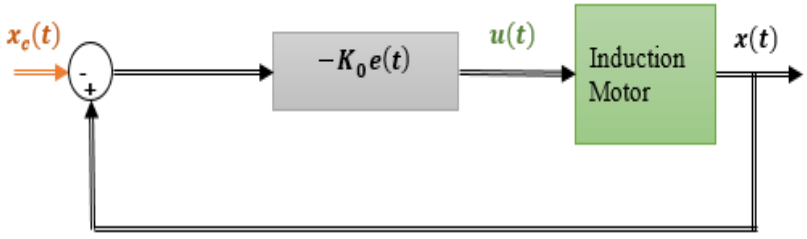

Figure 4.9 The state feedback control design

Combining (4.28) with (4.29), the dynamics of the control error becomes as:

$$\dot{e}(t) = (A_0 - BK_0)e(t) + A_0 x_c(t) + \emptyset(x) + Dn(t) \tag{4.30}$$

By using the MVT approach [11, 13, 14] (Section 3.2), we have:

$$\emptyset(x) = \emptyset_c(x_c) + \frac{\partial \emptyset}{\partial x}(\varepsilon)(x - x_c) \tag{4.31}$$

Where $\varepsilon \in [x, x_c]$

By substituting (4.31) in (4.30), the dynamics of the control error can be expressed as:

$$\dot{e}(t) = (A_0 - BK_0 + \frac{\partial \emptyset}{\partial x}(\varepsilon))e(t) + A_0 x_c(t) + \emptyset_c(x_c) + Dn(t) \quad (4.32)$$

Considering that the reference signal x_c is a stepwise signal, the component $\emptyset_c(x_c, u) = 0$

Utilizing the sector nonlinearity approach[13, 15, 16], the dynamics of the state feedback control error turn into:

$$\dot{e}(t) = \sum_{i=1}^{r} \mu_i(\xi)\,(A_0 - BK_0 + \mathcal{A}_i)e(t) + Dn(t) + A_0 x_c(t) \quad (4.33)$$

We define that:

$S_i = \breve{A}_i - BK_0$

where

$\breve{A}_i = A_0 + \mathcal{A}_i$ $\qquad D_w = [A_0 \quad D]$ $\qquad \bar{n}(t) = \begin{bmatrix} x_c(t) \\ n(t) \end{bmatrix}$

Such as $\mathcal{A}_i$ represent $\emptyset(x) - \emptyset_c(x_c)$ after the introducing the MVT and the sector nonlinearity approaches.

The dynamics of the state feedback error (4.33) is written as:

$$\dot{e}(t) = \sum_{i=1}^{r} \mu_i(\xi)\left(S_i e(t) + D_w \bar{n}(t)\right) \quad (4.34)$$

- ✓ **Synthesis for H_∞performance**

The existence of the disturbances $\bar{n}(t)$ will affect to the control performances. So as to minimize the effect of the disturbance $\bar{n}(t)$, the H_∞ performances has been taken into account [17].

$$\int_0^\infty e^T(t)\, e(t)\, dt \leq \gamma^2 \int_0^\infty \bar{n}^T(t)\, \bar{n}(t)\, dt \quad (4.35)$$

Consider the quadratic Lyapunov function as:

$$V\big(e(t)\big) = \bar{e}^T(t)Pe(t) \tag{4.36}$$

Where $P = P^T > 0$

So as to develop the asymptotic stability of (4.35) and to attain the H_∞ performance of the state control error, we have:

$$\dot{V}\big(e(t)\big) + e^T(t)e(t) - \gamma^2\bar{n}^T(t)\bar{n}(t) < 0 \tag{4.37}$$

The previous equation becomes an LMI's form as next:

$$\dot{e}^T(t)Pe(t) + e^T(t)P\dot{e}(t) + e^T(t)e(t) - \gamma^2\bar{n}^T(t)\bar{n}(t) < 0 \tag{4.38}$$

This is equivalent to:

$$\sum_{i=1}^{r}\mu_i(\xi)\, e^T(t)\big[{S_i}^T P + PS_i + I\big]e(t) + \bar{n}^T(t)\big[{D_w}^T P\big]e(t) + e^T(t)[PD_w]\bar{n}(t) - \gamma^2\bar{w}^T(t)\bar{w}(t) < 0 \tag{4.39}$$

Then, it is possible to present the last equation as:

$$[e^T(t) \quad \bar{n}^T(t)]\begin{bmatrix}\sum_{i=1}^{r}\mu_i(\xi)\left[{S_i}^T P + P\bar{S}_i + I\right] & PD_w \\ {D_w}^T P & -\gamma^2 I\end{bmatrix}\begin{bmatrix}e(t)\\ \bar{n}(t)\end{bmatrix} < 0 \tag{4.40}$$

The stability is considered by the following part:

$$\begin{bmatrix}\sum_{i=1}^{r}\mu_i(\xi)\left[{S_i}^T P + PS_i\right] + I & PD_w \\ {D_w}^T P & -\gamma^2 I\end{bmatrix} < 0 \tag{4.41}$$

After, we can present (4.41) as:

$$\begin{bmatrix}\sum_{i=1}^{r}\mu_i(\xi)\left[{S_i}^T P + PS_i\right] & PD_w \\ {D_w}^T P & -\gamma^2 I\end{bmatrix}\begin{bmatrix}I & 0\\ 0 & 0\end{bmatrix} < 0 \tag{4.42}$$

This main:

$$\begin{bmatrix} \sum_{i=1}^{r} \mu_i(\xi) \left[{S_i}^T P + P S_i \right] & P D_w \\ {D_w}^T P & -\gamma^2 I \end{bmatrix} \begin{bmatrix} I \\ 0 \end{bmatrix} [I \quad 0] < 0 \tag{4.43}$$

Depending on the Schur's complement, (4.43) becomes as follow:

$$\begin{bmatrix} \sum_{i=1}^{r} \mu_i(\xi) \left[{S_i}^T P + P S_i \right] & P D_w & I \\ {D_w}^T P & -\gamma^2 I & 0 \\ I & 0 & -I \end{bmatrix} < 0 \tag{4.44}$$

The stability depends on:

$$\begin{bmatrix} {S_i}^T P + P S_i & P D_w & I \\ {D_w}^T P & -\gamma^2 I & 0 \\ I & 0 & -I \end{bmatrix} < 0 \tag{4.45}$$

By applying the congruence transformation, multiplying to the right and to the left by the $diag\ [P^T, \quad I, \quad I]$ we get:

$$\begin{bmatrix} P^{-1} & 0 & 0 \\ 0 & I & 0 \\ 0 & 0 & I \end{bmatrix} \begin{bmatrix} {S_i}^T P + P S_i & P D_w & I \\ {D_w}^T P & -\gamma^2 I & 0 \\ I & 0 & -I \end{bmatrix} \begin{bmatrix} P^{-1} & 0 & 0 \\ 0 & I & 0 \\ 0 & 0 & I \end{bmatrix} < 0 \tag{4.46}$$

The previous equation can be developed to:

$$\begin{bmatrix} P^{-1} \left[{S_i}^T P + P S_i \right] P^{-1} & P^{-1} P D_w & P^{-1} \\ {D_w}^T P P^{-1} & -\gamma^2 I & 0 \\ P^{-1} & 0 & -I \end{bmatrix} < 0 \tag{4.47}$$

If we consider that $X^{-1} = P$ and $Y = K_0 P^{-1} = K_0 X$, we obtain the final LMI's to solving that are written in the following form:

$$\begin{bmatrix} \check{A}_i X + X\check{A}_i{}^T - BY - Y^T B^T + \alpha X & D_w & X \\ D_w{}^T & -\gamma^2 I & 0 \\ X & 0 & -I \end{bmatrix} < 0 \tag{4.48}$$

The exploiting of the YALMIP software computer allows finding the proportional controller gain that is gotten as:

$$K_0 = YX^{-1} \tag{4.49}$$

Where its value is:

$$K_0 = \begin{bmatrix} -474.1 & 0 & 1650 & 0.3 & 0.3 \\ 0.1 & -417.3 & 1.7 & 1775.2 & -908.4 \end{bmatrix}$$

4.4.1.3 Controller based observer applied to IM using the MVT theory:

In this part we will present an PI controller based observer using the MVT theory applied to the IM drive where the goals are to get the controller and the observer gains with:

- A systematic methodology
- The stability of all the system is proven
- The parameters don't depend on the IM states

✓ **The control law**

To eliminate the effects of disturbance and the parametric uncertainty in the steady state, it is better to add an integral action, so the control is rewritten as:

$$u(t) = -[K_1 \quad K_2] \begin{bmatrix} e(t) \\ e_I(t) \end{bmatrix} = K_I \bar{e}(t) \tag{4.50}$$

Such as the error state bound the integral action is:

$$e_I(t) = \int x(t) - x_c(t) \tag{4.51}$$

and $e(t)$ is as mentioned previously in (4.27).

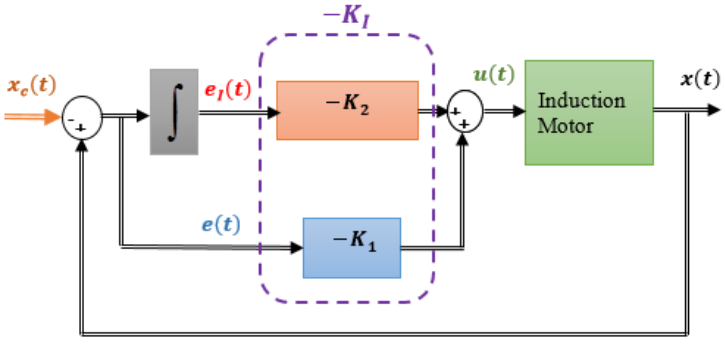

Figure 4.10 The PI control design

The combining of the MVT theory with the sector nonlinearity approach allows to get the following dynamics of the augmented state control error:

$$\dot{\bar{e}}(t) = \sum_{i=1}^{r} \mu_i(\xi)\,(\bar{S}_i \bar{e}(t)) + \bar{D}\bar{w}(t) \tag{4.52}$$

Where

$\bar{S}_i = \bar{A}_i - \bar{B}K_I$

And

$$\bar{A}_i = \begin{bmatrix} A_0 + \mathcal{A}_i & 0 \\ I & 0 \end{bmatrix} \qquad \bar{B} = \begin{bmatrix} B \\ 0 \end{bmatrix}$$

$$\bar{D} = \begin{bmatrix} A_0 & D \\ 0 & 0 \end{bmatrix} \qquad \bar{n}(t) = \begin{bmatrix} x_c(t) \\ n(t) \end{bmatrix}$$

- ✓ **The observer design**

We define the state estimation error as:

$$e_0(t) = x(t) - \hat{x}(t) \tag{4.53}$$

Passing by the same steps in sub-section 4.4.1.1, the dynamics of the estimation error can be written as:

$$\dot{e_0}(t) = \sum_{j=1}^{r} h_j(\delta)\left(AA_0 - L_0C_0 + AA_j\right)e_0(t) \tag{4.54}$$

Where $\delta \in [x, \hat{x}]$

And $C_0 = \begin{bmatrix} 1 & 0 & 0 & 0 & 0 \\ 0 & 1 & 0 & 0 & 0 \\ 0 & 0 & 0 & 0 & 1 \end{bmatrix}$

The global system (controller based observer) can be written as the next equation indicates:

$$\begin{bmatrix} \dot{\bar{e}}(t) \\ \dot{e}_0(t) \end{bmatrix} = \sum_{i=1}^{r}\sum_{j=1}^{r} \mu_i(\xi)h_j(\delta) \begin{bmatrix} A_i - B_0K_0 & 0 \\ \mathbf{0} & AA_0 - L_0C_0 + \mathcal{A}\mathcal{A}_j \end{bmatrix} \begin{bmatrix} \bar{e}(t) \\ e_0(t) \end{bmatrix} + A_0 \begin{bmatrix} x_c(t) \\ \mathbf{0} \end{bmatrix} + D \begin{bmatrix} n(t) \\ \mathbf{0} \end{bmatrix} \tag{4.55}$$

One can obtain the design of the PI controller parameters and the observer gain of the equation (4.55) by using the separation principle [18]. Consequently, one can separately analyze the stability of the equations by utilizing a quadratic Lyapunov function for control and observer as in (4.56) and (4.57) respectively, we have a common matrix for every state equation above ((4.52) and (4.54)) [19].

Consider the quadratic Lyapunov function for the controller and observer respectively as:

$$V\left(\bar{e}(t)\right) = \bar{e}^T(t)P\bar{e}(t) \tag{4.56}$$

$$VV(e_0(t)) = {e_0}^T(t)Se_0(t) \tag{4.57}$$

Then the stability expressed through the following LMI's that allow getting the observer and the controller gains separately[20].

$$P{\bar{A}_i}^T + \bar{A}_iP - M^T\bar{B}^T - \bar{B}M + \alpha P < 0 \tag{4.58}$$

And

$$AA_0^T S + SAA_0 + \mathcal{A}\mathcal{A}_j^T S + S\mathcal{A}\mathcal{A}_j - {C_0}^T N^T - NC_0 + \beta S < 0 \quad (4.59)$$

Where the PI controller parameters and the observer gains are gotten as:

$$\overline{K} = MP^{-1} \quad (4.60)$$

And

$$L_0 = S^{-1}N \quad (4.61)$$

Whereas their values are:

$\overline{K} = [K_1 \quad K_2]$ with:

$$K_1 = \begin{bmatrix} -551.4350 & -0.0093 & 656.80 & -0.0179 & 0.1558 \\ 0.0476 & -545.3837 & 1.0784 & 651.7380 & -215.0177 \end{bmatrix}$$

$$K_2 = \begin{bmatrix} 0.1972 & -0.0013 & -0.281 & 0 & 0 \\ -0.0003 & 0.2110 & -0.0001 & -0.028 & -0.0080 \end{bmatrix}$$

And

$$L_0 = 10^4 \begin{bmatrix} 1.2925 & -0.0543 & 0.0034 \\ 0.0544 & 1.2789 & -0.1554 \\ -0.0003 & 0.0001 & 0.0002 \\ 0.0001 & -0.0002 & 0.0001 \\ -0.0002 & 0.0771 & 0.3464 \end{bmatrix}$$

4.4.2 Simulation results and discussion

4.4.2.1 Extended observer based on the MVT approach:

The proposed extended observer design is applied to the IM drive so as to estimate all the ordinary IM states (i_{ds}, i_{qs}, $\emptyset_{rd}$, $\emptyset_{rq}$ and ω_r) and moreover the load torque (T_L) and the rotor position (θ_r) where the global scheme of the proposed extended observer is presented in figure 4.11. In figures 4.12 to 4.18, the real states have the red line, while the dashed green line indicates the estimated states. Initially, the motor is unloaded, after that, a load torque of 1N.m loads the IM at t = 2sec that is offered in figure 4.17. To show the effectiveness of the MVT observer, firstly, a reference speed is chosen 50 rad/sec for the first three seconds, then it has increased to the nominal speed (150 rad/sec) from 3sec to 6sec, whereas a low and negative speed of -20rad/sec is chosen

for the last three seconds. Secondly, the initial estimated states are taken as $[-2 \quad 4 \quad -0.4 \quad 0.2 \quad 20 \quad 0.4 \quad 6.2]$.

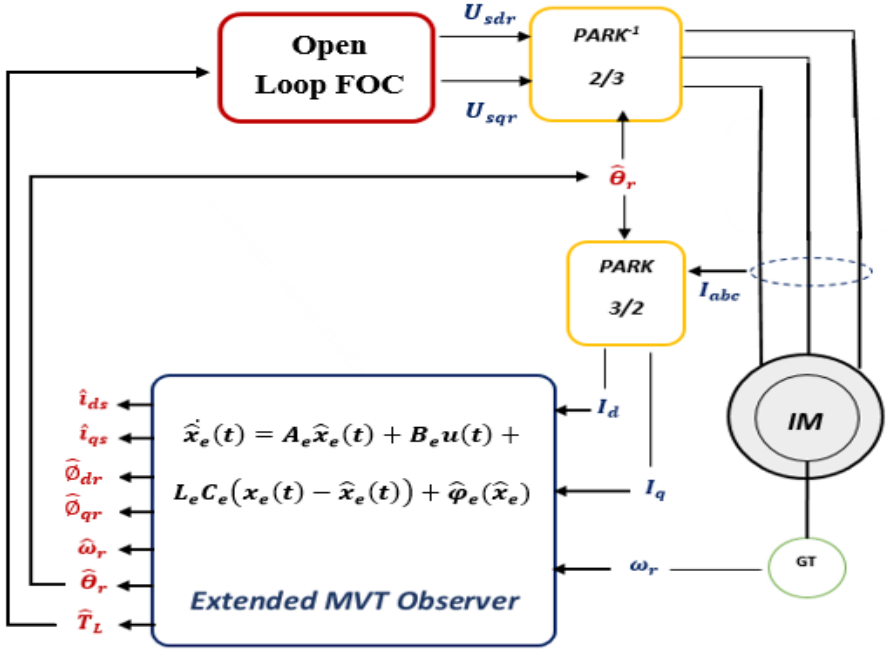

Figure 4.11 Global diagram of the extended MVT observer applied to IM

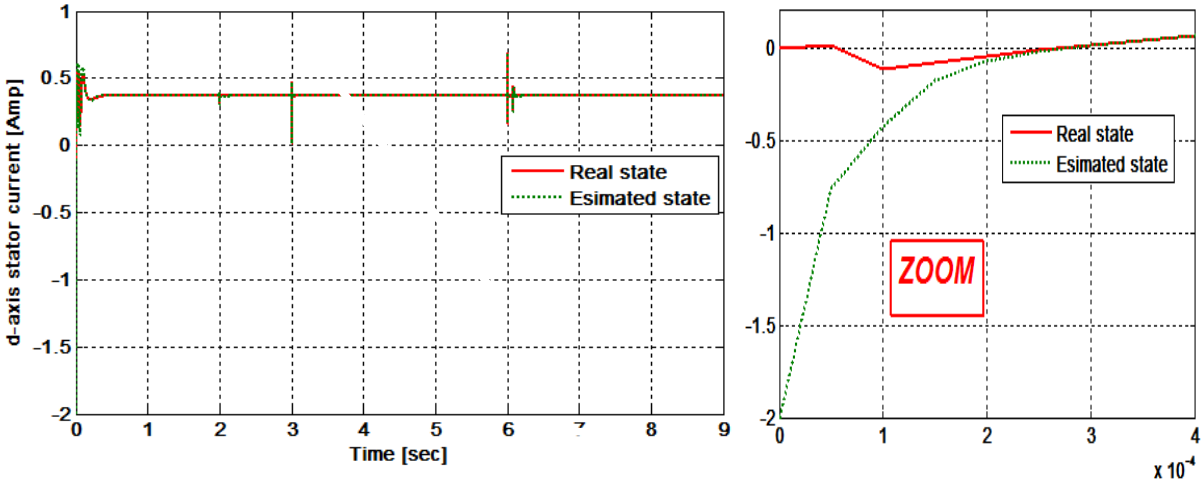

a) **b)**

Figure 4.12 The d-axis stator current and its estimation (a) and zoom (b)

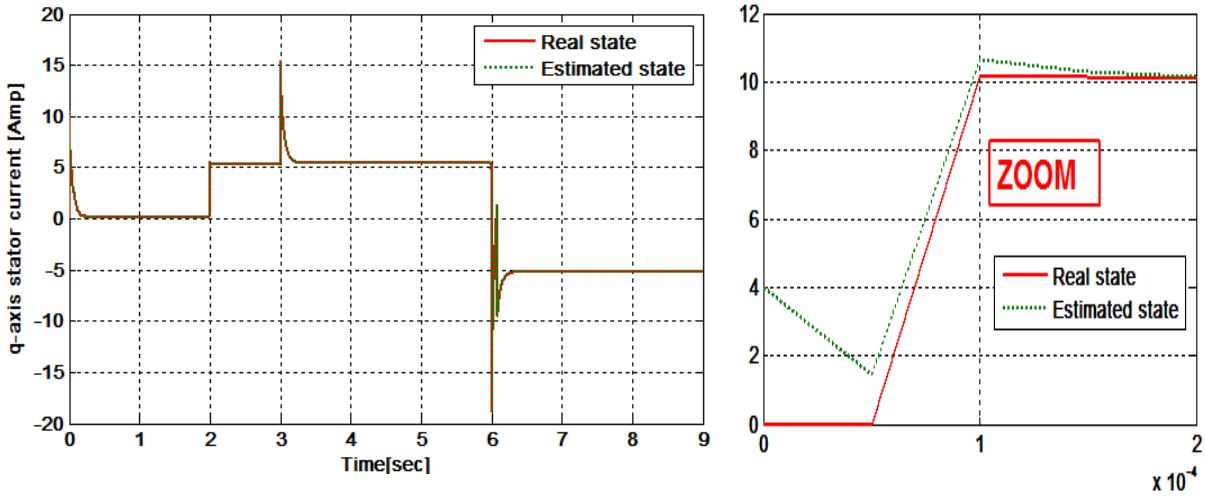

a) **b)**

Figure 4.13 The q-axis rotor current and its estimation (a) and zoom (b)

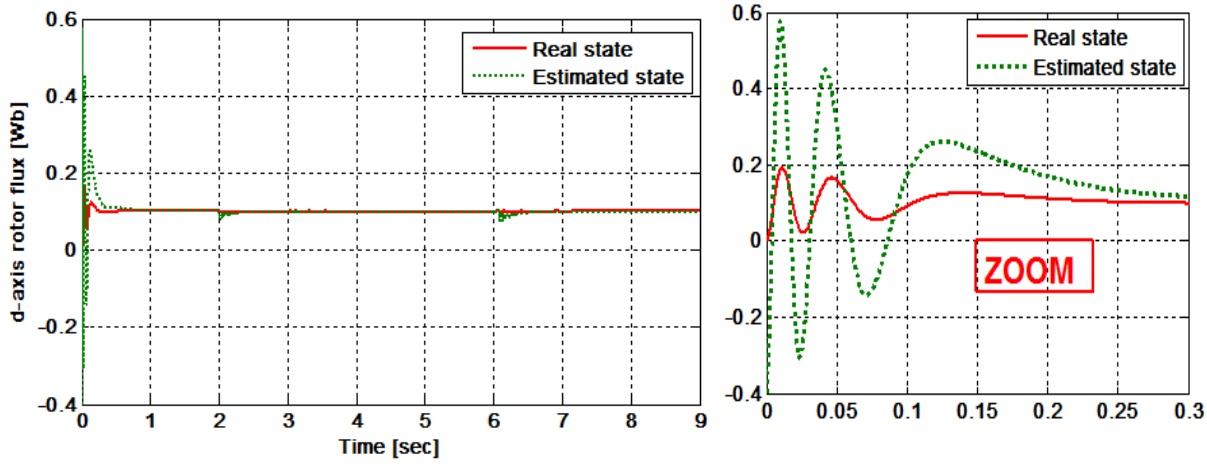

a) **b)**

Figure 4.14 The d-axis rotor flux and its estimation (a) and zoom (b)

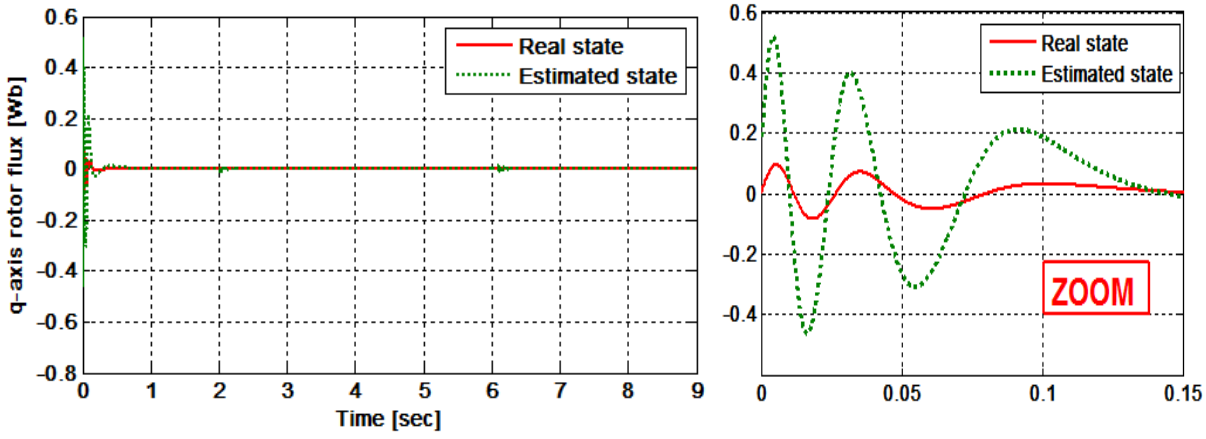

a) **b)**

Figure 4.15 The q-axis rotor flux and its estimation (a) and zoom (b)

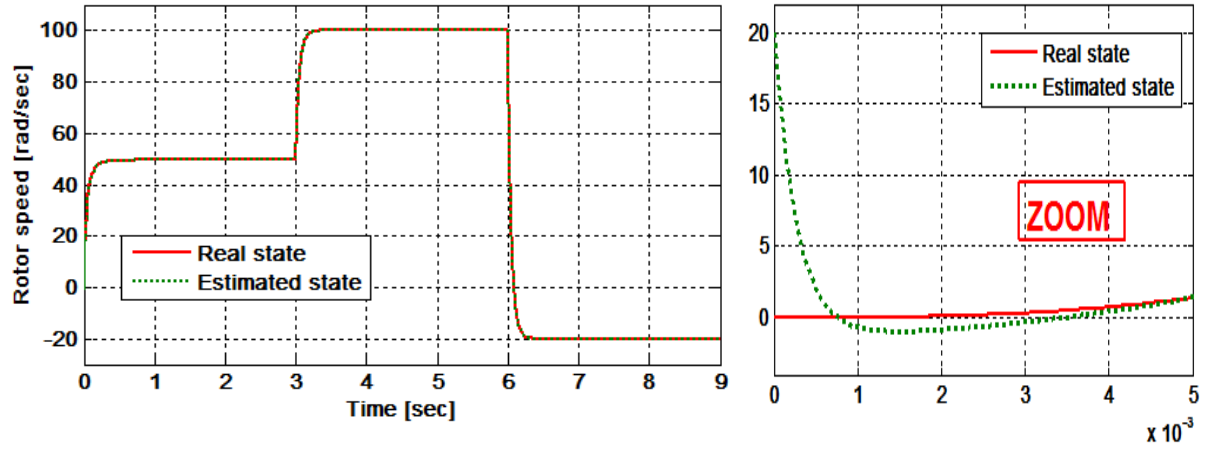

a) **b)**

Figure 4.16 The rotor speed and its estimation (a) and zoom (b)

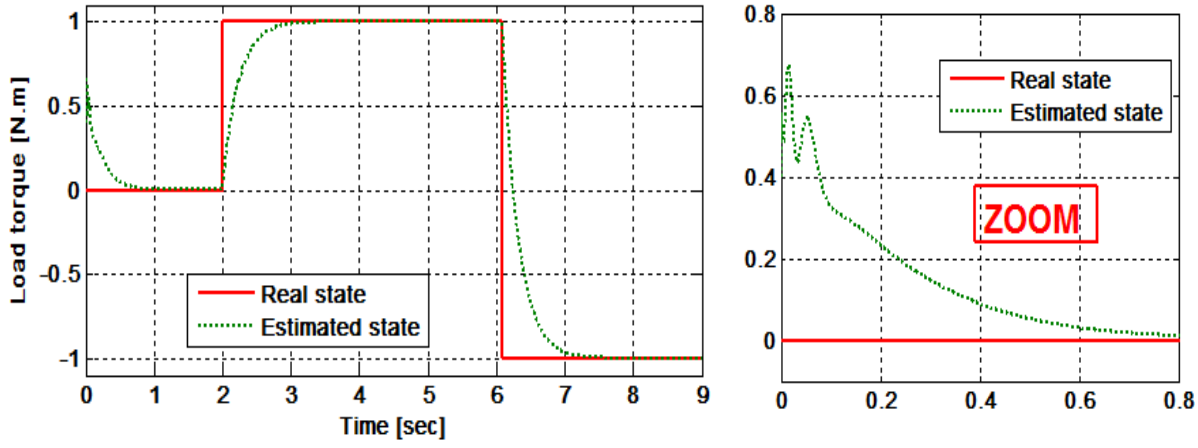

a) **b)**

Figure 4.17 The load torque and its estimation (a) and zoom (b)

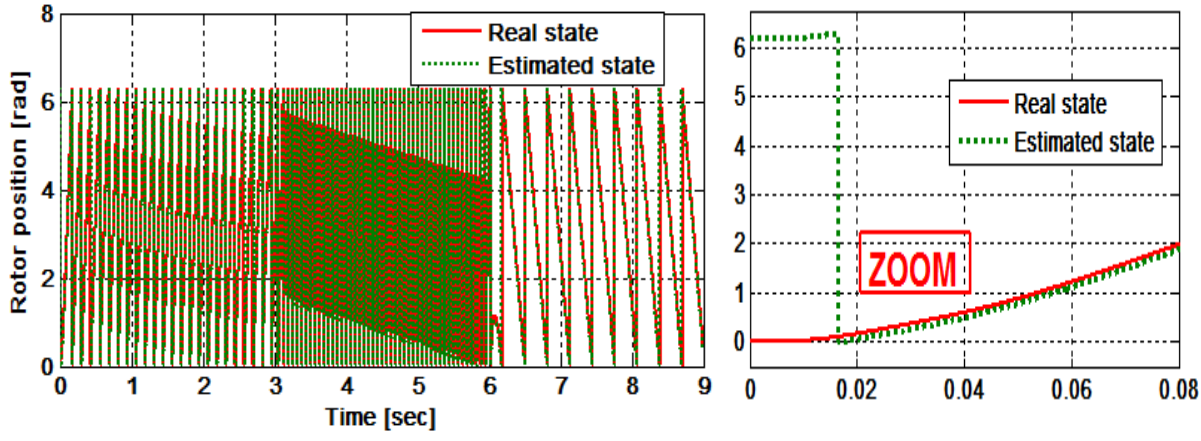

a) **b)**

Figure 4.18 The rotor position and its estimation (a) and zoom (b)

By analyzing the simulation results, the obtained performance of the extended MVT observer is very appropriate. The figures. 4.11 and 4.12 show that the estimated d and q-axis stator currents track their real states in fast response time and with a minimum estimation error which is about zero. The estimation error of the d and q-axis rotor flux is going rapidly toward zero as like as it expected in the figures 4.12 and 4.14. In figure 4.15, the estimated state of the rotor speed tracks its real with an estimation error toward zero even in presence of the load torque at the instant t=2sec. However the load torque and the rotor position are not considered as states of IM, but the

MVT extended observer has the capability to estimate them with an estimation error converge to zero with a response time less than 0.8sec for the load torque and less than 0.02sec for the state of the rotor position as indicated in figure 4.16 and 4.17, respectively. The results described above prove the effectiveness of the MVT approach through the extended observer design that makes a very complex nonlinear system that is the IM drive establishing to the observation conditions through one gain has calculated off-line in spite of the estimated states have intinal conditions different to zero. The key point of the MVT observers even in the presence of a high and coupled nonlinear terms in the system as in the IM machine by establishing the observation conditions by determining off-line a unique gain even in presence of the disturbance. The simplicity of this technic could reduce the cost and hardware implementation, without effecting on the effectiveness of the MVT approach compared to other approaches (sliding mode, MRAS, etc.).

4.4.2.2 Robust H_∞ controller based on the MVT approach:

The design of proposed control law (4.4.1.2) is implemented through an illustrative simulation test under the MATLAB/Simulink environment. The robust control based on MVT is applied to an IM which its parameters are mentioned in Appendix A. The proposed MVT control law has been tested in simulation results as presented in figure 4.18:

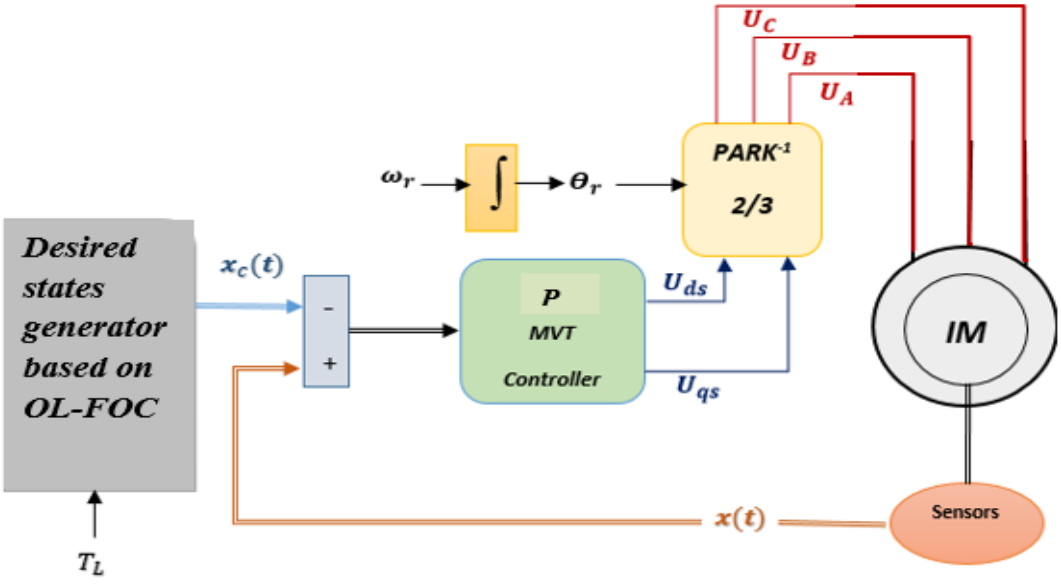

Figure 4.18 Global scheme of the P control law of the IM based on MVT

A rotor speed reference of 50 rad/s is chosen for the low-speed test that started from t = 0s and ends at t = 3sec. While for the high-speed test, a speed value of 150 rad/sec is applied between the instant t=3sec and t = 6s. For the reversing-speed operation, from the end of the previous test until to t = 9sec a rotor speed value is fixed at -150 rad/sec. in order to obtain the FOC conditions the q-axis rotor flux reference stays 0 Wb in all simulation time and the rotor flux reference of the value of 0.1 Wb has been oriented along the d-axis. For proving the robustness of the proposed approach, three disturbances are taken into consideration those are the load torque and the variation of the stator and rotor resistances. Initially, the motor is unloaded, after that, a load torque of 0.7 N.m is applied to the IM from t = 4s to the end of the simulation time. For the parameters variation test, At t= 2sec the R_r is considered to be 200% from the original value, while R_s increased to 150% of the original value at t= 7sec. All disturbances tests are presented in figure 4.24.

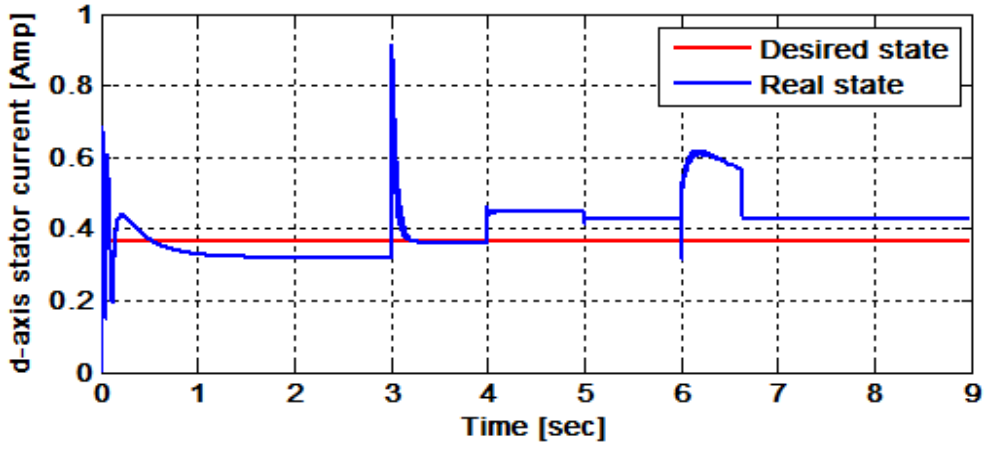

a)

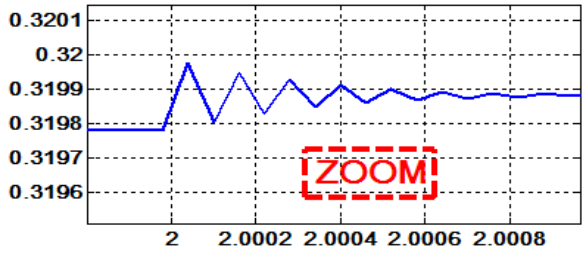

b)

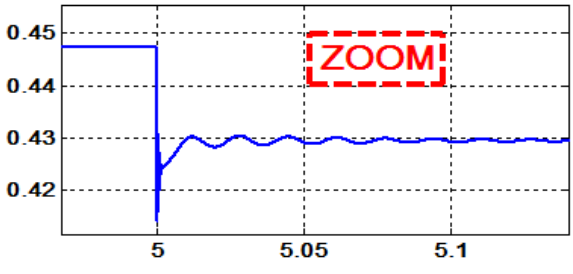

c)

Figure 4.19 **a)**-The d-axis stator current and its reference

b)- the rotor resistance effect

c)- the stator resistance effect

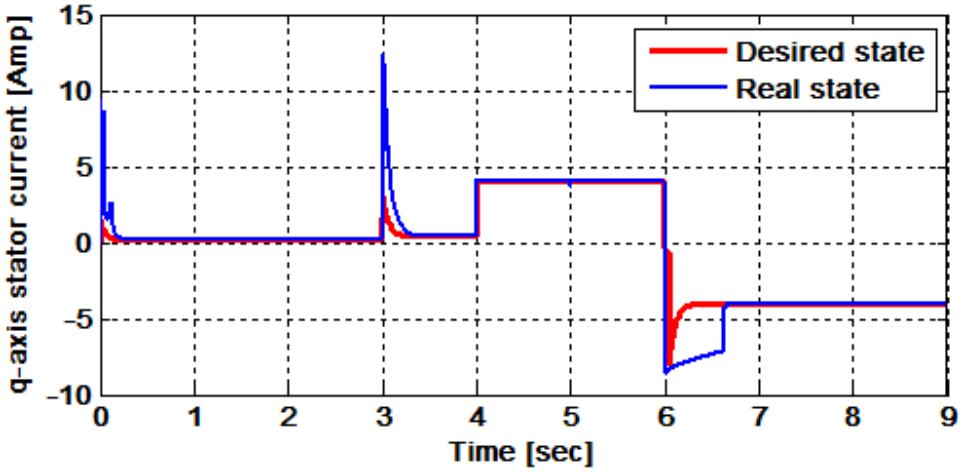

a)

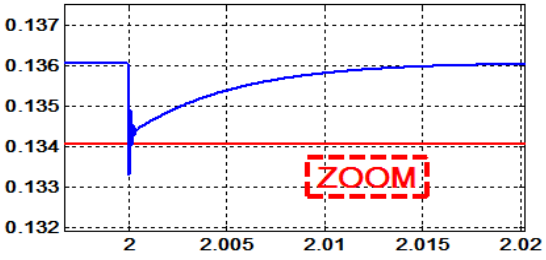

b)

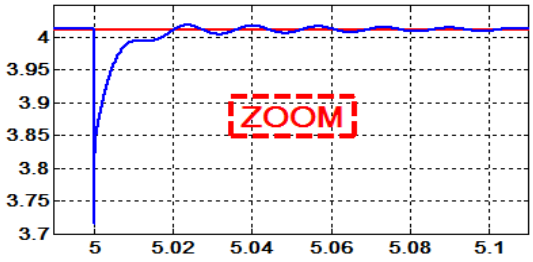

c)

Figure 4.20 **a)**-The q-axis stator current and its reference

b)- the rotor resistance effect

c)- the stator resistance effect

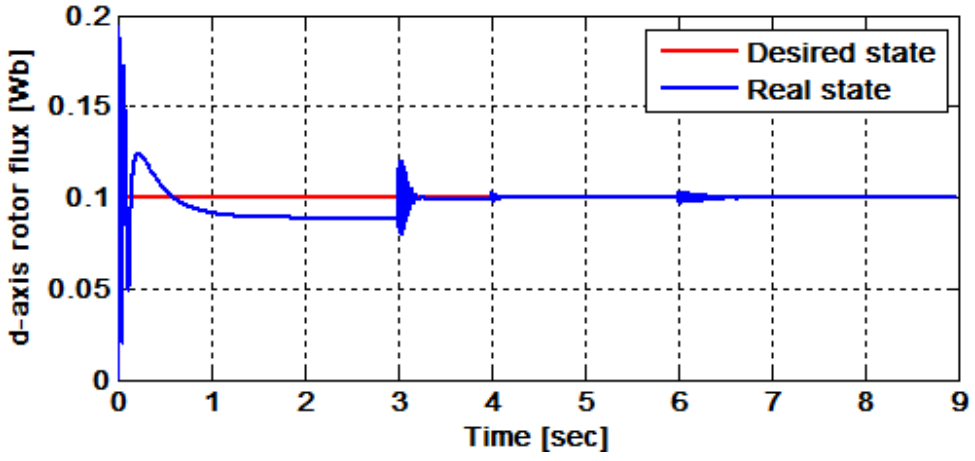

a)

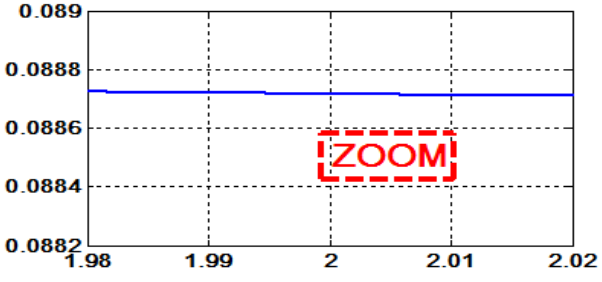

b)

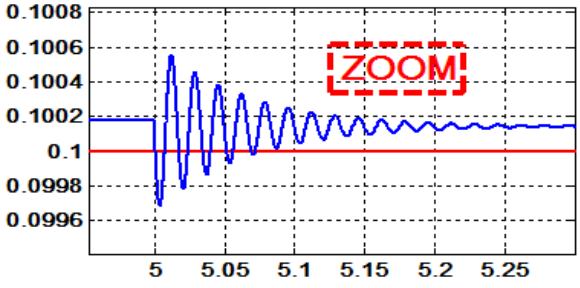

c)

Figure 4.21 **a)**-The d-axis rotor flux and its reference

b)- the rotor resistance effect

c)- the stator resistance effect

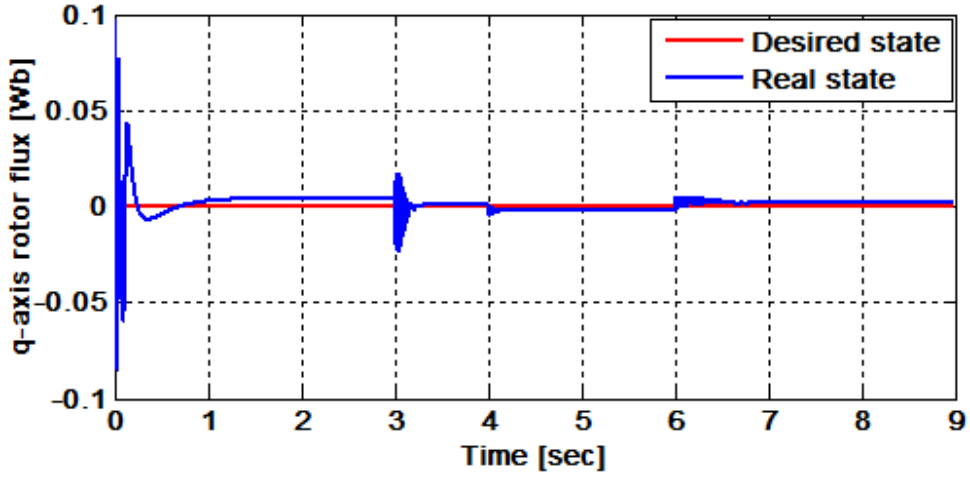

a)

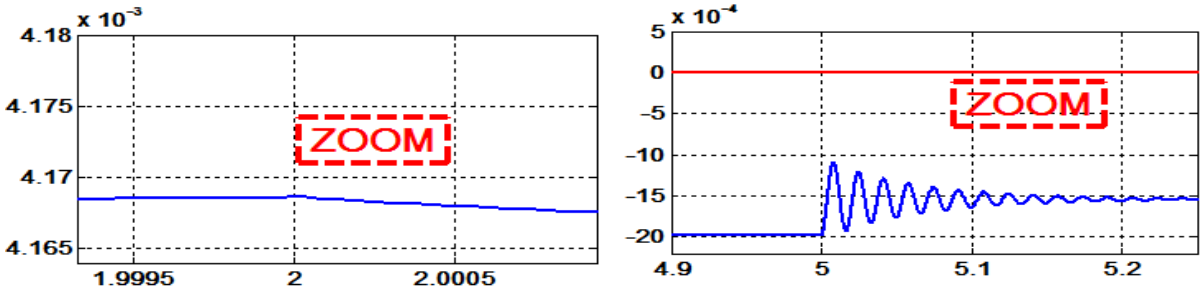

b) **c)**

Figure 4.22 **a)**-The q-axis rotor flux and its reference

b)- the rotor resistance effect

c)- the stator resistance effect

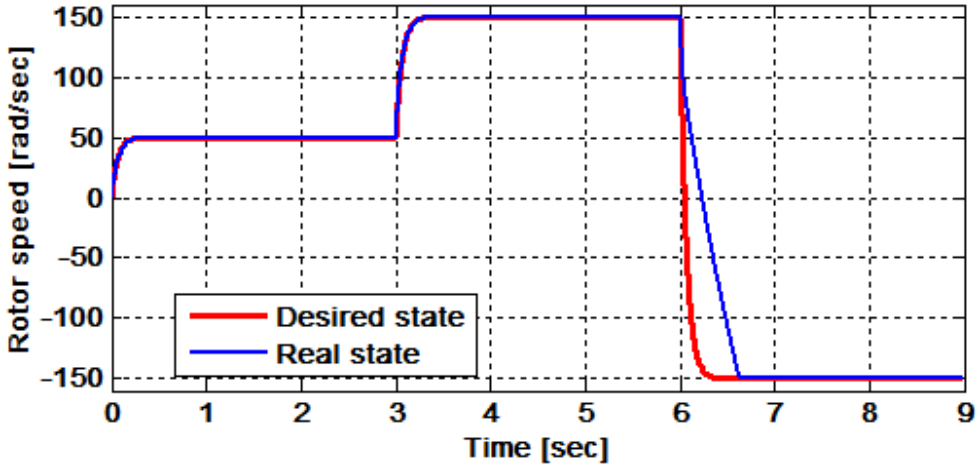

a)

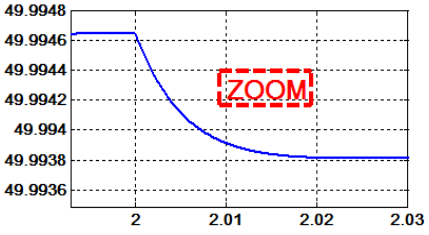

b)

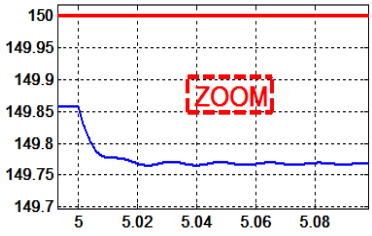

c)

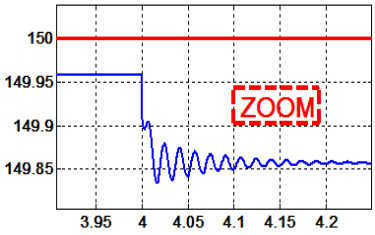

d)

Figure 4.23 **a)**-The rotor speed and its reference

b)- the rotor resistance effect

c)- the stator resistance effect

d)- the load torque effect

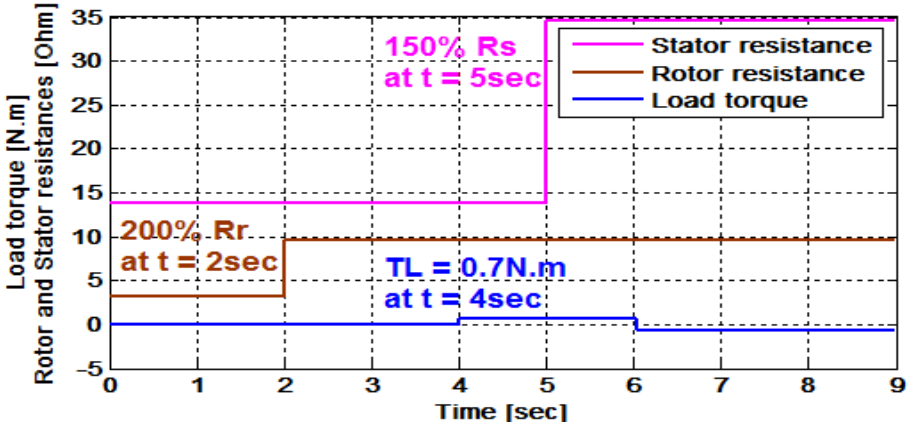

Figure 4.24 The load torque and parameters variations

The simulation results of the MVT robust control based H_∞ concept mentioned above show the effectiveness of this technic. For all the IM states it's clear that the real states still close to their desired values with a minimum errors. The rotor speed still close to its desired value with a minimum effect of the load torque and the parameters variations to the tracking error as figure 4.22 indicates. However of the high parameters variation of the rotor and stator resistances, the tracking error is approximately zero for all the IM states, this due to the independency between the controller gain and the IM states and the also to the missing of the decoupling block which is considered depend to the IM parameters in other methods of control, and this is why this approach compete for the previous technics.

4.4.2.3 PI controller based observer applied to IM based MVT:

The proposed control based observer design based MVT (sub-section 4.4.1.3) is implemented through an illustrative simulation check under the MATLAB/Simulink environment. The PI control based observer based on MVT is applied to an IM which its parameters are mentioned in Appendix A. The global scheme of the PI control based Luenberger observer based is presented in figure 4.25:

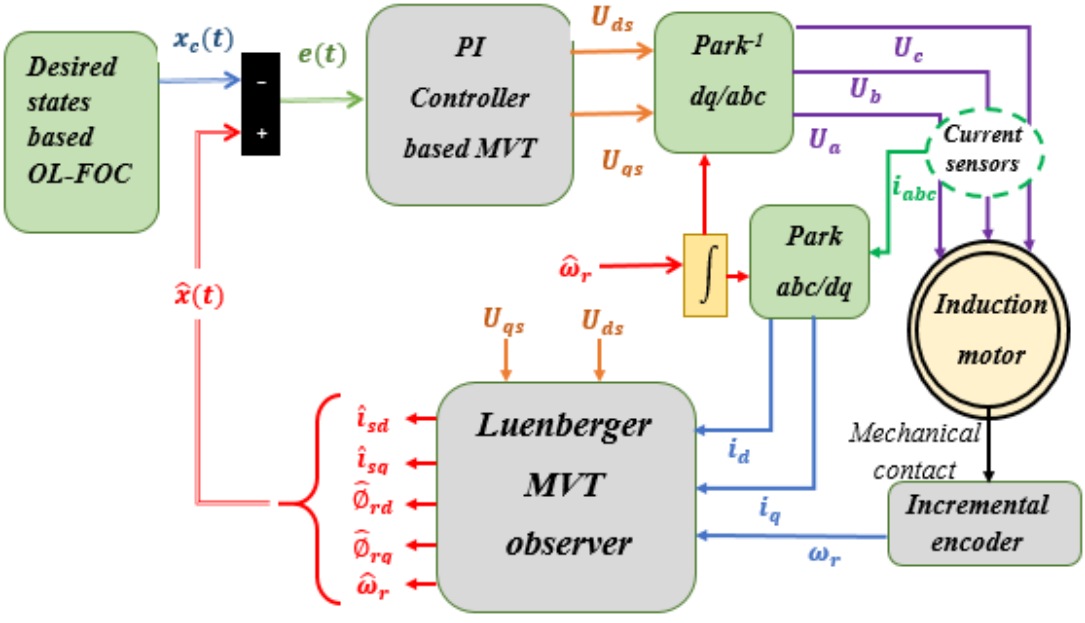

Figure 4.25 Global scheme of the PI control based observer of the IM based on MVT

The reference of the rotor speed has evenly divided into three thirds of the simulation time(6 sec); the first is chosen 50 rad/sec, after it has increased to 150 rad/sec and at last and for check the control based observer against the reversing and low-speed test, it has chosen -20 rad/sec . to show the robustness of the concept, a nominal load torque of 0.7 N.m is applied to the IM at t=3 sec as indicated in figure 4.31 to show the effectiveness of the MVT observer, the initial states are taken as: $[1.5 \quad 4 \quad 0.4 \quad -0.5 \quad 20]$. the desired states are presented in the red lines where the dashed green lines indicate the real states of the IM and the estimated states are mentioned by the black lines.

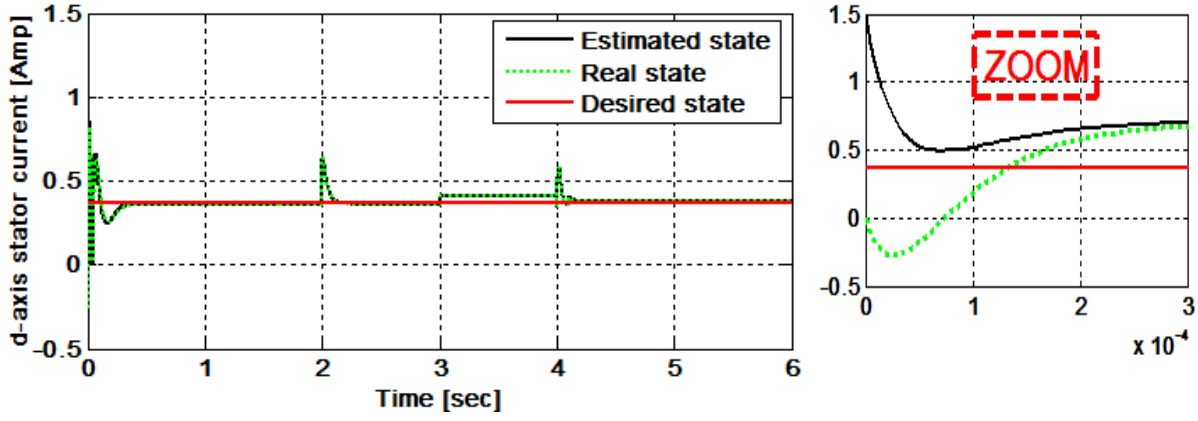

(a) **(b)**

Figure 4.26 The d-axis stator current with its desired and its estimation (a) and zoom in (b)

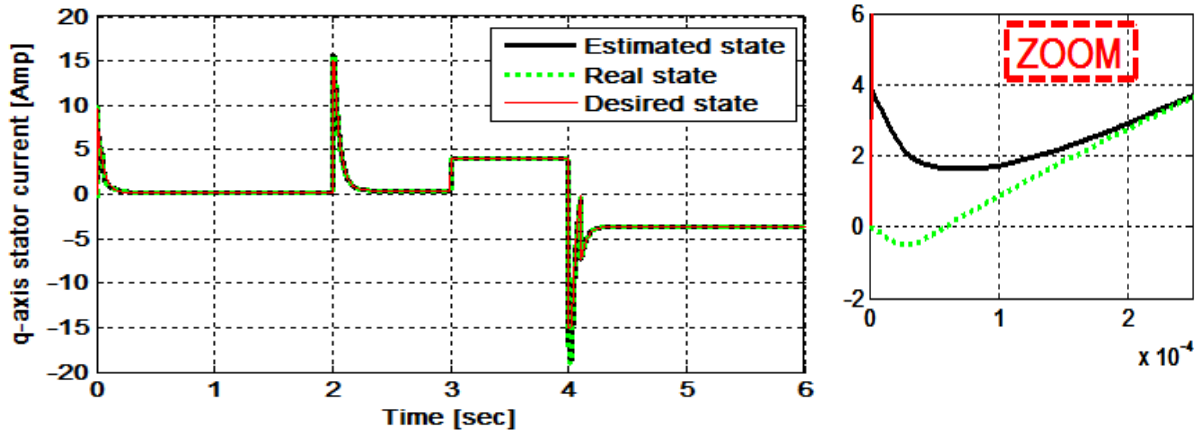

(a) **(b)**

Figure 4.27 The q-axis stator current with its desired and its estimation (a) and zoom in (b)

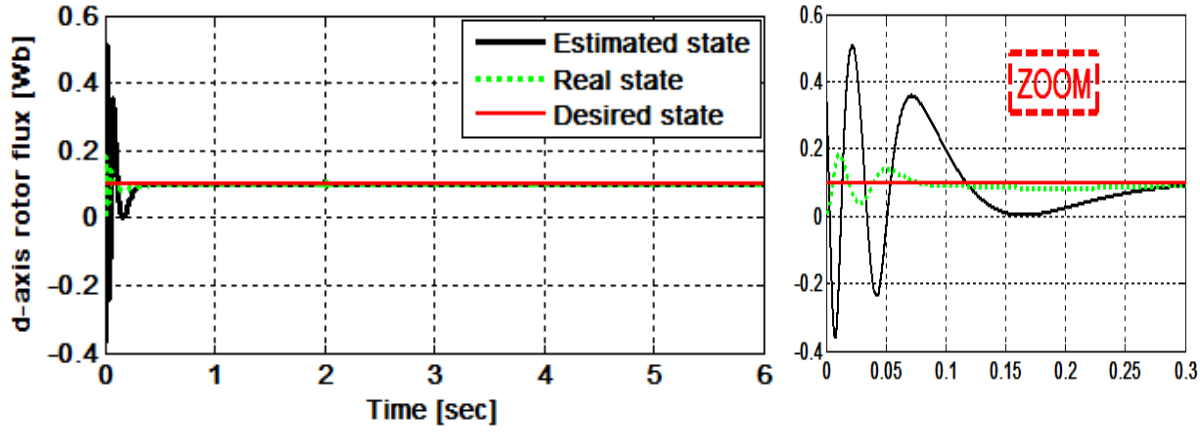

(a) **(b)**

Figure 4.28 The d-axis rotor flux with its desired and its estimation (a) and zoom in (b)

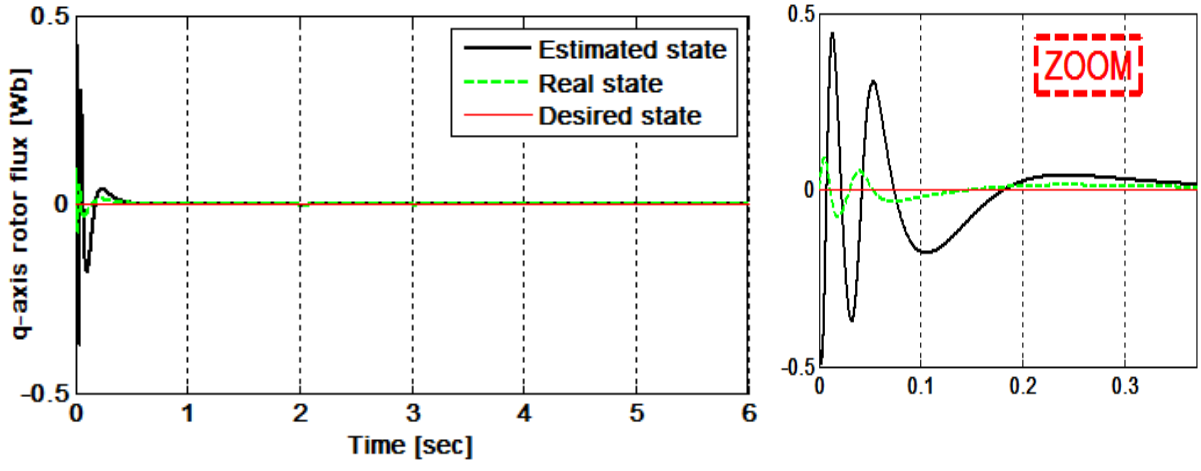

(a) **(b)**

Figure 4.29 The q-axis rotor flux with its desired and its estimation (a) and zoom in (b)

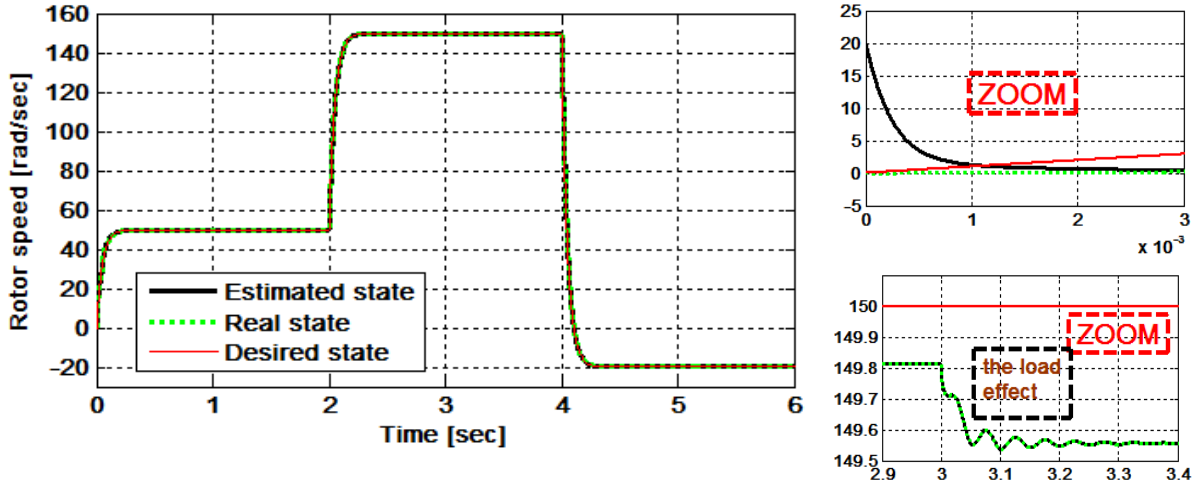

(a) **(b)**

Figure 4.30 The rotor speed with its desired and its estimation (a) and zooms in (b)

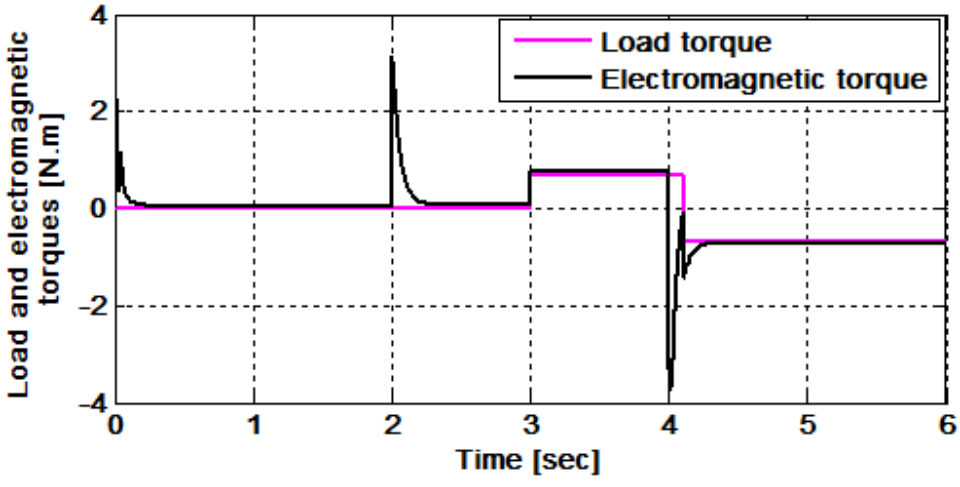

Figure 4.31 The load and electromagnetic torques

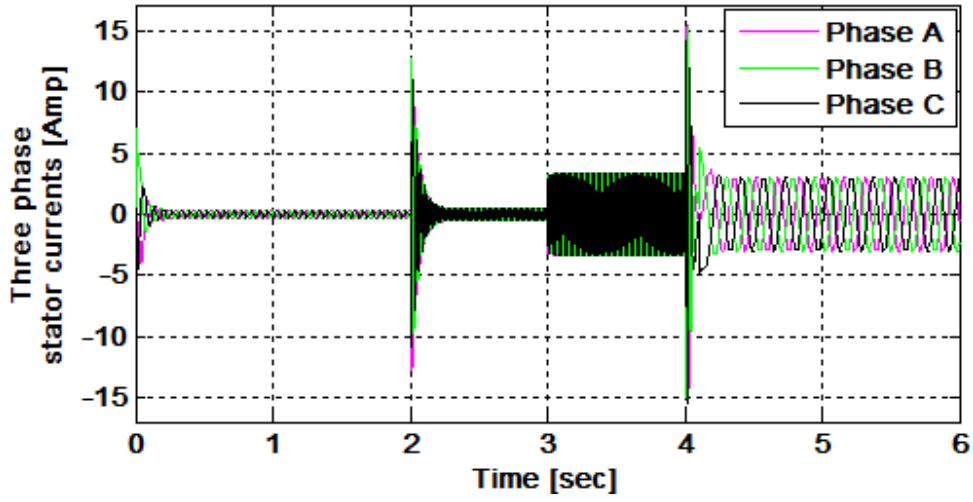

Figure 4.32 The three-phase stator currents

The real q-axis stator current tracks its desired at the same time where the estimated state does the same, it's clear from figures 4.27 and 4.31 that the q-axis stator current is a reproduction of the electromagnetic torque that proves that the FOC is assured. The estimated d-axis stator current follows its real where they track the desired value as shown in figure 4.26. It was also observed that the real and the estimated states of q-axis rotor flux stayed near zero ($\emptyset_{rq} = 0$), whereas its d-axis is around the rated rotor flux reference (0.1 Wb) which shows that the FOC is assured at the moment where the estimation errors is approximately zero as shown in figures 4.28 and 4.29. Based on figure 4.30, it has been observed that the estimated and the real states of the rotor speed are in closer proximity to its desired value. In despite of the application of the nominal load torque at t = 3 sec, the rotor speed still subject to the control and the estimation conditions with a minimum effect on these conditions. The estimated states are closed to their real values despite the fact that the starting conditions of the estimated states are not zero.

Through the simulation results given above, there is guaranteed success for the proposed PI-MVT controller -based observer and it can replace the other technics in the industrial applications due to its effectiveness, simplicity, and low cost.

4.4.2 Experimental results

To study the effectiveness of the proposed controllers and observers based on the MVT theory, some tests of control and states estimation of the IM were constructed in the laboratory of ***UTM-PROTON Future Drive Laboratory, University Technology Malaysia, Johor Bahru, Malaysia***. The set-up consists of a ¼ HP IM which its parameters are listed in Appendix A, a 3-phase voltage source inverter based IGBT 's, hall effect current sensors (La-55), incremental encoder, a DC motor considered as a load and a dSPACE 1104 controller board. A real photo of the experimental bench is presented in figure 4.33.

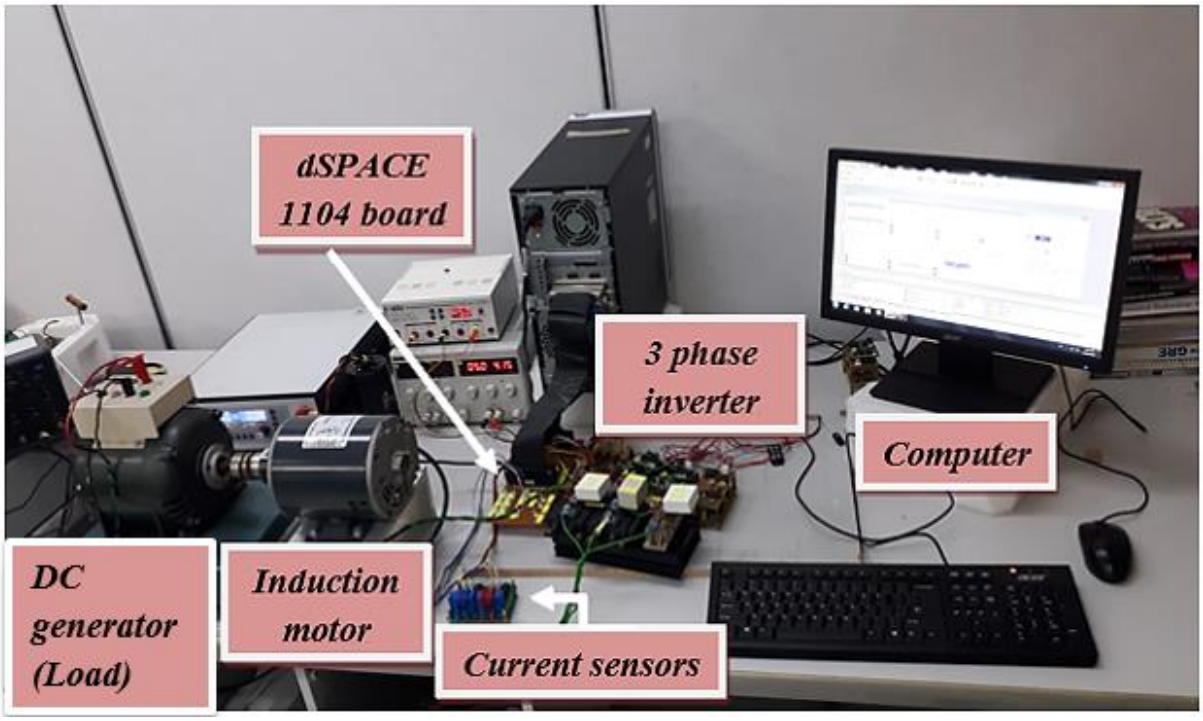

Figure 4.33 Real photo of the experimental bench

4.4.2.1 Robust H_∞ controller

The design of the proposed robust H_∞ for IM control strategy is previously shown in figure 3.18. As can be seen that the structure of the controller is similar to having 5 P controllers, one for each state. The desired states $[i_{sdr} \quad i_{sqr} \quad \emptyset_r \quad 0 \quad \omega_{rr}]^T$ are generated based on FOC conditions

($\emptyset_{rq}$=0) where the references generator should has the load torque. Two kind of control based MVT approach are compared in this part, the robust control and conventional control those presented in (a) and (b) respectively in the next figures in order to show the robustness of the robust control. The reference of the rotor speed is firstly chosen for null speed test. For the low speed test, a reference speed of 50rad/sec is chosen. Whereas a reference of 150rad/sec is taken for the high speed test. Finally for the reverse speed test, -150rad/sec is taken to prove the effectiveness of the control. The IM motor is unloaded firstly, then a nominal load torque of 0.7 N.m is applied through a DC generator to the IM.

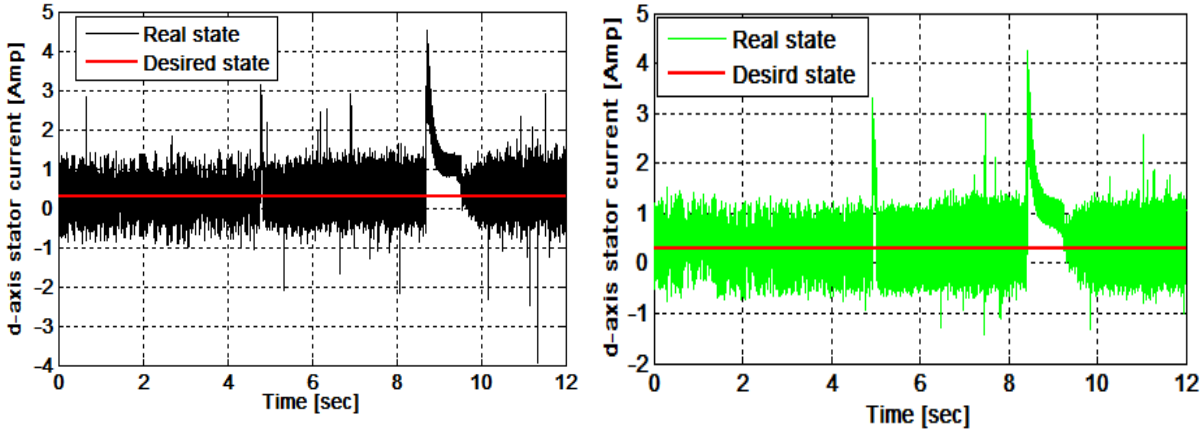

a) **b)**

Figure 4.34 The d-axis stator current

Robust control (a)

Conventional control (b)

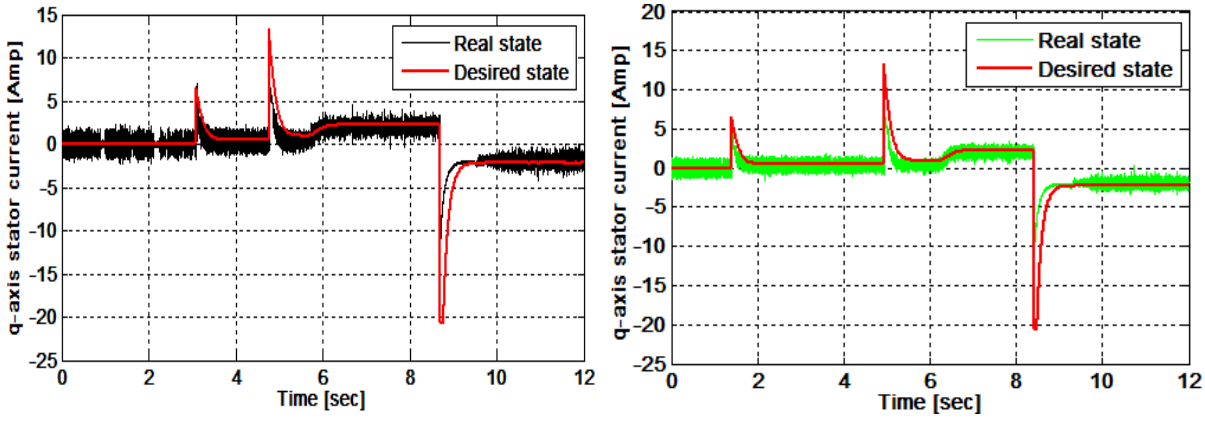

a) **b)**

Figure 4.35 The q-axis stator current

Robust control (a)

Conventional control (b)

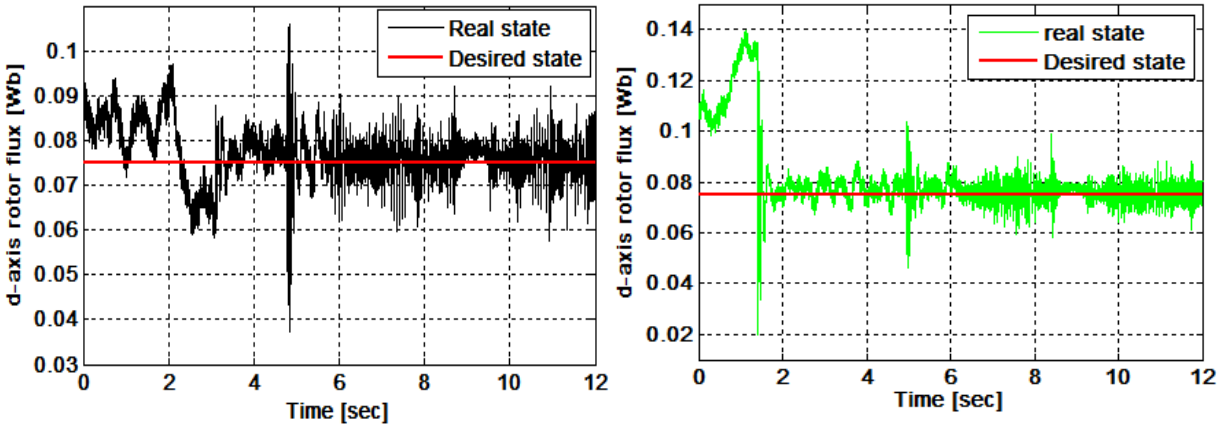

a) **b)**

Figure 4.36 The d-axis rotor flux

Robust control (a)

Conventional control (b)

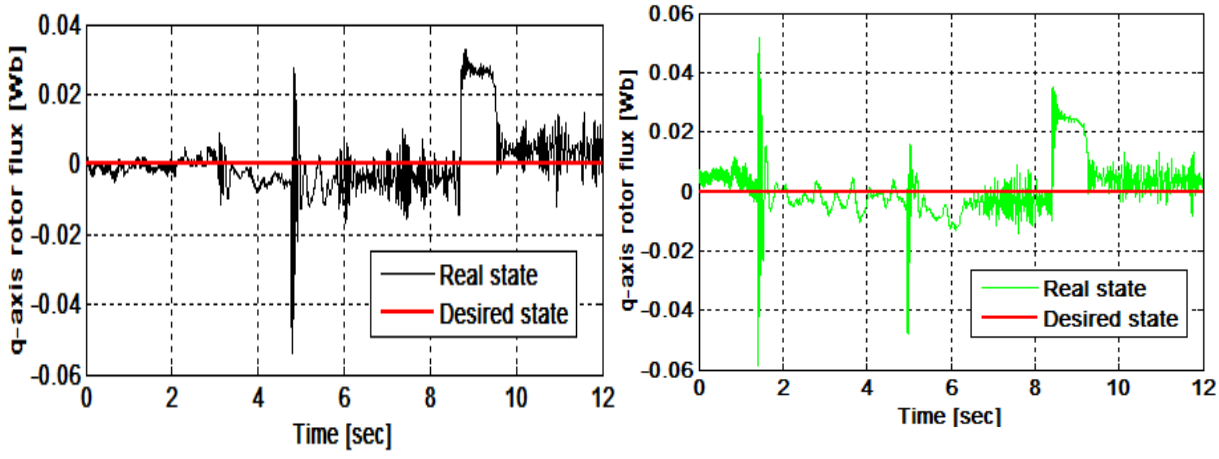

a) **b)**

Figure 4.37 The q-axis rotor flux

Robust control (a)

Conventional control (b)

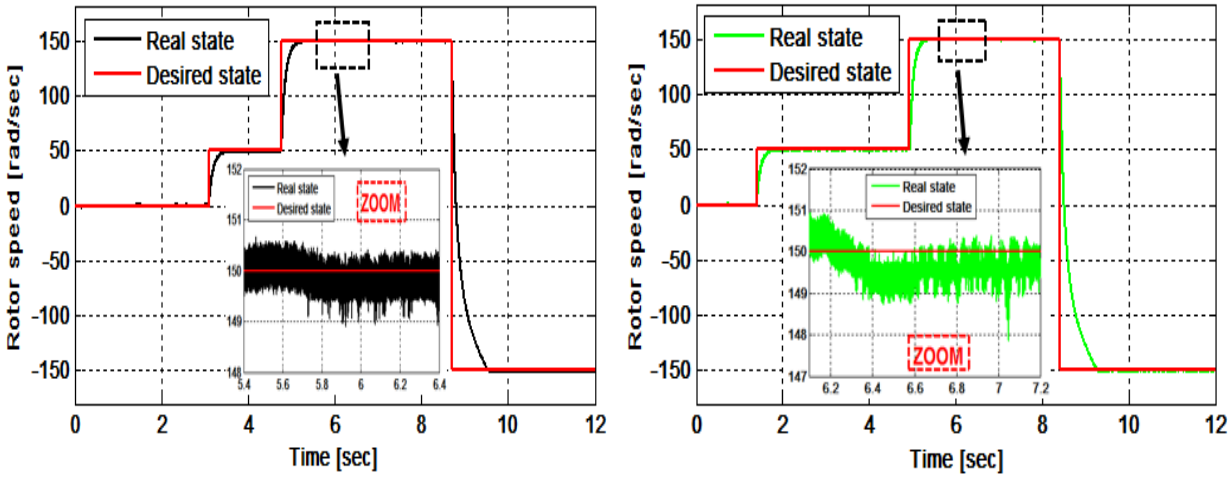

a) **b)**

Figure 4.38 The rotor speed

Robust control (a)

Conventional control (b)

Based on figures 4.34 and 4.35, the d and q axis stator currents are track their desired values with a minimum error approximately zero in all experimental time even in the application of the nominal load torque. The robust H_∞ control also show a minimum tracking error for the null speed

test except for the rotor fluxes as presented in figures 4.36 and 4.37. The effect of the load torque is not observable for the robust control where the speed decrease by 1rad/sec at the moment of application of the load torque for the normal control as indicated in figure 4.38.

It's clear from the previous experimental results the success of the robust control against the normal one that is also acceptable. However the MVT approach is simple to implement, These results show the effectiveness of the MVT approach, which can be considered to replace the previous hard and complex technics in industrial applications.

4.4.2.2 PI controller based observer

The proposed PI control based observer strategy based on MVT approach is shown in figure 4.25. As can be seen that the structure of the controller is similar to having 5 PI controllers, one for each state. The desired states $[i_{sdr} \quad i_{sqr} \quad \emptyset_r \quad 0 \quad \omega_{rr}]^T$ are generated from the load torque and FOC conditions ($\emptyset_{rq}$ = 0). Where as in linear systems, a Lupberger observer is applied to the IM. By measuring the two line currents and the rotor speed, the MVT observer estimates all the IM states $[i_{sd} \quad i_{sq} \quad \emptyset_{rd} \quad \emptyset_{rq} \quad \omega_r]^T$. The reference of the rotor speed is firstly chosen for null speed test. For the high speed test, a reference speed of 150rad/sec is taken. Whereas a reference of 20rad/sec is taken for the low speed test. The IM motor is unloaded firstly, then a nominal load torque of 0.7 N.m is applied to the IM at t=5.3sec through a DC generator. Because of the missing of the flux sensor, we present just the desired and estimated of the d and q-axis rotor fluxes as figures 4.41 and 4.42 indicate.

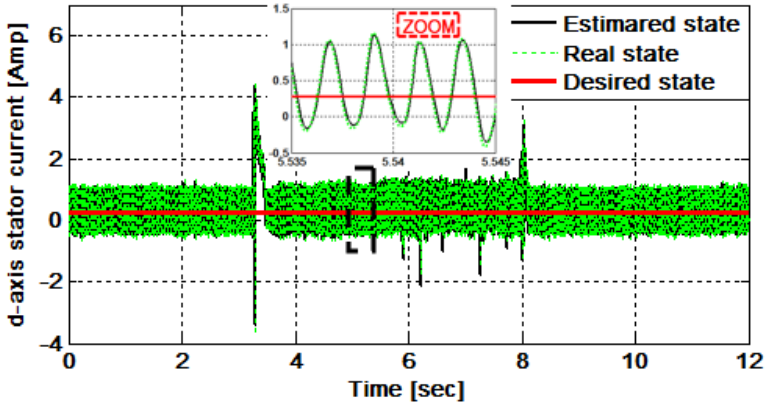

Figure 4.39 The d-axis stator current

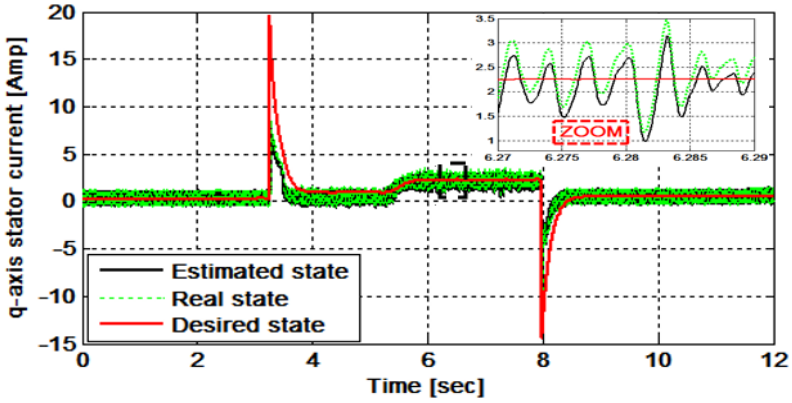

Figure 4.40 The q-axis stator current

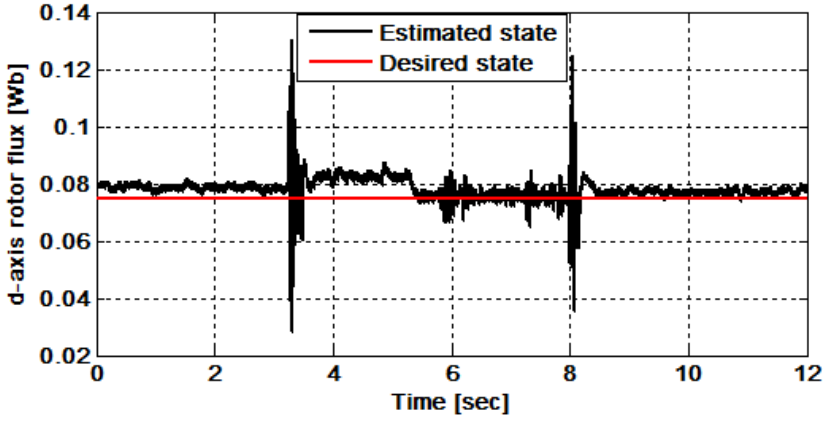

Figure 4.41 The d-axis rotor flux

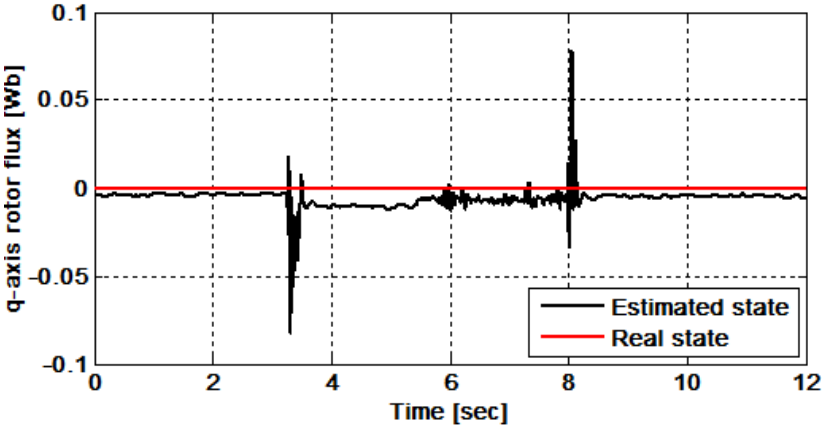

Figure 4.42 The q-axis rotor flux

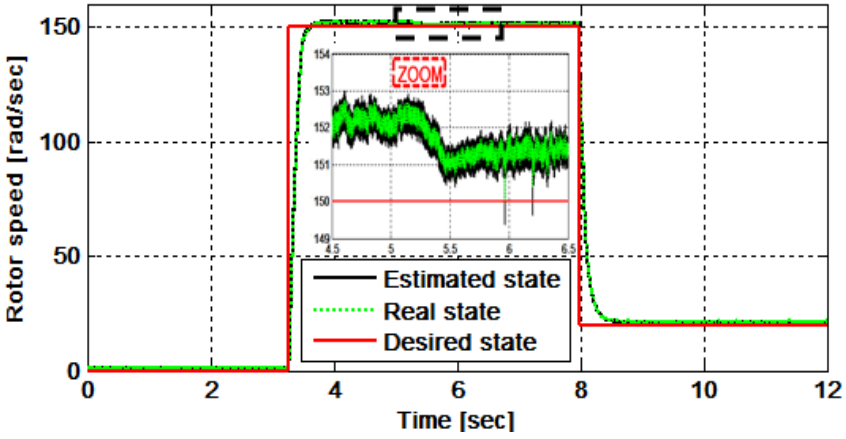

Figure 4.43 The rotor speed

The estimation error of d and q axis stator currents is approximately zero, where the real and estimated states of them are around the desired states as proposed in figures 4.39 and 4.40 respectively. A maximum tracking error of 0.008 Wb for the d-axis rotor flux, where it doesn't exceed 0.01Wb for the q-axis rotor flux as shown in figures 4.41 and 4.42 respectively. The figure 4.43 indicates the success of the PI control based observer based on the MVT through a minimum effect of the load torque to the control and estimation errors and a minimum effect of them against different speeds test.

The MVT approach for control based observer not only has a systematic and proven methodology, the parameters of the controller and observer have been calculated separately and don't depend on the IM states, but also has good performances and efficiency as the previous experimental results show. These advantages of the MVT allow seeing this strategy in the industrial applications in the next years.

4.4 Conclusion

In this chapter, we have firstly modeled the IM drive system in the two axes rotating frame, OL-FOC and references generation are presented after, then the design, the simulation results, and different experiments are mentioned for control and states estimation based on the MVT approach of the IM such as the extended observer, the robust control and controller based observer.

Despite the high complexity, the strong nonlinearity and the coupled IM system, The obtained simulation and experimental results show the effectiveness of the MVT approach. By a unique gain has been calculated offline and doesn't depend on the IM states, the MVT approach allows the IM system to submit to the control and the estimation conditions. Due to the efficiency, the robustness, the simplicity and the low cost of the MVT approach, we can see this technic in industrial applications in the next years.

References

[1] H. Su and K. T. Chong, "Induction machine condition monitoring using neural network modeling," *IEEE Transactions on Industrial Electronics*, vol. 54, pp. 241-249, 2007.

[2] S. Abu Saad, "The Untilisation of Information Available in a Sensorless Control System of an AC Induction Motor for Condition Monitoring," University of Huddersfield, 2015.

[3] A. Hughes and W. Drury, *Electric motors and drives: fundamentals, types and applications*: Newnes, 2013.

[4] A. H. Bonnett and T. Albers, "Squirrel cage rotor options for AC induction motors," in *Pulp and Paper Industry Technical Conference, 2000. Conference Record of 2000 Annual*, 2000, pp. 54-67.

[5] A. M. Trzynadlowski, *Control of induction motors*: Elsevier, 2000.

[6] D. R. Patrick and S. W. Fardo, *Industrial process control systems*: The Fairmont Press, Inc., 2009.

[7] M. Y. HAMMOUDI, "Contribution à la commande et à l'observation dans l'association convertisseurs machine," Université Mohamed Khider-Biskra, 2015.

[8] H. B. Zina, M. Allouche, M. Souissi, M. Chaabane, and L. Chrifi-Alaoui, "Robust sensor fault-tolerant control of induction motor drive," *International Journal of Fuzzy Systems*, vol. 19, pp. 155-166, 2017.

[9] H. B. Zina, M. Allouche, M. Souissi, M. Chaabane, L. Chrifi-Alaoui, and M. Bouattour, "A Takagi-Sugeno fuzzy control of induction motor drive: experimental results," *International Journal of Automation and Control*, vol. 12, pp. 44-61, 2018.

[10] O. Zeghib, A. Allag, M. Allag, and B. Hamidani, "An Extended MVT Observer Designed for Induction Motor Drive," *Mediterranean Journal of Measurement and Control,* vol. 13, pp. 805-811, 2017.

[11] M. Y. Hammoudi, A. Allag, M. Becherif, M. Benbouzid, and H. Alloui, "Observer design for induction motor: an approach based on the mean value theorem," *Frontiers in Energy,* vol. 8, pp. 426-433, 2014.

[12] H. b. Zina, M. Allouche, M. Souissi, M. Chaabane, L. Chrifi-Alaoui, and M. Bouattour, "Descriptor observer based fault tolerant tracking control for induction motor drive," *automatika,* vol. 57, pp. 703-713, 2016.

[13] A. Allag, A. Benakcha, M. Allag, I. Zein, and M. Y. Ayad, "Classical state feedback controller for nonlinear systems using mean value theorem: closed loop-FOC of PMSM motor application," *Frontiers in Energy,* vol. 9, p. 413, 2015.

[14] D. Ichalal, B. Marx, J. Ragot, and D. Maquin, "Brief paper: State estimation of Takagi-Sugeno systems with unmeasurable premise variables," *IET Control Theory & Applications,* vol. 4, pp. 897-908, 2010.

[15] M. Y. Hammoudi, M. H. Benbouzid, N. Rizoug, and A. Allag, "New state observer based on Takagi-Sugeno fuzzy controller of induction motor," in *Systems and Control (ICSC), 2015 4th International Conference on*, 2015, pp. 145-150.

[16] G. Phanomchoeng, "State, parameter, and unknown input estimation problems in active automotive safety applications," 2011.

[17] A. Moez, S. Mansour, C. Mohamed, and M. Driss, "Takagi-Sugeno Fuzzy Control of Induction Motor," *Proc. Int. Journal of Electrical and Electronics Engg*, vol. 2, 2009.

[18] J. Yoneyama, "Nonlinear control design based on generalized Takagi–Sugeno fuzzy systems," *Journal of the Franklin Institute,* vol. 351, pp. 3524-3535, 2014.

[19] K. Tanaka and H. O. Wang, *Fuzzy control systems design and analysis: a linear matrix inequality approach*: John Wiley & Sons, 2004.

[20] D. Ichalal, B. Marx, S. Mammar, D. Maquin, and J. Ragot, "How to cope with unmeasurable premise variables in Takagi–Sugeno observer design: Dynamic extension approach," *Engineering Applications of Artificial Intelligence,* vol. 67, pp. 430-435, 2018.

Chapter 5:
Diagnosis and fault tolerant control of the induction motor based on the T-S fuzzy approach

5.1 Introduction:

The IM's are the most machines that are used in industrial applications due to its simple construction, robustness, and low cost[1]. In order to reach a high efficiency and with the development of the power electronics components, the control of the IM's become an integral part of the actual industrial application. The control or the estimation of the states of the IM drives never happened without the using of sensors to get the IM states in order to control them. In the industry, these sensors are partially or completely exhibiting of corruption in any moment, which leads to a lot of issues may reach the losing of all the system if it doesn't stop in the appropriate moment that is so impossible to do without diagnosis and FTC approaches.

The objective is now to use it in order to actively reconfigure the control law by eliminating (or at least minimizing) the sensor fault effect on the system. Based on T-S representation of the IM, the FTC approach has been proved with a systematic methodology in order to get the extended fuzzy observer gains that estimates the IM states and moreover the sensor fault, and also to get the fuzzy robust controller gains that makes the IM subject to the control conditions in the two cases faulty and healthy sensors. In the current chapter, we will present the T-S form, of the IM, the design of the FTC approach based on the T-S fuzzy model of the IM and the simulation results and discussion and it's ended by a conclusion.

5.2 T-S model of the IM

In the last chapter, we present the nonlinear model of the IM as in (4.9) indicate.

To ensure the field-oriented control strategy(the rotor flux is oriented on the d-axis and its q-axis is null), the electrical speed of the stator in the rotating synchronous d-q frame must be chosen as:

$$\omega_s = n_p\omega_r + \frac{M}{\tau_r \emptyset_r} i_{sq} \tag{5.1}$$

Where $\emptyset_r$ is the rotor flux reference.

Then this nonlinear model can be represented in the following form:

$$\begin{cases} \dot{x}(t) = A_x x(t) + Bu(t) + v(t) \\ y(t) = Cx(t) \end{cases} \tag{5.2}$$

Where:

$$A_x = \begin{bmatrix} -\gamma & \omega_s & \frac{k_s}{\tau_r} & k_s n_p \omega_r & 0 \\ -\omega_s & -\gamma & -k_s n_p \omega_r & \frac{k_s}{\tau_r} & 0 \\ \frac{M}{\tau_r} & 0 & -\frac{1}{\tau_r} & \frac{M}{\tau_r \emptyset_r} i_{sq} & 0 \\ 0 & \frac{M}{\tau_r} & -\frac{M}{\tau_r \emptyset_r} i_{sq} & -\frac{1}{\tau_r} & 0 \\ 0 & 0 & \frac{n_p M}{J L_r} i_{sq} & -\frac{n_p M}{J L_r} i_{sd} & -\frac{b}{J} \end{bmatrix}$$

With

$$x(t) = [i_{sd} \quad i_{sq} \quad \emptyset_{rd} \quad \emptyset_{rq} \quad \omega_r]^T$$

$$B = \begin{bmatrix} \frac{1}{\sigma Ls} & 0 & 0 & 0 & 0 \\ 0 & \frac{1}{\sigma Ls} & 0 & 0 & 0 \end{bmatrix}^T$$

$$u(t) = \begin{bmatrix} U_{ds} \\ U_{qs} \end{bmatrix}$$

$$v(t) = \begin{bmatrix} 0 & 0 & 0 & 0 & -\frac{1}{J}T_L \end{bmatrix}^T$$

$$C = \begin{bmatrix} 1 & 0 & 0 & 0 & 0 \\ 0 & 1 & 0 & 0 & 0 \end{bmatrix}$$

The fuzzy model can be constructing using the well-known sector nonlinearity technique. The system (5.2) is constituted by the following three nonlinearities:

$$\begin{cases} z_1(t) = i_{sd}(t) \\ z_2(t) = i_{sq}(t) \\ z_3(t) = \omega_r(t) \end{cases} \tag{5.3}$$

The local weighting functions are defined by:

$$\begin{cases} F_{1j}(t) = \dfrac{z_j(t) - z_{j\,min}}{z_{j\,max} - z_{j\,min}} \\ F_{2j}(t) = \dfrac{z_{j\,max} - z_j(t)}{z_{j\,max} - z_{j\,min}} \end{cases} \tag{5.4}$$

Thus we can transform the nonlinear terms under the following shape:

$$z_j(t) = F_{1j}(t) z_{j\,max} + F_{2j}(t) z_{j\,min}; \quad j = \{1,2,3\} \tag{5.5}$$

Consequently, the global fuzzy model of the IM can be written in the following form[2, 3]:

$$\begin{cases} \dot{x}(t) = \sum_{i=1}^{8} \mu_i(z(t)) \big(A_i x(t)\big) + Bu(t) + v(t) \\ y(t) = Cx(t) \end{cases} \tag{5.6}$$

Where

$$\begin{cases} \mu_i(z(t)) = \dfrac{h_i(z(t))}{\sum_{i=1}^{8} h_i(z(t))}; \\ h_i(z(t)) = \prod_{j=1}^{3} F_{ij}\left(z_j(t)\right) \\ \mu_i(z(t)) > 0\,, \sum_{i=1}^{8} h_i(z(t)) = 1 \end{cases}$$

5.3 Observer-Based Fault-Tolerant Tracking Control

5.3.1 Reference model

The references states are generated under FOC conditions by substituting the real states of the IM model by the desired states, where the dynamics of the desired states is as follows[4]:

$$\dot{x}_c(t) = A_c x_c(t) + r(t) \tag{5.7}$$

Where

$x_c(t) = [i_{sdr} \quad i_{sqr} \quad \emptyset_r \quad 0 \quad \omega_{rr}]^T$

$$A_c = \begin{bmatrix} -\gamma & \omega_{sr} & \dfrac{k_s}{\tau_r} & k_s\, n_p \omega_{rr} & 0 \\ -\omega_{sr} & -\gamma & -k_s\, n_p \omega_{rr} & \dfrac{k_s}{\tau_r} & 0 \\ \dfrac{M}{\tau_r} & 0 & -\dfrac{1}{\tau_r} & \dfrac{M}{\tau_r \emptyset_r} i_{sqr} & 0 \\ 0 & \dfrac{M}{\tau_r} & -\dfrac{M}{\tau_r \emptyset_r} i_{sqr} & -\dfrac{1}{\tau_r} & 0 \\ 0 & 0 & \dfrac{n_p M}{J L_r} i_{sqr} & -\dfrac{n_p M}{J L_r} i_{sdr} & -\dfrac{b}{J} \end{bmatrix}$$

And

$$r(t) = [B \quad I] \begin{bmatrix} u_r(t) \\ v(t) \end{bmatrix}$$

With

$u_r(t) = \begin{bmatrix} U_{sdr} \\ U_{sqr} \end{bmatrix}$ where U_{sdr} and U_{sqr} are calculated as indicated in equation (4.14) in the last chapter.

The reference model (5.7) can be described via T–S fuzzy model where the global fuzzy reference model is inferred as:

$$\dot{x}_c(t) = \sum_{n=1}^{8} \mu_n(z_r(t))\big(A_{cn}x_c(t)\big) + r(t) \tag{5.8}$$

5.3.2 Sensor fault tolerant control design

In order to point up the proposed approach, the fault is injected to the T-S model (5.6) that represents the model of the IM. The faulty system can be written in the following structure:

$$\begin{cases} \dot{x}(t) = \sum_{i=1}^{8} \mu_i(z(t))\big(A_i x(t)\big) + Bu(t) + v(t) \\ y(t) = Cx(t) + Dg(t) \end{cases} \tag{5.9}$$

Where $g(t)$ denote the sensor fault. *D* is of appropriate dimension and assumed to be of full column rank.

Construct the augmented descriptor system consisting of the system (5.9) and the sensor fault as follows:

$$\begin{cases} \tilde{E}\dot{\tilde{x}}(t) = \sum_{i=1}^{8} \mu_i(z(t))\left(\tilde{A}_i\tilde{x}(t)\right) + \tilde{B}u(t) + \tilde{H}v(t) + \tilde{D}x_f(t) \\ y(t) = \tilde{C}\tilde{x}(t) + x_f(t) \end{cases} \tag{5.10}$$

Where

$$x_f(t) = Dg(t), \tilde{E} = \begin{bmatrix} I_n & 0 \\ 0 & 0 \end{bmatrix}, \tilde{x}(t) = \begin{bmatrix} x(t) \\ x_f(t) \end{bmatrix}, \tilde{A}_i = \begin{bmatrix} A_i & 0 \\ 0 & -I_p \end{bmatrix},$$

$$\tilde{B} = \begin{bmatrix} B \\ 0 \end{bmatrix}, \tilde{H} = \begin{bmatrix} I \\ 0 \end{bmatrix}, \tilde{D} = \begin{bmatrix} 0 \\ I_p \end{bmatrix}, \tilde{C} = [C \quad 0].$$

and the vector $x_f(t)$ is considered as an auxiliary state of the augmented system (5.10).

The following fuzzy observer is constructed to estimate simultaneously system state and the sensor fault

$$\begin{cases} E\dot{x}_f(t) = \sum_{i=1}^{8} \mu_i(z(t)) \left(N_i x_f(t)\right) + \tilde{B}u(t) \\ \hat{\tilde{x}}(t) = x_f(t) + Ly(t) \end{cases} \tag{5.11}$$

Where $x_f(t)$ is the auxiliary state vector and $\hat{\tilde{x}}(t)$is the state estimation vector while *L* are the gain matrices of the observer. The estimation error is defined as:

$$\tilde{e}(t) = \tilde{x}(t) - \hat{\tilde{x}}(t) = \begin{bmatrix} e_0(t) \\ e_f(t) \end{bmatrix} \tag{5.12}$$

Where $e_0(t)$ represent the state estimation error and $e_f(t)$ represent the fault estimation error.

Through (5.10) and (5.11) we can obtain:

$$\begin{aligned} &\left(\tilde{E} + EL\tilde{C}\right)\tilde{x}(t) - E\hat{\tilde{x}}(t) \\ &\qquad = \sum_{i=1}^{8} \mu_i(z(t)) \left(\left(\tilde{A}_i + N_i L\tilde{C}\right)\tilde{x}(t) - N_i\hat{\tilde{x}}(t) + \left(\tilde{D} + N_i L\right)x_f(t)\right. \\ &\qquad \left. + \tilde{H}v(t)\right) \end{aligned} \tag{5.13}$$

As in[5], if we choose:

$$\begin{cases} N_i = \tilde{A}_i + N_i L \tilde{C} \\ E = \tilde{E} + E L \tilde{C} \\ \widetilde{D} = -N_i L \end{cases} \tag{5.14}$$

The dynamic error can be written as the following form:

$$E\tilde{e}(t) = \sum_{i=1}^{8} \mu_i(z(t)) \left(N_i \tilde{e}(t) + \widetilde{H} v(t) \right) \tag{5.15}$$

In order to ensure the constraints (5.14), the observer parameters are chosen as:

$N_i = \begin{bmatrix} A_i & 0 \\ -C & I_p \end{bmatrix}$, $L = \begin{bmatrix} 0 \\ I_p \end{bmatrix}$ and $E = \begin{bmatrix} I_n & 0 \\ RC & R \end{bmatrix}$ with R is a nonsingular matrix.

Then the dynamics of the state estimation error can be written as follows:

$$\tilde{\dot{e}}(t) = \sum_{i=1}^{8} \mu_i(z(t)) \left(S_i \tilde{e}(t) + H_e v(t) \right) \tag{5.16}$$

With

$S_i = E^{-1} N_i = \begin{bmatrix} A_i & 0 \\ -CA_i - R^{-1}C & R^{-1} \end{bmatrix}$ and $H_e = E^{-1}\widetilde{H} = \begin{bmatrix} I_n \\ -C \end{bmatrix}$

The following fuzzy controller is employed to deal with the above control system design. The goal is to design the control law such that the system state converges toward the reference state given by even in presence of a sensor fault. The control strategy is illustrated in figure 4.1. The following structure is proposed for the control law[6, 7]:

$$u(t) = \sum_{i=1}^{8} \mu_i(z(t)) \left(-x_f(t) + K_i \left(\hat{x}(t) - x_c(t) \right) \right) \tag{5.17}$$

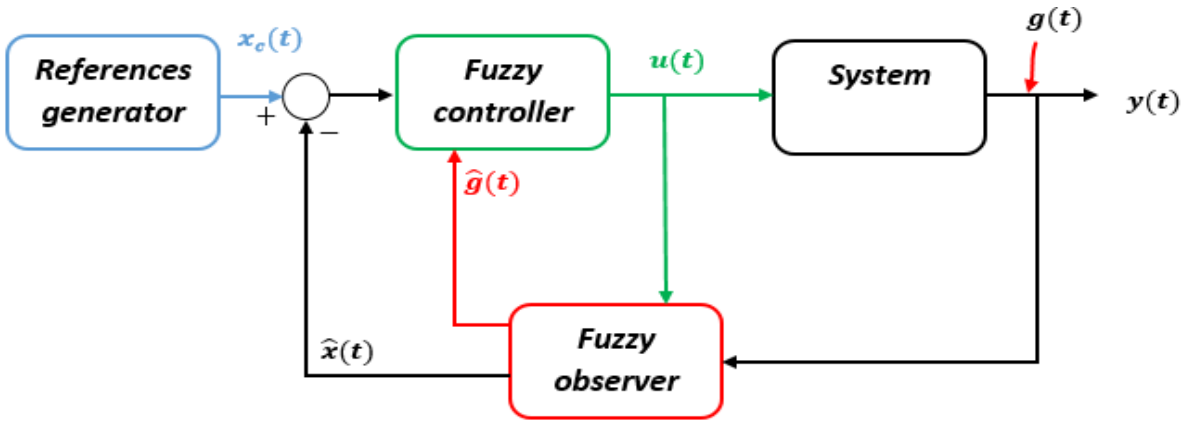

Figure 5.1 Fault tolerant control scheme

The control error is defined as follows:

$$e_c(t) = x_c(t) - \hat{x}(t) \tag{5.18}$$

Then it's possible to get the dynamics of the tracking error as follows using (5.8),(5.10) and (5.17):

$$\dot{e}_c(t) = \sum_{n=1}^{8}\sum_{i=1}^{8} \mu_n(z_r(t))\mu_i(z(t))(A_i + BK_i)e_c(t) - BK_i e_0(t) + (A_i - A_{cn})x_c(t) + v(t) - r(t) \tag{5.19}$$

We construct an augmented system containing the tracking, the estimation and the fault error as presented in the next equation:

$$\dot{e}_a(t) = \sum_{n=1}^{8}\sum_{i=1}^{8} \mu_n(z_r(t))\mu_i(z(t))(A_{ai}e_a(t) + T_{in}\rho(t)) \tag{5.20}$$

Where

$$e_a(t) = \begin{bmatrix} e_c(t) \\ e_0(t) \\ e_f(t) \end{bmatrix}, \rho(t) = \begin{bmatrix} v(t) \\ r(t) \\ x_c(t) \end{bmatrix}, A_{ai} = \begin{bmatrix} A_i + BK_i & BK_i & 0 \\ 0 & A_i & 0 \\ 0 & -CA_i - R^{-1}C & R^{-1} \end{bmatrix},$$

$$T_{in} = \begin{bmatrix} I & -I & A_i - A_{cn} \\ I & 0 & 0 \\ -C & 0 & 0 \end{bmatrix}$$

in order to ensure a minimum effect of the disturbances to the tracking error, an H_∞ performance is introduced to do so where it's as follows:

$$\int_0^{t_f} {e_a}^T \tilde{Q}\, e_a dt = \gamma^2 \int_0^{t_f} \rho(t) dt \tag{5.21}$$

Where

$$\tilde{Q} = \begin{bmatrix} Q & 0 & 0 \\ 0 & 0 & 0 \\ 0 & 0 & 0 \end{bmatrix}$$

the objective is now to use it in order to actively reconfigure the control law by eliminating (or at least minimizing) the fault effect on the system, and able to force the output of the IM to tracks the reference signal in both the faulty and fault-free cases.

Theorem 5.1 [8](For the proof of theorem 5.1, see Appendix B): For a given positive scalar δ, the closed loop fuzzy system in (5.20) is asymptotically stable and the H_∞ performance is guaranteed with an attenuation level γ and provided that the signal $\rho(t)$ is bounded, if there exist symmetric positive-definite matrices P_1, P_2 and P_3 and matrices J_i, β and the scalar γ satisfying the following LMI constraint

$$\begin{bmatrix} Ж_{in} & Л_{in} \\ * & \Gamma_{in} \end{bmatrix} < 0\ ; \quad for\ i,n = 1,\ldots,8 \tag{5.22}$$

Where

$$Ж_{in} = \begin{bmatrix} Ж_{1,1} & -BJ_i & 0 & 0 & 0 & I & -I & A_i - A_{cn} \\ * & -2\delta P_1 & 0 & 0 & 0 & 0 & 0 & 0 \\ * & * & -2\delta I & 0 & 0 & 0 & 0 & 0 \\ * & * & * & -2\delta I & 0 & 0 & 0 & 0 \\ * & * & * & * & -2\delta I & 0 & 0 & 0 \\ * & * & * & * & * & -2\delta I & 0 & 0 \\ * & * & * & * & * & * & -2\delta I & 0 \\ * & * & * & * & * & * & * & -2\delta I \end{bmatrix}$$

$$Л_{in} = \begin{bmatrix} 0 & 0 & 0 & 0 & 0 & 0 & 0 & P_1 \\ \delta I & 0 & 0 & 0 & 0 & 0 & 0 & 0 \\ 0 & \delta I & 0 & 0 & 0 & 0 & 0 & 0 \\ 0 & 0 & \delta I & 0 & 0 & 0 & 0 & 0 \\ 0 & 0 & 0 & \delta I & 0 & 0 & 0 & 0 \\ 0 & 0 & 0 & 0 & \delta I & 0 & 0 & 0 \\ 0 & 0 & 0 & 0 & 0 & \delta I & 0 & 0 \\ 0 & 0 & 0 & 0 & 0 & 0 & \delta I & 0 \end{bmatrix}$$

$$\Gamma_{in} = \begin{bmatrix} \Gamma_{1,1} & 0 & \Gamma_{1,3} & 0 & P_2 & 0 & 0 & 0 \\ * & -\gamma^2 I & 0 & 0 & 0 & 0 & 0 & 0 \\ * & * & \Gamma_{3,3} & 0 & -P_3 C & 0 & 0 & 0 \\ * & * & * & -\gamma^2 I & 0 & 0 & 0 & 0 \\ * & * & * & * & -\gamma^2 I & 0 & 0 & 0 \\ * & * & * & * & * & -\gamma^2 I & 0 & 0 \\ * & * & * & * & * & * & -\gamma^2 I & 0 \\ * & * & * & * & * & * & * & -Q^{-1} \end{bmatrix}$$

With

$Ж_{1,1} = A_i P_1 + P_1 {A_i}^T - BJ_i - B^T {J_i}^T$

$\Gamma_{1,1} = P_2 A_i + {A_i}^T P_2$

$\Gamma_{1,3} = {A_i}^T C^T P_3 - C^T \beta$

$\Gamma_{3,3} = -\beta^T - \beta$

$R = (-\beta^{-1} P_3)^{-1}$

$K_i = J_i {P_1}^{-1}$

Then the tracking control performance is guaranteed and the sensor fault can be estimated by:

$$\hat{g}(t) = (D^T D)^{-1} D^T [0 \quad I_n] \hat{\hat{x}}(t) \tag{5.23}$$

The previous theorem derives a condition that guarantees the stability of the closed-loop system and the trajectory tracking performances. The result is expressed in the form of LMI's which can be easily solved by using the YALMIP software computer[9].

5.4 Simulation results

The proposed FTC design based T-S fuzzy approach (figure 5.1) is implemented through an illustrative simulation check under the MATLAB/Simulink environment. The FTC is applied to an IM which its parameters are mentioned in Appendix A. The global scheme of the FTC concept is presented in figure 5.3:

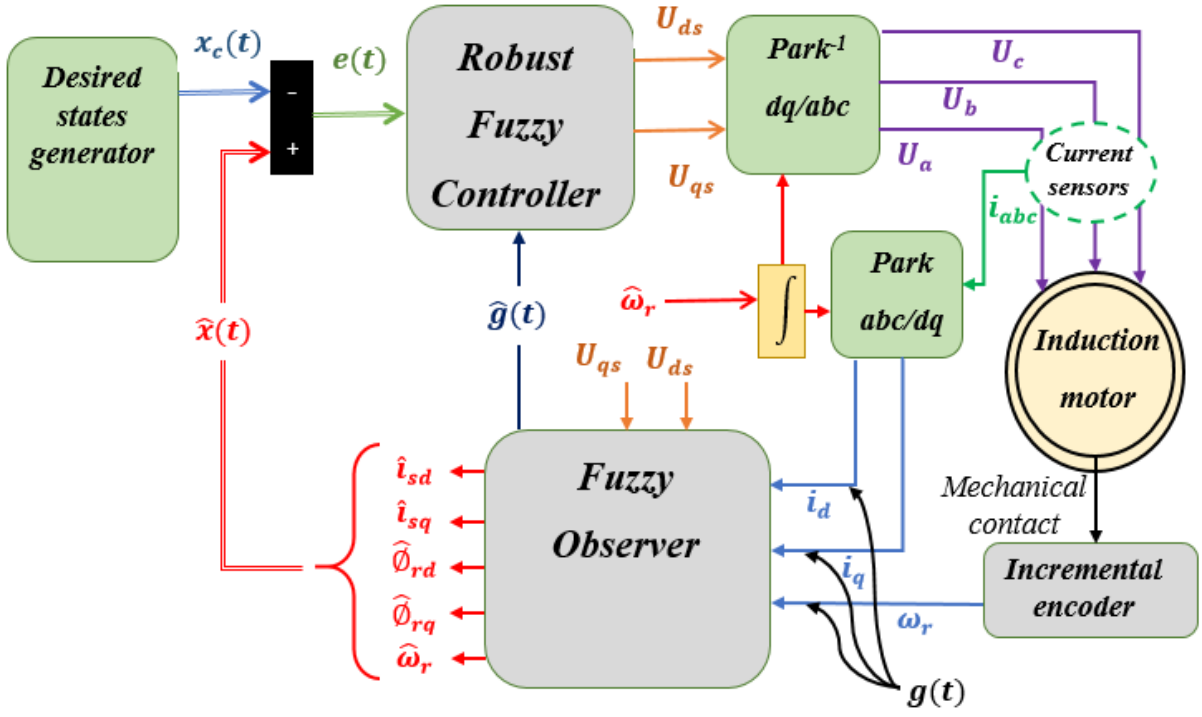

Figure 5.2 the global scheme of the proposed FTC approach applied to IM

The design of the FTC approach for IM control strategy has been previously shown in figure 4.3. The desired states are generated based on FOC conditions ($\emptyset_{rq}$=0) where the references generator should has the load torque as well presented in sub-section 5.3.1. Two kind of control based T-S fuzzy approach are compared in this part, the control and estimation with FTC and without FTC those presented in (a) and (b) respectively in the next figures in order to show the effectiveness of

the FTC concept. The reference of the rotor speed is firstly chosen 50rad/sec for low speed test, whereas a reference of 150rad/sec is taken for the high speed test at t=4.5sec. The IM motor is unloaded firstly, then a nominal load torque of 0.7 N.m is applied to the IM at t=3sec. In this simulation test, it considered that the faults are happened as follows:

$$d\ and\ q-axis\ stator\ current \begin{cases} 0\ for\ t \in [0,1] \\ 2\ for\ t \in [1,4] \\ 0\ for\ t \in [4,7] \end{cases}$$

$$rotor\ speed \begin{cases} 0\ for\ t \in [0,1] \\ 50\ for\ t \in [1,4] \\ 0\ for\ t \in [4,7] \end{cases}$$

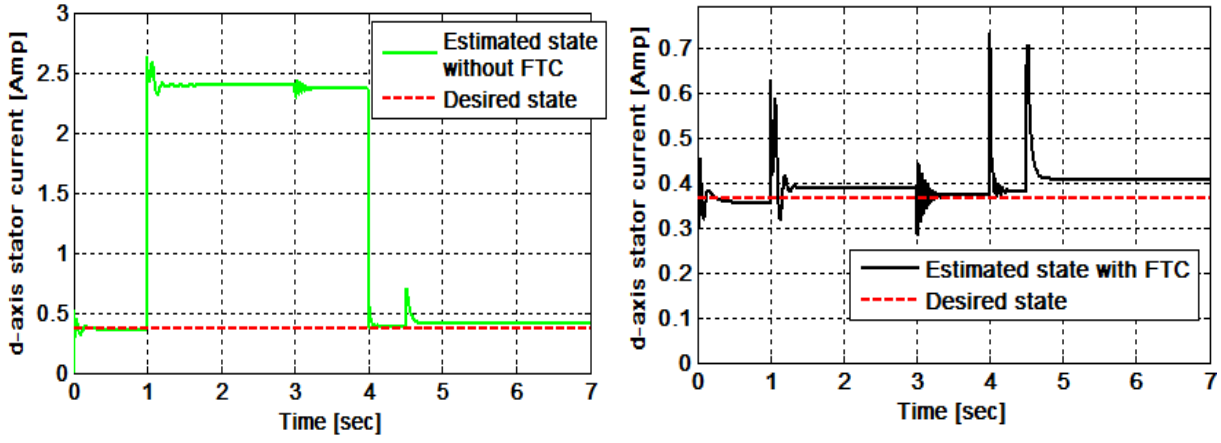

a) **b)**

Figure 5.3 The d-axis stator current

Without FTC (a)

With FTC (b)

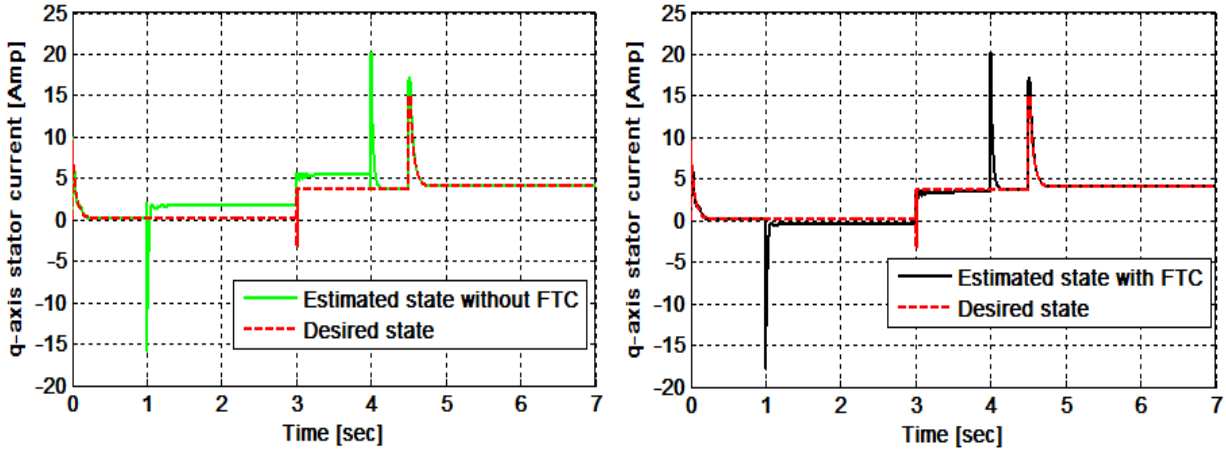

a) **b)**

Figure 5.4 The q-axis stator current

Without FTC (a)

With FTC (b)

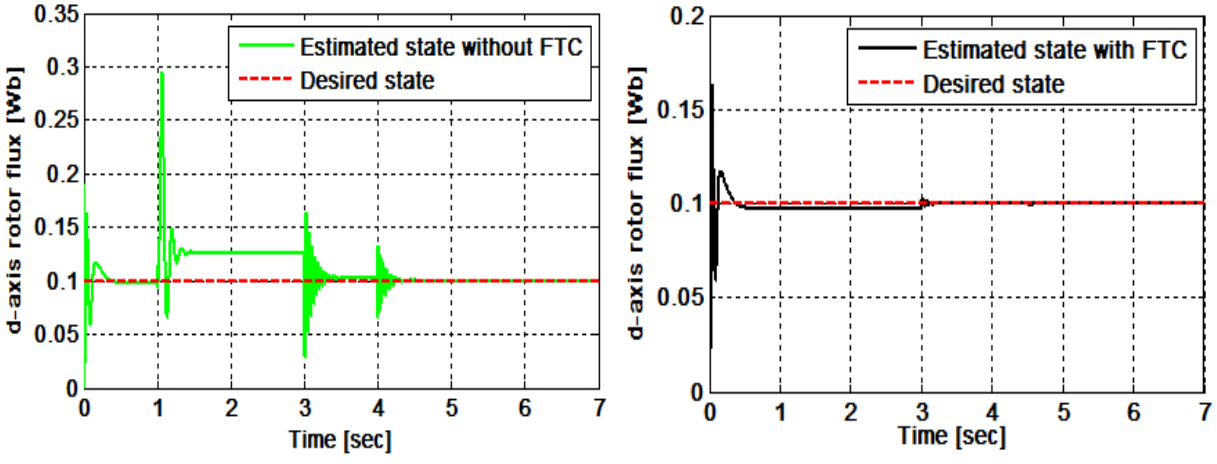

a) **b)**

Figure 5.5 The d-axis rotor flux

Without FTC (a)

With FTC (b)

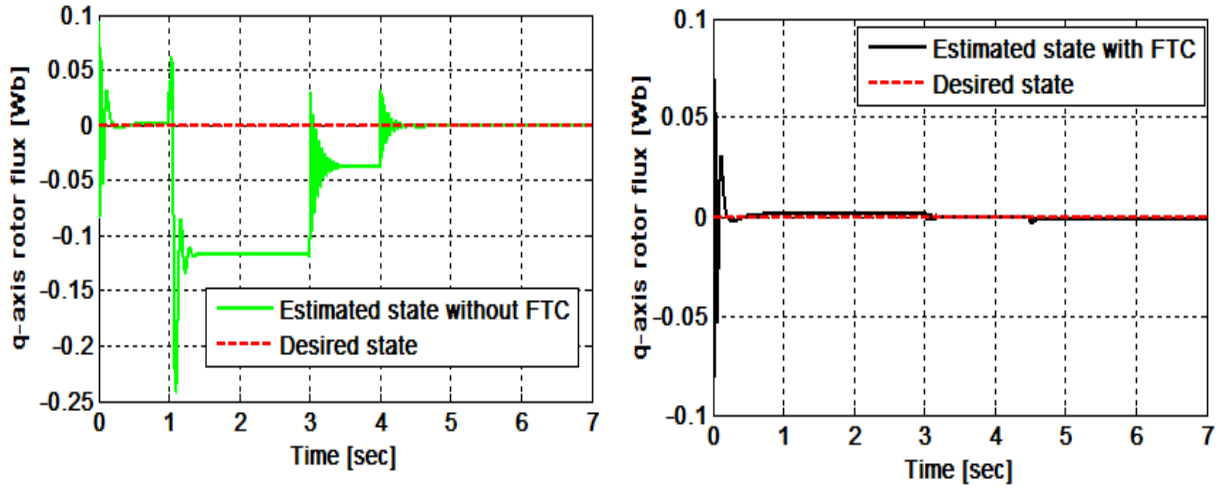

a) **b)**

Figure 5.6 The q-axis rotor flux

Without FTC (a)

With FTC (b)

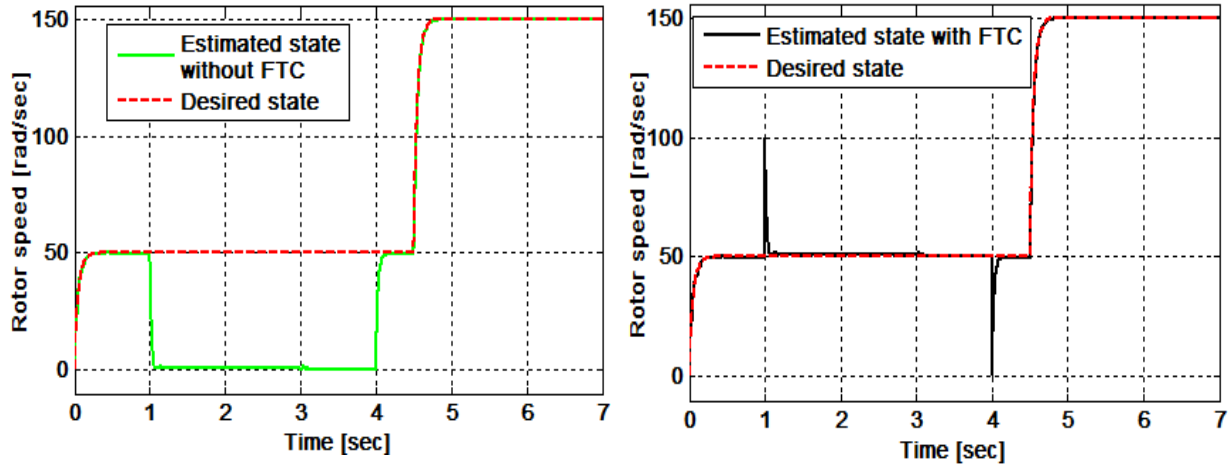

a) **b)**

Figure 5.7 The rotor speed

Without FTC (a)

With FTC (b)

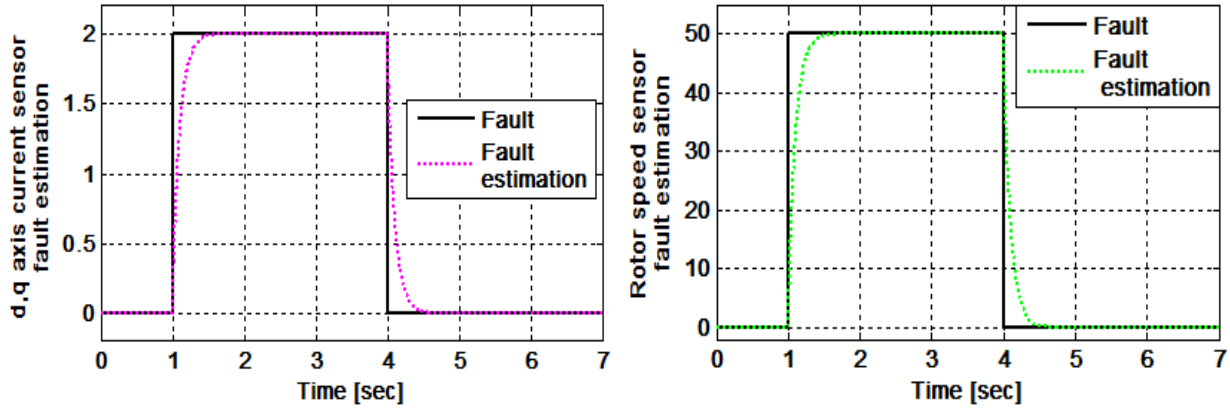

a) **b)**

Figure 5.8 The faults estimation

d and q axis currents fault (a)

Rotor speed fault (b)

Based on the simulation results mentioned above for the control of the IM with and without FTC approach, we can illustrate:

- The using of the FTC approach allow the real states of the IM to stay close to their desired states even in presence of sensor faults, otherwise, without FTC, it's noted that the appearance of the sensor fault effects the tracking error with considerable values.
- As known, most of the control theories are based on FOC conditions. Without FTC approach the q-axis rotor flux no longer stays zero when the sensor faults have done and you can't know how the IM behave. Whereas for the case with FTC, the FOC conditions are ensured through a tracking error approximately zero in faulty and healthy situations.
- A sensor fault can cause a set of problems may reach until the loss of the IM him-self through the high currents those move in the IM windings. With the FTC, we avoid this issue by taking into consideration the sensor fault in the control law and that allow to respect the IM constraints.
- For the diagnosis part, it possible to detect the type of the sensor fault and in which sensor is it, this through the estimation of the sensor faults as indicated in figure 5.8.

- Because of the T-S fuzzy approach has a systematic and proven methodology in order to obtain the controller and observer gains, and the effectiveness of the FTC has been shown, this approach can be used in the industry in the following years.

5.5 Conclusion

In this chapter, the design of the observer based FTC tracking of the IM drive system based on the transferring of the IM nonlinear model to the T-S form is distinctly presented, then simulation results about the FTC approach are mentioned in order to affirm the effectiveness of the presented approach is mentioned hereafter. Without the FTC concept, a sensor fault can cause a set of issues such as the loss of the control track, the loss of the FOC conditions that control theories based on it, and may reach the loss of the IM through the high currents those move in the IM windings. The using of the FTC approach make possible to eliminate or minimize the sensor fault effect to the control condition with the detection of the sensor fault kind and in which sensor is it. Due to the efficiency, the robustness, the proven and the systematic methodology for the stability proving and the low cost of the FTC approach based T-S fuzzy approach, we can see this technic in industrial applications in the next years in order to avoid the damage and control losing of the electrical machines.

References

[1] M. Y. Hammoudi, A. Allag, M. Becherif, M. Benbouzid, and H. Alloui, "Observer design for induction motor: an approach based on the mean value theorem," *Frontiers in Energy*, vol. 8, pp. 426-433, 2014.

[2] H. B. Zina, M. Allouche, M. Souissi, M. Chaabane, L. Chrifi-Alaoui, and M. Bouattour, "A Takagi-Sugeno fuzzy control of induction motor drive: experimental results," *International Journal of Automation and Control*, vol. 12, pp. 44-61, 2018.

[3] M. Y. Hammoudi, M. Benbouzid, N. Rizoug, and A. Allag, "New State Observer Based On Takai-Sugeno Fuzzy Controller of Induction Motor," in *2015 IEEE ICSC*, 2015, pp. 145-150.

[4] M. Allouche, M. Chaabane, M. Souissi, D. Mehdi, and F. Tadeo, "State feedback tracking control for indirect field-oriented induction motor using fuzzy approach," *International Journal of Automation and Computing*, vol. 10, pp. 99-110, 2013.

[5] H. b. Zina, M. Allouche, M. Souissi, M. Chaabane, L. Chrifi-Alaoui, and M. Bouattour, "Descriptor observer based fault tolerant tracking control for induction motor drive," *automatika*, vol. 57, pp. 703-713, 2016.

[6] D. Ichalal, B. Marx, J. Ragot, S. Mammar, and D. Maquin, "Sensor fault tolerant control of nonlinear Takagi–Sugeno systems. Application to vehicle lateral dynamics," *International Journal of Robust and Nonlinear Control*, vol. 26, pp. 1376-1394, 2016.

[7] D. Ichalal, B. Marx, J. Ragot, and D. Maquin, "Fault tolerant control for Takagi-Sugeno systems with unmeasurable premise variables by trajectory tracking," in *IEEE International Symposium on Industrial Electronics, ISIE 2010*, 2010, p. CDROM.

[8] H. B. Zina, M. Allouche, M. Souissi, M. Chaabane, L. Chrifi-Aloui, and C. France, "Fault Tolerant Control for Induction Motor Drive Using Descriptor Approach," *WSEAS TRANSACTIONS on SYSTEMS and CONTROL*, vol. 10, pp. 624-631, 2015.

[9] O. Zeghib, A. Allag, M. Allag, and B. Hamidani, "An Extended MVT Observer Designed for Induction Motor Drive," *Mediterranean Journal of Measurement and Control*, vol. 13, pp. 805-811, 2017.

Chapter 6:
Conclusions and future work

6.1 Conclusions

The work presented in this thesis aims to show that the algorithms based on the nonlinear the MVT theory and sector non-linearity must be used to the dynamics model of the nonlinear systems and to design stable and robust structures. The main contributions of this study lie with two topics. Firstly, the development of control methodologies based on the MVT approach essentially on the control without mechanical sensor of a three-phase IM where the influence of the parameters uncertainties and/or disturbances on the performances command is taken into account. Secondly, a robust fault tolerant trajectory tracking control scheme was proposed for the IM system affected by load torque disturbance, and speed and currents sensors fault.

Indeed, the methods of robust and sensor-less control based on other techniques generally suffer from a limited area of convergence and a relatively high sensitivity vis-à-vis uncertainties and/or disturbances but also robustness in the presence of a parameters variation of the nonlinear system. We have tried to make both educational and practical manual that should allow the designer to dealing with the control of electrical drives, we hope consistent and not too forbidding, combining theory, implementation practical and many applications of three-phase IM control techniques, which can be realized.

The Using of the sensor fault estimation given by the descriptor observer based on the T-S fuzzy approach, the control law allows to avoid (at least minimize) the fault effect on all the system and can ensure at the same time a robust tracking control performance.

In order to best situate our contribution in relation to existing works, a state of the art was presented in the second chapter. We first recalled the main results of state estimation theory and

the feedback control for the class of nonlinear systems, as well as the faults kinds and their effect on the IM drive.

Representation, synthesis and analysis tools such as MVT theory and the T-S fuzzy approach are necessary to implement the control techniques developed. These tools are summarized in the third chapter of this thesis.

Then, the next chapter (4) illustrates the application of the results mentioned in this paper to the model IM machine. After a brief presentation of the three-phase IM machine, we presented the different steps in order to obtain the final non-linear model of the IM in the two axes rotating frame (d,q). Three applications based on the MVT theory are designed for IM; first application concerns the extended observer- that estimates the IM states and moreover the rotor position and the load torque, the second application concerns a robust control of IM, where the third application is a PI control based observer for IM. These applications are proven through simulations and experimental tests and the results are shown.

The application of the FTC approach based on the T-S fuzzy approach to the IM drive is the topic of the fifth chapter where the fault is chosen in the sensors of the speed and currents. The goal is to design an observer that estimate the IM states as well as the sensor fault and also to design in the same time a robust control that takes into consideration the sensors faults and ensure the submission of the IM to the control tracking conditions. This concept is checked through an illustrative simulation and the results prove the effectiveness of the approach.

6.2 Future works

The work presented in this thesis opens a number of perspectives. In the short term, we intend to apply the analytical approach of the control and the observation used in this thesis to other types of electrical machines (synchronous machines, double fed IM,…). It seems to us that such a study could improve the performance of the control and the state's estimation of electrical machines with or without a mechanical sensor.

In long term, The design of the FTC approach for non-linear systems described by the MVT theory, and the implementation of it through experimental trials for the IM drive and other electrical machines. the stability analysis can be enhanced through the using of the Ricatti equation

and other methods instead of the Lyapunov function. We have shown the efficiency of this approach with simulations where the machine has undergone a load torque and important parametric variations, this work can be considered in the industrial application in the future if it has been checked through experimental tests. Nevertheless, a thorough study of the loss of observability must be carried out because during the implementation we have assumed that the states of the IM are observable at every moment.

Appendix A:

The parameters of the used induction motor

Parameter name	Parameter symbol	Parameter value	Parameter unit
Nominal power	P_n	186.5	Watt
Pole pair number	n_p	2	/
Rotor inductance	L_r	0.281	Henry
Stator inductance	L_s	0281	Henry
Rotor resistance	R_r	3.21	Ohm
Stator resistance	R_s	13.8	Ohm
Mutual inductance	M	0.257	Henry
Moment of inertia	J	0.001875	Kg/m^2
Friction coefficient	b	0.00052	Nm/rad/s

Figure A.1 The nameplate of the used IM

Appendix B:

Proof of theorem 5.1

Consider the following candidate Lyapunov function for the augmented system (5.20)

$$V(e_a(t)) = {e_a}^T(t)\tilde{P}e_a(t) \tag{B.1}$$

The time derivative of the candidate Lyapunov function is:

$$\dot{V}(e_a(t)) = \sum_{i=8}^{8}\sum_{n=8}^{8} \mu_n(z_r(t))\mu_i(z(t)) \left[{e_a}^T(t)\left({A_{ai}}^T\tilde{P} + \tilde{P}A_{ai}\right)e_a(t) + \rho(t)^T {T_{in}}^T\tilde{P}e_a(t) + {e_a}^T(t)\tilde{P}T_{in}\rho(t)\right] \tag{B.2}$$

To achieve the performance required by (5.21) and the closed loop stability of (5.20) the following inequality must hold

$$\dot{V}(e_a(t)) + {e_a}^T(t)\tilde{Q}e_a(t) - \gamma^2\rho(t)^T\rho(t) \leq 0 \tag{B.3}$$

By substituting (B.2) in (B.3) the inequality become as:

$$\sum_{i=8}^{8}\sum_{n=8}^{8} \mu_n(z_r(t))\mu_i(z(t)) \begin{bmatrix} e_a(t) \\ \rho(t) \end{bmatrix}^T FF \begin{bmatrix} e_a(t) \\ \rho(t) \end{bmatrix} \leq 0 \tag{B.4}$$

With

$$FF = \begin{bmatrix} {A_{ai}}^T\tilde{P} + \tilde{P}A_{ai} + \tilde{Q} & \tilde{P}T_{in} \\ {T_{in}}^T\tilde{P} & \gamma^2 I \end{bmatrix}$$

The LMI (B.4) is satisfied if

$$\begin{bmatrix} {A_{ai}}^T\tilde{P} + \tilde{P}A_{ai} + \tilde{Q} & \tilde{P}T_{in} \\ {T_{in}}^T\tilde{P} & \gamma^2 I \end{bmatrix} \leq 0 \tag{B.5}$$

With $\tilde{P} = diag[P_1 \quad P_2 \quad P_3]$ and $\beta = {P_3}/{R}$ the inequality (B.5) become as:

$$\begin{bmatrix} \pi_{11} & -P_1BK_i & 0 & P_1 & -P_1 & P_1(A_i - A_{cn}) \\ * & \pi_{22} & \pi_{23} & P_2 & 0 & 0 \\ * & * & \pi_{33} & -P_3C & 0 & 0 \\ * & * & * & -\gamma^2 I & 0 & 0 \\ * & * & * & * & \gamma^2 I & 0 \\ * & * & * & * & * & \gamma^2 I \end{bmatrix} \leq 0 \tag{B.6}$$

Whereas

$\pi_{11} = P_1(A_{ai} + BK_i) + (A_{ai} + BK_i)^T P_1 + Q$

$\pi_{22} = P_2 A_{ai} + {A_{ai}}^T P_2$

$\pi_{23} = -C{A_{ai}}^T + C^T \beta^T$

$\pi_{33} = -\beta^T - \beta$

Because of (B.6) contains a nonlinear terms, and in order to transfer it to an LMI, the following partitioning is required

$$\vartheta = \begin{bmatrix} \vartheta_{11} & \vartheta_{12} \\ \vartheta_{21} & \vartheta_{22} \end{bmatrix} \tag{B.7}$$

Where

$$\vartheta_{11} = \pi_{11}$$

$$\vartheta_{12} = [-P_1BK_i \quad 0 \quad P_1 \quad -P_1 \quad P_1(A_i - A_{cn})]$$

And ϑ_{21} and ϑ_{22} represent the lower blocks of (B.6)

By multiplying (B.7) by $Z = diag\left({P_1}^{-1}X\right), X = diag({P_1}^{-1} \quad I \quad I \quad I \quad I)$

Then the inequality follows that:

$$\begin{bmatrix} {P_1}^{-1}\vartheta_{11}{P_1}^{-1} & {P_1}^{-1}\vartheta_{12}X \\ X\vartheta_{21}{P_1}^{-1} & X\vartheta_{22}X \end{bmatrix} \leq 0 \tag{B.8}$$

The inequality need $X\vartheta_{22}X$ to be negative, and to achieve this constraint we have

$$X\vartheta_{22}X \leq -2\delta X - \delta^2 {\vartheta_{22}}^{-1} \tag{B.9}$$

Now the stability is expressed in LMI form that can be easily solved that is as follows

$$\begin{bmatrix} {P_1}^{-1}\vartheta_{11}{P_1}^{-1} & {P_1}^{-1}\vartheta_{12}X & 0 \\ X\vartheta_{21} & -2\delta X & \delta I \\ 0 & \delta I & \vartheta_{22} \end{bmatrix} \leq 0 \qquad \text{(B.10)}$$

This LMI is the same as in (5.21) if we substitute $\vartheta_{11}, \vartheta_{12}, \vartheta_{21} and\ \vartheta_{22}$ by their original values.